BACK-CALCULATING DESIGN PARAMETERS FOR PILES IN MARINE SOILS FROM HIGH-STRAIN DYNAMIC TESTS

BY

AHMED H. BUKHARY

A Thesis Presented to the

DEANSHIP OF GRADUATE STUDIES

KING FAHD UNIVERSITY OF PETROLEUM & MINERALS

DHAHRAN, SAUDI ARABIA

In Partial Fulfillment of the
Requirements for the Degree of

MASTER OF SCIENCE

In

CIVIL ENGINEERING

May, 2017

KING FAHD UNIVERSITY OF PETROLEUM & MINERALS

DHAHRAN- 31261, SAUDI ARABIA

DEANSHIP OF GRADUATE STUDIES

This thesis, written by **AHMED HASSAN MOHAMMED BUKHARY** under the direction of his thesis advisor and approved by his thesis committee, has been presented to and accepted by the Dean of Graduate Studies, in partial fulfillment of the requirements for the degree of **MASTER OF SCIENCE IN CIVIL ENGINEERING**.

Prof. Naser A. Al-Shayea
(Advisor)

Dr. Salah U. Al-Dulaijan
Department Chairman

Dr. Prakasha S. Kuppalli
(Member)

Prof. Salam A. Zummo
Dean of Graduate Studies

Prof. Sahel N. Abduljauwad
(Member)

26/7/2017

Date

I am immensely proud to dedicate this work to my parents for all what they gave and still giving and for their indescribable support.

ACKNOWLEDGMENTS

I am genuinely grateful to my supervisor Prof. Naser Al-Shayea without whom it would have been difficult to complete this work standing over me as I carried out every assignment; dedicating his precious time and providing invaluable advice through the entire research period. My foremost thanks go to him as the man who taught me how to commit to high research values. Under his supervision, I was given the opportunity to see the solution for real soil problems and the meaning behind the results of each laboratory test I have conducted through the eyes of the expert taking measures in relation to them.

I would like to pay tribute to the calm professionalism of Dr. Prakasha Kuppalli of Saudi Aramco, my thesis committee member whom I would rather call my co-advisor for his valuable guidance. There are a few people who can guide one to discover the reality of what it is like to be the professional engineer being in the middle of geotechnical problems solving. Dr. Kuppalli, with no doubts, is one of them.

I am thankful to Prof. Sahel Abduljauwad for his valuable comments and inputs which had a positive impact on the quality of the work.

Acknowledgment is due to King Fahd University of Petroleum and Minerals for providing all necessary facilities and support for my M.Sc. thesis. I would also like to acknowledge Saudi Aramco for their cooperation and support through providing the technical reports, and Fugro-Suhaimi Limited for offering marine soil samples.

I extend my thanks to the other members of the geotechnical research group who made my time as part of the group very pleasant and enjoyable by their friendship and the enthusiasm they brought to my work.

Personally, I am deeply indebted to my parents for their unconditional support over the years.

Finally, I would like to thank everyone who contributed to or provided any help or support to this research in any mean.

TABLE OF CONTENTS

LIST OF TABLES

LIST OF FIGURES

NOMENCLATURE

A	cross-sectional area of the pile (in^2)
A_s	side surface area of pile
A_p	gross end area of the pile
API	American Petroleum Institute
BOR	Beginning of Restrike
β	dimensionless shaft friction factor, for sands
CAPWAP	CAse Pile Wave Analysis Program
D	diameter of the pile (inches)
DMS	Dynamic Monitoring System (dynamic pile monitoring)
d_t	displacement of the top of the pile (inches)
D_{10}	effective grain size, grain size corresponds to 10% of the soil sample passing by weight
D_c	degree of crushing
$D_{c\%}$	degree of crushing expressed as percentage
D_r	Relative density of soil (%)
EOD	End of initial Drive
E	modulus of elasticity of the pile (psi)
$f(z)$	unit shaft friction, in stress units
f_{lim}	limiting skin friction
FOS	factor of safety
G_s	Specific gravity of soil
HPA	Hammer Performance Analyser
H_0	null hypothesis of statistical test
H_1	alternative hypothesis of statistical test
ICP	Imperial College Pile approach
K_0	coefficient of lateral earth pressure at rest
L	length of the pile (inches)
LL	liquid limit (%)

NR	not reported
$\mathbf{N_q}$	dimensionless bearing capacity factor
OCR	Over Consolidation Ratio
PL	plastic limit (%)
PI	plasticity index (%)
PDA	Pile Driving Analyser
PIT	Pile Integrity Tester
$\mathbf{p_0'(z)}$	effective vertical stress at depth z
$\mathbf{p_{0,\ tip}'}$	effective vertical stress at the pile tip
Q	applied test load (lbs)
$\mathbf{Q_c}$	axial pile ultimate capacity in compression, in force units
$\mathbf{Q_{f,c}}$	shaft friction capacity in compression, in force units
$\mathbf{Q_p}$	end bearing capacity, in force units
q	unit end bearing at the pile tip, in stress units
$\mathbf{q_c}$	cone tip resistance
SEM	Scanning Electron Microscope
$\mathbf{SF_{DMS}}$	Shaft Friction in stress units estimated by Dynamic Monitoring System
$\mathbf{SF_{API}}$	Shaft Friction in stress units estimated by API standards = $\mathbf{f(z)}$
$\mathbf{s_u}$	undrained shear strength of the soil at the point in question, in stress units
WCI	Wasted Capacity Index
W.C.	soil water content (%)
XRD	X-ray diffraction
z	depth below the original seafloor
$\boldsymbol{\alpha}$	dimensionless shaft friction factor, for clays
$\boldsymbol{\alpha_\alpha}$	the level of significance
$\boldsymbol{\gamma}$	unit weight of the soil
$\boldsymbol{\mu}$	mean of population
$\boldsymbol{\mu_0}$	hypothesised population mean
$\boldsymbol{\sigma}$	standard deviation

η	population median
$\boldsymbol{\delta_0}$	hypothesised difference between two population means

ABSTRACT

Full Name : Ahmed Hassan Mohammed Bukhary

Thesis Title : Back-Calculating Design Parameters for Piles in Marine Soils from High-Strain Dynamic Tests

Major Field : Civil Engineering

Date of Degree : May, 2017

With the increasing need to develop more marginal oilfields, and continuing new finds worldwide, offshore structures are now frequently constructed in regions where unpredictable clay and sand including young calcareous sediments, are predominately present. The constituent particles of calcareous sediments for instance, are highly variable, consisting of the skeletal remains of marine organisms or precipitate grains. Offshore structures are often founded on piles in these materials. The present methodology of design parameters of these piles is based upon geotechnical investigation, and adopting the American Petroleum Institute standard (API RP 2Geo), and verified using high strain pile test results. The initiation of this research was a result of increasing awareness within the oil industry that this design methodology is overconservative. The study evaluates the degree of this overconservatism through performing back-analysis of soil parameters, and carrying out statistical analysis on the collected data. Over 100 offshore geotechnical investigation and dynamic pile monitoring (DMS) reports were collected for a number of marine platforms installed at 5 major fields within the Arabian Gulf. Necessary data of piles which restrike was performed on were compiled from the reports. Design parameters were back-calculated and then statistically analysed. The study concluded that the

relationship between DMS and API design parameters varies, generally with DMS parameters being larger. Regression plots yielded an overconservative factor of 2.36, 1.50, 2.03, 1.71, and 1.76 for very loose, loose, medium dense, dense, and very dense silica sand layers, respectively. While for carbonate sand, the overconservative factor was as high as 3.67. Similarly, overconservative factor for clayey layers with OCR = 1, $1 < OCR \leq 4$, and OCR > 4 were estimated at 1.90, 1.44, and 1.35, respectively. Furthermore, adjusted overconservative factors were suggested based on statistical evaluation of the difference between the DMS and API design parameters for sand and clay. Moreover, the crushability of marine carbonate sands was investigated by means of an experimental programme and compared with that of quartzitic sand. Test results showed an average crushability of 65% for carbonate sand, compared to a negligible 2% for quartzitic sand.

ملخص الرسالة

الاسم الكامل: أحمد حسن محمد بخاري

عنوان الرسالة: الحساب العكسي لعوامل تصميم الخوازيق في التربة البحرية من الاختبارات الديناميكية عالية الانفعال

التخصص: هندسة مدنية

تاريخ الدرجة العلمية: مايو 2017

مع تزايد الحاجة إلى تطوير حقول نفطية هامشية، واستمرار الاكتشافات النفطية الجديدة في جميع أنحاء العالم، كثيرا ما يتم تشييد المنشآت البحرية في المناطق التي توجد فيها عادة تربة طينية او رملية بما فيها التي تحتوي رواسب جيرية حديثة لا يمكن التنبؤ بسلوكها . الجسيمات المكونة لهذه الرواسب متغيرة للغاية، وتتألف من بقايا الهياكل العظمية للكائنات البحرية. غالبا ما تؤسس المنشآت البحرية على خوازيق في هذه المواد . تستند الطريقة المتبعة حاليا لتصميم هذه الخوازيق البحرية على معيار المعهد الأمريكي للبترول API RP 2Geo ومن ثم التحقق من هذه المعاملات عن طريق نظام CAPWAP لتقدير القدرة التحميلية للخازوق عن طريق الاحتكاك والارتكاز. فكرة هذا المشروع نبعت نتيجة لزيادة الوعي داخل صناعة النفط بأن منهجية التصميم هذه متحفظة وبالتالي تقود الى نتائج غير اقتصادية ومكلفة . تقيم هذه الدراسة درجة هذا التحفظ الزائد من خلال إجراء تحليل خلفي لعوامل التصميم، وإجراء تحليلات إحصائية للبيانات المجمعة .وقد تم جمع أكثر من 100 تقرير جيوتقني بحري وتقارير مراقبة أداء الخوازيق ديناميكيا لعدد من المنصات البحرية التي تم تركيبها في 5 حقول رئيسية في الخليج العربي .وقد جمعت البيانات اللازمة من الخوازيق التي تم عليها إعادة الطرق من التقارير .تم حساب عوامل التصميم عكسيا ومن ثم تحليلها إحصائيا .وخلصت الدراسة إلى وجود عامل تحفظ يبلغ 2.36, 1.50, 2.03, 1.71 و 1.76 لطبقات رمل السيليكا المفككة جدا, المفككة, المتوسطة الكثافة, الكثيفة, والكثيفة جدا، على التوالي. بينما وجد عامل تحفظ قدره 3.67 للتربة الرملية الكربونية. وبالمثل، تم تقدير عامل تحفظ للطبقات الطينية والتي لها نسبة زيادة تصلب (OCR) تساوي 1، OCR بين 1 و4، وOCR أكبر من 4 عند 1.90, 1.44, و 1.35 على التوالي. تم اقتراح عوامل تحفظ معدلة استناداً الى نتائج تقييم احصائي للفرق بين معاملات التصميم المحسوبة والمقدرة بمعيار API ونظام CAPWAP على التوالي .وعلاوة على ذلك، تمت دراسة نسبة سحق الرمال الكربونية البحرية عن طريق تجارب معملية وتمت المقارنة مع عينة رمل الكوارتز .أظهرت نتائج الاختبارات ان متوسط قابلية السحق 65٪ للرمل الكربوني، مقابل 2٪ فقط بالنسبة لرمال الكوارتز .

CHAPTER 1

INTRODUCTION

1.1 General

A number of geotechnical problems are likely to be involved in the design of marine structures. Typical examples are the difficulties associated with foundation which are well-recognised. Offshore construction experiences clearly demonstrated the dangers of applying design criteria of piles in silica sand to those driven in calcareous material. Moreover, modifications are believed to be required for American Petroleum Institute (API) capacity determination procedure for piles driven into some offshore sand and clay fields in the Arabian Gulf due to the especial nature of soil in these locations.

1.2 Importance of the Research

The present design methodology of pile foundation for offshore structures is based on geotechnical investigations and adopting API RP 2Geo [1] recommendations to determine the design parameters, which are verified by performing the high-strain dynamic test (i.e., DMS) in the field. The DMS data indicate that API estimates are overconservative. A research is needed to evaluate and remove this degree of overconservatism. The research is intended to aid in determining better design parameters, which would bring about more economical design of offshore piles in marine soils.

1.3 Objectives of the Research

This research is intended to:

- evaluate the degree of overconservatism in design parameters estimated in accordance with API recommendations for piles driven into marine sand and clay in the Arabian Gulf. The overconservatism is to be expressed in terms of a factor for practicality purpose.
- study the degree of crushability of calcareous/carbonate sand for some soil samples collected from different offshore fields in the Arabian Gulf, and its contribution to the reduced shaft friction values of piles installed in such soils.

1.4 Organisation of the Thesis

The organisation of this thesis is as follows: Chapter 2 highlights common types of offshore structures used in oil industry and their associated pile foundation. It also outlines the existing methods for determination of axial pile capacity with some emphasis on API guidelines and the dynamic approach using Pile Driving Analyser (PDA) and CAse Pile Wave Analysis Program (CAPWAP). The last section in this chapter casts some light on marine calcareous soil and summarises some of their famous classification systems.

Chapter 3 presents the methodology of the work followed, starting with compiling and organising field data, passing through carrying out back-calculation and statistical analyses, and ending with performing experimental program on soil samples.

Chapter 4 discusses the results obtained. The evaluation of shaft friction and alpha factor is presented and discussed by means of interpreting results of the statistical analyses. Moreover, the chapter presents the outcomes of the experimental assessment of the degree of crushing of carbonate sand samples.

Chapter 5 gives a summary and conclusions of this thesis, and discusses possible directions for future work. Last but not the least, is a list of references cited, then the Appendix which contains a detailed tabulation of compiled field data for marine sand and clay layers used in this research.

CHAPETR 2

LITERATURE REVIEW

2.1 General

The beginning of offshore geotechnology can be traced back to the late 1940s, precisely in 1947 when the first offshore oil rig ‘Superior’ was installed in only 6-m-deep water, and 30 Km from Louisiana coast, USA [2], [3]. The need for safe foundations for similar offshore structures mainly for hydrocarbon recovery has attracted the interest of geotechnical engineers to involve in and develop this area. Basically, the practice associated with offshore geotechnical engineering stemmed from the onshore practice. However, there was a major tendency towards the divergence of the two application areas over the last 30 years, due to the fundamental differences in the scale of foundations and anchoring systems, as well as in the construction techniques. Offshore geotechnical engineering has evolved through the years as speciality. Now there are over 7000 offshore platforms all over the world embedded in water with different depths, some of which exceed 2000 m [2], [4].

2.2 Features of Offshore Geotechnical Engineering

Marine or offshore geotechnics are quite analogous to onshore geotechnics; nonetheless, there is a number of features that distinguish the geotechnical engineering for offshore conditions, which include:

- The cost of site investigations and pile installation are enormously higher. Hiring suitable vessels typically costs millions of English pounds.
- The behaviour of seafloor soils, especially carbonate soils, is often unusual unlike terrestrial soils.
- Waves constitute an additional loading component which is large and cyclic in nature.
- It is generally not possible to apply modifications to the design during construction since they would be prohibitively expensive even if these modifications are technically feasible.
- Despite foundation stiffness influences the dynamic response of the structure, more emphasis is placed upon capacity, or ultimate limit state.

2.3 Types of Offshore Structures

An offshore or marine structure may be defined as one which has no fixed access to dry land and which should stand stable in different weather conditions [5]. Offshore structures are constructed to serve various roles in different water depths and environments. Their types are so many, and covering them all is beyond the scope of this research; however, light will be shed upon some of the common types of offshore platforms. Further information can be found in the references at the end of this thesis.

2.3.1 Fixed Platforms

Fixed platforms are usually built for hydrocarbon production and in certain conditions when the water depth is shallow. Their "legs" are usually made of concrete or steel and

they are fixed to the seafloor with piles. The stability of these types of platforms is high; as they are fixed to the seafloor which is considered to be a main advantage. Movement due to wind waves are quite limited. However, their use in deep water is uncommon, since it is not economically feasible to construct very long legs [6], [7].

2.3.2 Compliant Platforms

The concept of compliant platforms is based on the movement of the structure with wind and waves as opposed to resisting them. Water depths of 300 to 800 m are considered suitable for construction of such platforms. Compliant platforms have a structure of a steel truss supported by piles. Lena was the first compliant tower built in the early 1980s in the Gulf of Mexico with a total height reaches 400 m [8].

2.4 Offshore Pile Foundation

It has been a well-recognised engineering practice to favour the use of pile foundations over shallow foundations whenever soil conditions at the surface are considered problematic (e.g. soft, expansive, etc.), or when a high horizontal component of loads is present which would bring about sliding of a surface foundation. Depending upon the geotechnical conditions at a particular engineering site, the type of pile foundations to be adopted is selected. Generally, the diameter of offshore piles varies from 0.76 m for wellhead conductors to larger than 4 m for monopile foundations, with a typical range of 25 to 100 mm diameter to wall thickness ratio.

Since time is an essential factor during the installation of any offshore platform driven steel piles are the traditional and most preferable type of foundation for offshore steel platforms. Choosing bored type of piles would mean more time for the vessel to stay in duty, and consequently, immense amount of spending. A typical small jacket structure has a pile at each corner of the platform, while in contrast a group of piles at each corner is usually the case in major platforms. The North Rankin A platform located in the North-West Shelf near Australia, and the Goodwyn platform are good examples. Eight piles were constructed at each corner of the former, while five were sufficient to carry the load imposed by the latter.

In general, three criteria must be satisfied in the design of offshore piles and pile group [2], [7]:

a) Axial and lateral capacities are adequate;
b) Load-deformation response is acceptable;
c) Piles installation is feasible, meaning that the available equipment is technically capable of driving the piles to the design depth.

Pile foundation design should be optimised for cost by shortening the installation time and reducing the material used through minimising the number of piles and their length.

2.4.1 Types of Offshore Piles

This section describes two types of pile foundations which are commonly used for offshore structures. Greater attention is given to driven steel piles since they are by far the most preferably used type for offshore platforms and moreover, are the subject of this study.

Driven Steel Piles

The open-ended driven steel tube pile is the most common offshore type. Which is typically driven into the seafloor by means of a hammer, so this type is basically a displacement pile (i.e., installation of the pile is done by displacing as opposed to removing the soil). Specifying the dimensions is by the diameter and the wall thickness. Dimeter is usually provided in multiples of 6 inches, and wall thickness is at $\frac{1}{4}$ inches intervals. Typical range of diameter to wall thickness ratio is 20 to 60. The lower value denotes the ultimate curvature that a steel rolling machine can offer, while the highest value represents a limit below which the curvature should be maintained so as to avoid wall-buckling effects [9]–[11].

The detailed pile design including the wall thickness and the rest of pile section features is referred to by the term "pile make-up". A driving shoe may be used at the lower end of the pile to facilitate the driving process. It usually has a thicker wall section to account for the non-uniformities in the soil and rock while advancing the pile and more importantly for the stress concentrations. Generally, piles are designed with a constant wall thickness; nevertheless, and because the imposed loads on the central sections are of lower order of magnitude, hence thinner wall thickness can be used at these parts. In contrast, the upper section must have a thicker wall so as to withstand the high stresses during the operational phase of the platform design life. The sleeves at the bottom of platform legs, and the shear connections attached to the sleeves are usually the means to transfer the structural loads to the piles.

Driven steel piles have design considerations that are mainly associated with issues of drivability which typically include soil plug, refusal, and tip damage. Such issues are especially considered of high significance when driving into dense sand or sediments with high level of cementation. When the driving resistance exceeds the hammer capacity, the design penetration cannot be reached and a refusal has occurred. Pile tip integrity is immensely important. Should the pile tip get damaged before the final penetration is reached, buckling of the pile tip, and subsequently collapse during driving may likely take place [12]. Consequently, the change of pile shape can cause a reduction in the capacity or even lead to a premature refusal. An example of a case in which premature refusal has taken place which dictated involvement of substantial remedial works is reported by [13].

Limitations of driven piles lie mainly in the hindering that a cemented caprock layer may cause which can eventually lead to pile tip damage. Very low shaft resistance can be obtained when driven piles are advanced into calcareous sand or compressible and cemented soils in general.

Drilled and Grouted Piles

In strong cemented formations, drilling and grouting is the only possible solution for piling. In uncemented to weak formations, high bearing capacities can be achieved, although borehole instability can be a problem, and drilling mud often reduces skin friction. Following the tests in the early 1970's by [14], [15] offshore Australia, the design limit for peak skin friction of 100 kPa came to be accepted. Murff [16] pointed out that many of the early field tests did not take the piles to failure. Later tests have illustrated that this figure is probably extremely conservative. Tests on cemented material from offshore Australia suggest peak skin friction is in excess of 500 kPa [17], [18].

2.4.2 Pile Capacity

Piles are the usual foundation solution adopted for the support of offshore platforms on continental shelves, and a number of projects in the Arabian Gulf have encountered a variety of uncemented and lithified calcareous sediments in the last 50 years. In virtually every case the load carrying capacities of the piles chosen are thought to have been severely over-estimated.

The prediction of ultimate axial capacity of a single pile is the first step in the design of deep foundation. The numerous applications of piles in civil engineering practice have encouraged many investigators to study the essential factors affecting pile behaviour under axial and even under lateral loading [19]. The reliability of pile installation to the required depth of penetration should be ensured in the design. It must also be checked that the stiffness and strength of the foundation are sufficient enough to resist the design loads.

Determination of an open-ended tubular pile capacity should involve performance of two calculations: one allowing for unplugged failure and one accounting for plugged failure. Various components of resistance that ought to be overcome for each failure mechanisms are shown in Figure 1.

The axial capacity of driven piles is usually determined either:

a) from the results of load testing, either static or dynamic; or
b) from different pile capacity estimation methods;

The load carrying capacity of a pile is the load the pile is subjected to which will cause failure. It can be calculated from vertical equilibrium as the sum of the total shaft resistance, and the ultimate tip resistance.

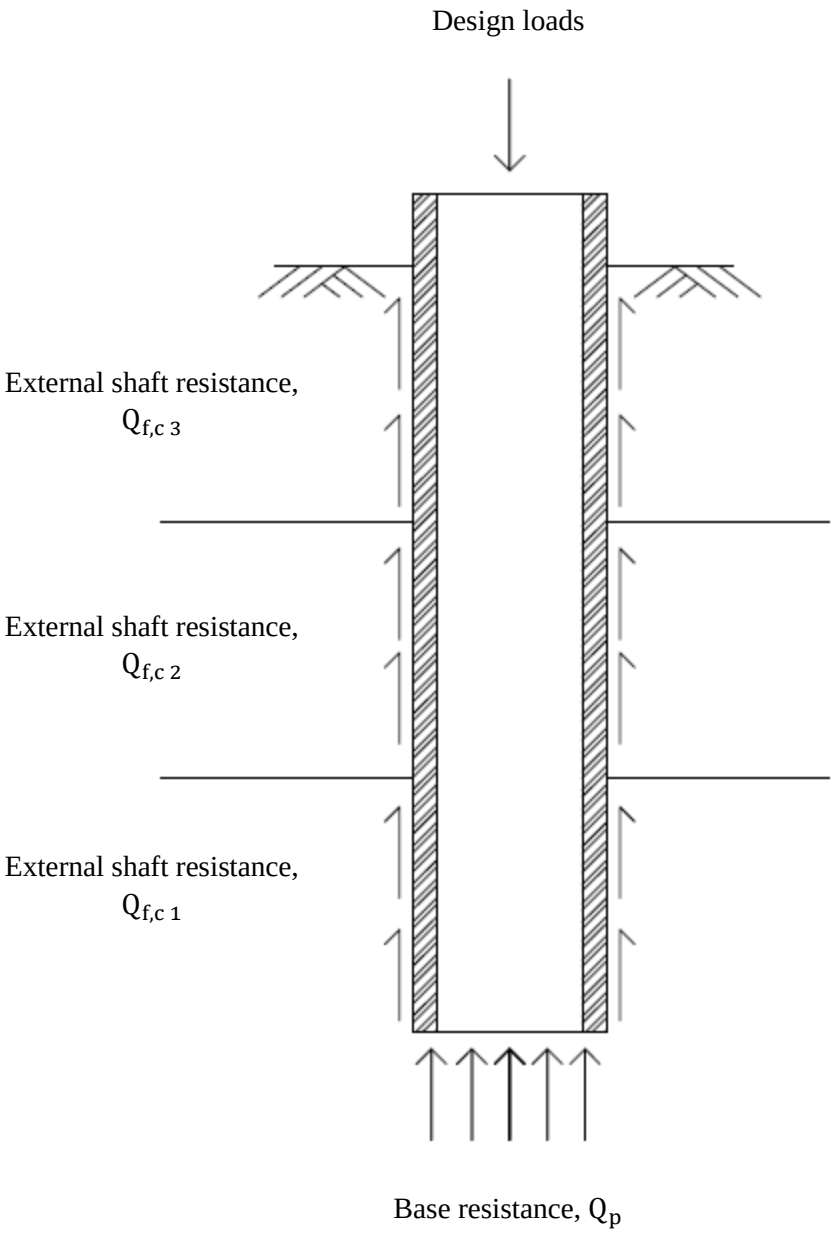

Figure 1: Pile capacity mechanisms installed through layered soil [2]

Unit skin friction is a function of the effective overburden pressure, the coefficient of lateral earth pressure, and the friction angle between the soil and pile wall.

In carbonate sands, bearing capacities are significantly lower at a given stress level than for silica sand [20]. Furthermore, On the basis of a series of studies reported by Golightly [20], the reduced Rigidity Indices defined as the ratio between shear strength and stiffness for compressible carbonate sands, lead to reduced bearing capacity N_q values and thereby, low unit end bearing value.

2.4.3 Axial Capacity of Driven Pile from Static Load Testing

In the static load test, piles are commonly loaded to twice the design load or to failure. The load is usually applied with a jack against a reaction beam connected to anchor piles. Following is an incremental unloading of the pile. Depending upon the type of load test, the increment of loading as well as monitoring procedure and time is varying. The "Standard Test Method for Piles Under Static Axial Load" of ASTM D1143 [21] is recommended by Hannigan [22], while AASHTO 2002 [23] recommends the use of Davisson criteria [24] to evaluate the design capacity. In this method, Davisson sets the intersection of the pile top displacement and a line offset to the elastic deformation portion of the pile loading as where the pile fails. This indicated line is addressed by the following equation [25], [26]:

$$d_t = \frac{QL}{EA} + (0.15 + 0.008D) \qquad (2.1)$$

where, d_t: displacement of the top of the pile (in)

Q: applied test load (lbs)

A: cross-sectional area of the pile (in^2)

E: modulus of elasticity of the pile (psi)

L: length of the pile (in)

D: diameter of the pile (in)

Major drawbacks of the static load testing of piles include the high cost and its inability to provide any information about the quality of installation and driving efficiency [25], [26].

2.4.4 Axial Pile Capacity from High-Strain Dynamic Test

Design and installation of pile foundations for different offshore structures is more challenging when complicated soil strata exist. The complexity gets even higher when the piles to be driven are very heavy and long, have large diameter, and/or the required depth of penetration is immense, etc. While driving the pile, issues such as pile integrity, performance of the hammer, driveability and penetration into the different soil strata, and pile load carrying capacity are the major concerns.

High-Strain Dynamic Test (HSDT) was introduced more than 40 years ago, and has been in use to monitor the installation of pile, determine static soil resistance to driving of the pile, evaluate the long term static soil resistance, as well as to evaluate the total settlement of the pile under the measured capacity [27], [28].

Some advantages of high strain dynamic pile test include quickness, portability, cost-effectiveness, possibility of stresses evaluation, distribution of soil resistance, and the availability of heavy duty hammers capable of performing large pile driving operations. These make it the most reliable option to address the concerns associated with marine piles design and installation.

The HSDT is administrable at any point during the installation of the pile, which allows the pile to be tested for any suspected damage or misalignment during driving process. Moreover, the appropriateness of the hammer used for driving in terms of efficiency, stroke, and fuel setting can be checked. The Pile Driving Analyser (PDA®) provided by Pile Dynamics, Inc. (PDI), is used in HSDT to collect data during striking process, and then a computer program, such as the CAPWAP® (CAse Pile Wave Analysis Program) of Pile Dynamics, Inc. (PDI), is employed to refine the data and subsequently estimate the pile in situ capacity [25]. The following is a general summary of dynamic measurements available to solve typical deep foundation problems.

Pile Driving Analyser (PDA):

Pile top strain and acceleration measurements which are converted to force and velocity records, respectively are the basis for the results calculated by the PDA. The PDA computes average pile force and velocity thereby eliminating bending effects, immediately after it conditions, calibrates and displays these signals. The PDA calculates the results using closed form Case Method solutions, based on the one-dimensional linear wave equation. Figure 2 shows recent PDA announced by PDI, Inc. in 2014.

Hammer Performance Analyser (HPA)

Radar technology in the Hammer Performance Analyser™ (HPA) is used to evaluate the ram velocity. It should be pointed out that the ram ought to be visible in order for this unit to be applicable. A PC can automatically process the impact velocity results or they can alternatively be recorded on a strip chart.

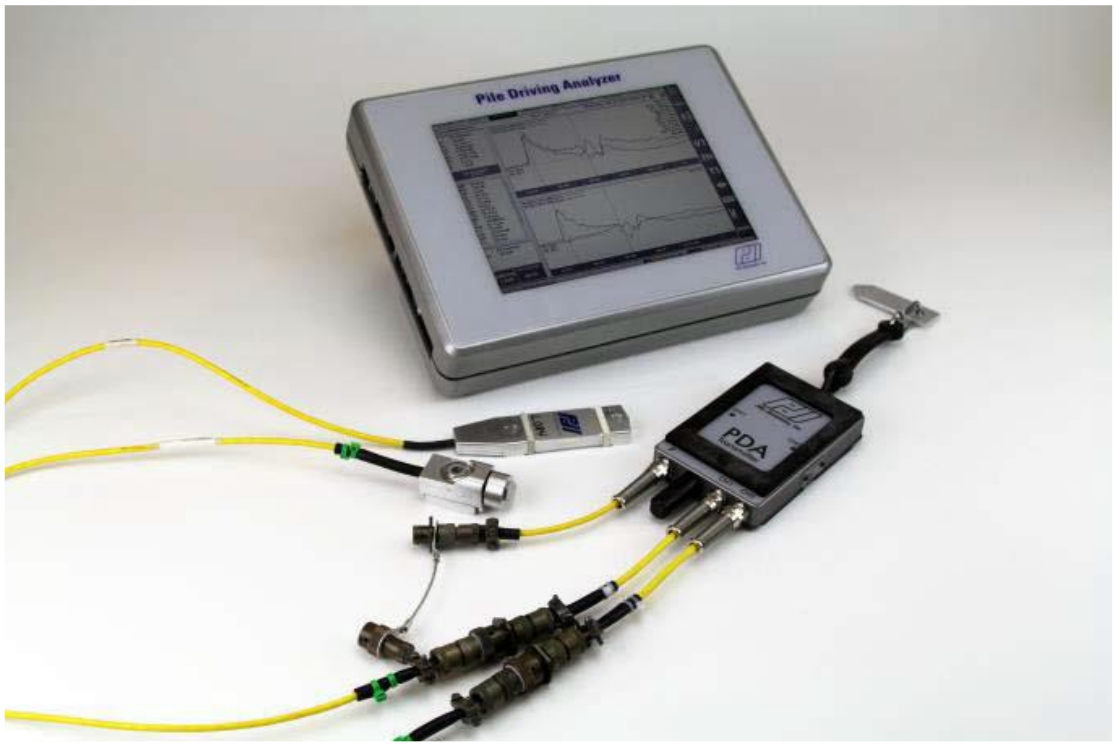

Figure 2: The new PDA 8G (8th generation PDA) [64]

CAPWAP

In addition to total and static bearing capacity values, the solution of the CAse Pile Wave Analysis Program includes shaft resistance, end bearing, damping factors, and soil stiffness values because it combines the Case Method measurements and the wave equation pile and soil model.

A number of unknowns is iteratively calculated by signal matching in this method. In contrast to what a GRLWEAP analysis necessities making hammer performance assumptions, the CAPWAP program works with the pile top measurements. Moreover, certain assumptions associated with soil behaviour are required in both Case Method and GRLWEAP. On the other hand, the CAPWAP calculates these soil parameters based on the dynamic measurements.

Limitations of CAPWAP Analyses

Lai and Kou [29] evaluated the reliability of PDA and CAPWAP for prediction of in situ pile capacity. Their investigation yielded that the CAPWAP has more reliably predicted capacities than the PDA, which was basically attributed to the fact that CAPWAP analysis refines the Smith damping factor employed in capacity prediction.

Nonetheless, when CAPWAP predictions were compared with static capacity analysis using Davisson failure criteria, it could over predict the static capacity by up to a factor of 1.15. Moreover, CAPWAP analysis could give under-predicted results by a factor down to 0.4 from hammer limitations or from soil disturbance when compared to static testing.

A study to investigate the reliability of dynamic measurements at predicting the measured static capacity calculated by the Davisson method was conducted by Long et al. [30]. A

comparison was made between Engineering News, WEAP, Gates, Measured Energy, PDA, and CAPWAP methods in terms of value of predicting capacity evaluated by the Wasted Capacity Index (WCI) of each method. WCI is a measure of the inefficiency of a method at predicting capacity. In other words, the uncertainty associated with each method. It basically compares the needed amount of additional capacity for a pile to meet a specified level of certainty. Typically, the lower the WCI, the better the prediction. The different methods were compared for a 99% reliability of prediction. The results yielded that when using EOD data for predicting capacity, the Measured Energy approach appears to be superior with WCI of only 1.9, while CAPWAP performing at virtually the same level as the rest of methods (WCI = 2.4). In contrast, CAPWAP method takes the lead when BOR data is used evidenced by a reduced WCI of 1.6, which clearly reflects the reliability of this method at the beginning of restrike. The time at which these BOR tests were conducted was not reported however.

Pile Integrity Tester (PIT)

The Pile Integrity Tester™ (PIT) is used to examine the concrete piles or shafts and H-steel piles for any major defects. It is also used to assess the length of different deep foundations, except pipe steel piles. The PTI utilises the "Pulse-Echo Method"; hence, only motion measurements (e.g., acceleration) at the pile top produced by a light hammer impact are required. "Transient Response Method" is another concept the PIT supports. Additional measurement of the hammer force and an analysis in the frequency domain are required in this method. Another advantage of the PIT is that it may be used to evaluate the unknown length of deep foundations of existing structures.

2.4.5 Determination of Pile Capacity:

Pile foundation design and installation in Saudi Arabia is usually performed in accordance with API 2011 [8], SAES-M-005 2011 [21], and SAES-Q-004 2010 [22].

The following general equation is used to determine the ultimate axial capacity, Q_c of piles in compression:

$$Q_c = Q_{f,c} + Q_p = f(z)A_s + qA_p \quad (2.2)$$

where, Q_c: axial pile ultimate capacity in compression, in force units

$Q_{f,c}$: shaft friction capacity in compression, in force units

Q_p: end bearing capacity, in force units

$f(z)$: unit shaft friction, in stress units

A_s: side surface area of pile

q: unit end bearing at the pile tip, in stress units

A_p: gross end area of the pile

Shaft Friction and End Bearing in Cohesionless Soils

Unit shaft friction at given depth for pipe piles installed in cohesionless soil can be calculated using the following formula (API 2011) [1]:

$$f(z) = \beta p_0'(z) \quad (2.3)$$

where, β: dimensionless shaft friction factor, for sands

$p_0'(z)$: effective vertical stress at depth z

At the other end of the spectrum, the unit end bearing, q, in stress units, is determined by:

$$q = N_q p'_{0,\ tip} \tag{2.4}$$

where, N_q: dimensionless bearing capacity factor

$p'_{0,\ tip}$: effective vertical stress at the pile tip

Shaft Friction and End Bearing in Cohesive Soils

Equation 2.5 below can be used to compute the unit shaft friction, f(z), in stress units at a given depth, z [1]:

$$f(z) = \alpha s_u \tag{2.5}$$

While the unit end bearing is evaluated in stress units by:

$$q = 9 s_u \tag{2.6}$$

where, α: dimensionless shaft friction factor, for clays

s_u: undrained shear strength of the soil at the point in question, in stress units

The factor α can be determined by equation (2.7):

$$\alpha = 0.5\varphi^{-0.5} \text{ for } \varphi \leq 1.0 \tag{2.7}$$

$$\alpha = 0.5\varphi^{-0.25} \text{ for } \varphi > 1.0$$

where,

$$\varphi = \frac{s_u}{p'_0(z)} \text{ at depth, } z \tag{2.8}$$

with the constraint that $\alpha \leq 1.0$

It must be pointed out that although these equations represent the current industry standard and a simplified model that has been in practice for long time, it does not give any information about axial pile displacements which are considered highly important for serviceability purposes, especially when load conditions are non-extreme. The above-discussed model is based on a quasi-static and monotonic application of the axial loads and the complexity associated with the interaction between pile and soil in the field is not reflected by this model [1].

Ras Tanajib Modification:

It has been observed that soil resistance to driving of piles driven in the Safaniya Field to shallow depths were as high as 10 times greater than the static pile capacity determined in accordance with the API standards. It was then decided that a discrepancy of this magnitude must be addressed and further investigated. So, 8 offshore sites were selected and a total of 26 pullout tests were performed in 1982 on 0.51 to 0.76 m diameter open-ended pipe piles which had depth of penetration of 11 to 22 m. Tensile capacities were found to be 2.5 to 6 times greater than determined static pile capacity [33]. Helfrich et al. [34] and Al-Shafei et al. [35] described details of load tests performed in 1983 on two open-ended pipe piles 18 m long, 0.61 m diameter driven into the very dense sand at Ras Tanajib Field, and based on which a new procedure was developed to determine the capacity of piles driven into dense sand. The engineering design parameters of this method is summarised in Table 1.

Table 1: Design parameters, Ras Tanajib Method [36]

Soil Type	Silt content %	Carbonate content %	q_c (MPa)	∅ (deg.)	K	f_{max} (kPa)	N_q	q_{max} (MPa)
Medium dense sand and silty sand	< 25	< 20	4 – 12	30	0.8	100	20	10
Very dense sand and silty sand	< 25	< 20	> 12	35	0.8	150	40	12
Very dense, overconsolidated sand and silty sand	< 25	< 20	> 40	40	1.0	200	70	15

Imperial College Pile (ICP) Approach

The ICP design methods for estimating axial capacity of piles driven in sand and clays were the outcomes of an extensive research conducted by Imperial College London between 1980 and 2005 [37] to obtain a better understanding of pile behaviour. Tests were performed at six fields in the UK and France where wide range of soil conditions was covered. Jardine et al. [38] and Lehane et al. [39] presented pile load test database studies that demonstrated the reliability and accuracy of the ICP approach over other traditional design methods. Using ICP methods requires some essential geotechnical parameters to be available such as:

- Continuous profiles of CPT / PCPT tip resistance;
- Soil-steel interface friction angles for sand and clay determined from ring shear tests;
- Yield stress ratio in case of clays determined from in situ tests (e.g. CPTs or field vane tests) or laboratory tests (e.g. triaxial or oedometer tests);

- Sensitivity of clay achieved in laboratory either by oedometer test or undrained triaxial test on undisturbed and remoulded samples.

Additionally, other routinely measured properties in well-planned site investigation and characterisation studies are also required. Typical examples of these properties are: Atterberg limits, unit weights, gradation curves, and water contents alongside a record of the groundwater table fluctuation.

Jardine et al. [37] provided an overview of the ICP design methods together with an experience-based guidance on their application by reference to 40 turbines founded on large diameter steel piles for the North Sea Borkum West II wind farm project. The authors reported some key conclusions, a summary of which is as follows:

- The effective stress based ICP methods yield more reliable pile design in terms of axial capacity predictions than traditional methods.
- Important phenomena such as aging and cyclic loading effects are often neglected in conventional design methods. ICP approach addresses such phenomena and loading conditions which makes it advantageous.

2.5 Marine Calcareous / Carbonate Sand

Three types of sediments are predominately covering the sea floor: brown clays, siliceous soils, and calcareous soils [40]. The latter soil types are formed from the skeletons of micro-organisms in the sea. Upon the death of these creatures, their skeletons which are composed mainly of calcium carbonate slowly sink into the sea to settle eventually on the sea floor,

and build into thick layers over millennia allowing the calcium carbonate to dissolve slowly in the seawater [3], [40]. The experience of dealing with calcareous sediments while piling can be traced back to the mid 1960's in the Arabian Gulf. Open-ended piles which were designed in accordance with pure end-bearing or drilled and grouted solutions, were noticed to free fall through uncemented carbonate sands [20].

The term 'calcareous' means "containing calcium carbonate". The term 'carbonate' is usually taken to mean "containing over 50% by weight of calcium carbonate". The 'carbonate compensation depth' (CCD) is the water depth below which the rate of dissolution of calcium carbonate exceeds the rate of supply of carbonate materials. The magnitude of CCD depth depends on temperature and other factors; although, 3.5 – 5 Km is a typical range [3]. It is not possible for the carbonate soil deposits to form below the CCD; nonetheless, events such as flowslides can transport them to such depths. These carbonate soils can have very complicated shapes and are soft in comparison with siliceous soils. An electron photomicrograph of a calcareous sand is shown in Figure 3. Commonly, sea sediments that are formed from the organic remains of the ocean life are termed oozes [40].

Through much of the warmer seas of the world, calcareous sands exist—for instance, they are observed along the south and west coasts of Australia, and offshore of Brazil.

Typical calcareous sands give relatively high friction angles when tested in laboratory; notwithstanding, they exhibit field behaviour that is significantly different from sands.

It is worth mentioning that great bearing values can be developed; however, immense deformation is associated. Furthermore, friction on piling can reach almost zero. Virtually,

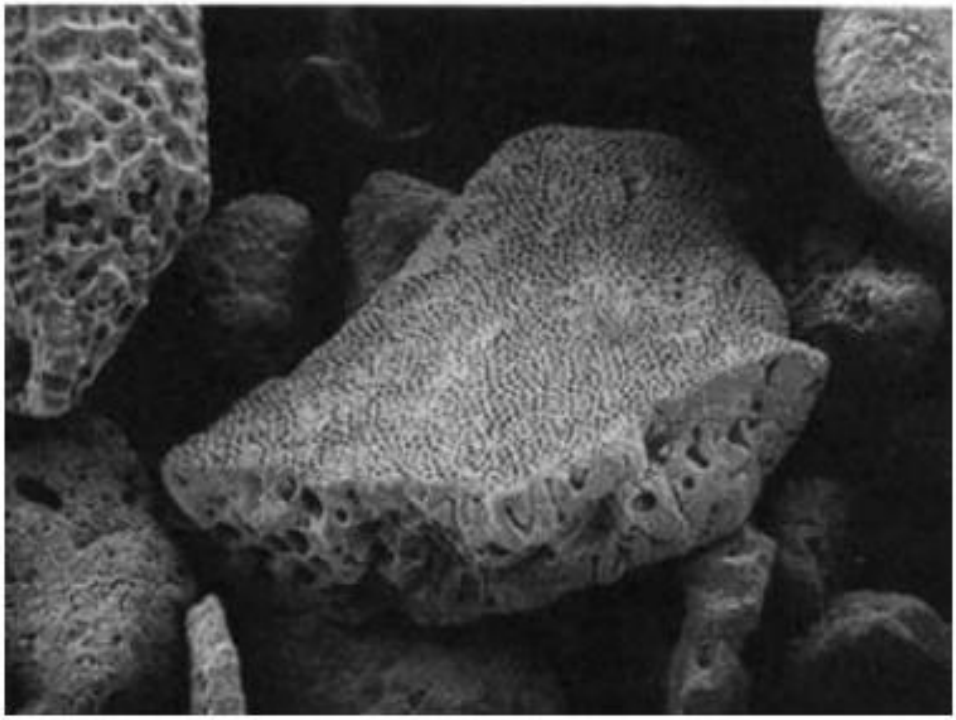

Figure 3: Electron photomicrograph of calcareous sand from Guam. Magnification is 45 × [55]

the shells exert no effective pressure against the wall of the pile due to their high crushability. As a result, advancing the pile through hammering can get very easy; nonetheless, the pile would develop low uplifting capacity. Gerwick [41] reported that in an extreme case in which the force required to pull a pile driven 60 m into these calcareous sands was measured slightly higher than the pile weight. Calcareous sands that have no cementation are relatively impermeable, and thus liquefaction is a potential concern [41].

Golightly [20] conducted a comprehensive study on four carbonate sands: a skeletal molluscan sand in an uncemented and artificially cemented state, a coralline sand, a mixed skeletal/oolitic sand, and an algal sand. Through investigating the basic grain properties alongside a mineralogical and microscopic study he concluded that the densities and strengths of particle of carbonate sands are quite low, while they have very high surface areas and particle angularities, when compared to non-carbonate sands. Also, there is intraparticle porosity present in skeletal sands. Furthermore, based upon laboratory test programme for evaluating the strength and stiffness for each type in the dense state, he concluded that uncemented carbonate sands exhibit the following:

- High compressibility;
- A curved failure envelope at very low stress levels;
- Strong volumetric contraction due to low density and susceptibility to particle crushing;
- High positive pore pressure generation when sheared undrained;
- A steady state in void ratio / mean effective stress space which differs considerably from that of silica sand;
- Low stiffness; and
- Low strength in constant volume direct shear tests.

The behaviour of the oolitic non-skeletal sand is intermediate between the silica and skeletal carbonate sands.

Parameters derived from the testing programme were used in a cavity expansion model to predict pile limit end-bearing values of less than 3 MPa. Rigidity indices are very low, and decrease rapidly with depth.

A load transfer analysis is developed which predicts low values of pile limit skin friction similar to those found from a back-analysis of field and model tests in carbonate sands.

Several case histories have been reported that describe some of the unusual characteristics of foundations on carbonate soils and their often poor performance. It has been shown from numerous pile load tests that piles driven into weakly cemented and compressible carbonate sands and silts mobilise only a fraction of the capacity (as low as 15 %) predicted by conventional design and/or prediction methods for siliceous material [1].

For sands containing greater amounts of carbonate than that of siliceous soils (i.e., more than 20%), the unit skin friction and end bearing resistance are calculated based on Kolk, [42] recommended method:

For sands comprising carbonate content ranging between 20 and 80%:

- the unit skin friction is calculated based on the unit skin friction of a siliceous sand of same relative density and on the unit skin friction calculated for a carbonate sand (carbonate content > 80%, $K\tan\delta = 0.14$ and $f_{lim} = 15$ kPa);
- the limiting end bearing is calculated based on the limiting unit end bearing of a siliceous sand of same relative density and on the limiting unit end bearing defined for a carbonate sand ($q_{lim} = 3$ MPa).

2.5.1 Typical Geotechnical Profiles

The purpose of marine geotechnical investigations is to acquire detailed information on the sub seabed soil condition and the geotechnical properties at each of these soils' localities. This is to enable engineering analyses to be performed in a more reliable way, for a number of purposes such as selection of design soil parameters, estimation of pile capacity, estimation of axial and lateral load deflection of piles, evaluation of mudmat bearing capacity, etc. Offshore geotechnical reports present not only field (boreholes) data, but also necessary onshore laboratory testing results (e.g., water contents, density, carbonate content, undrained shear strength, etc.). Data are presented in graphical and tabular forms, and as logs as can be seen in Figures 4 to 8. The figures show typical geotechnical profiles in U offshore field in the Arabian Gulf which contains calcareous sand and clay layers.

Objectives of dynamic pile monitoring typically include calculation of pile driving stresses, monitoring of the hammer and driving system performance, and evaluation of pile capacity. Further analyses of static pile capacity are usually completed using the CAPWAP computer program.

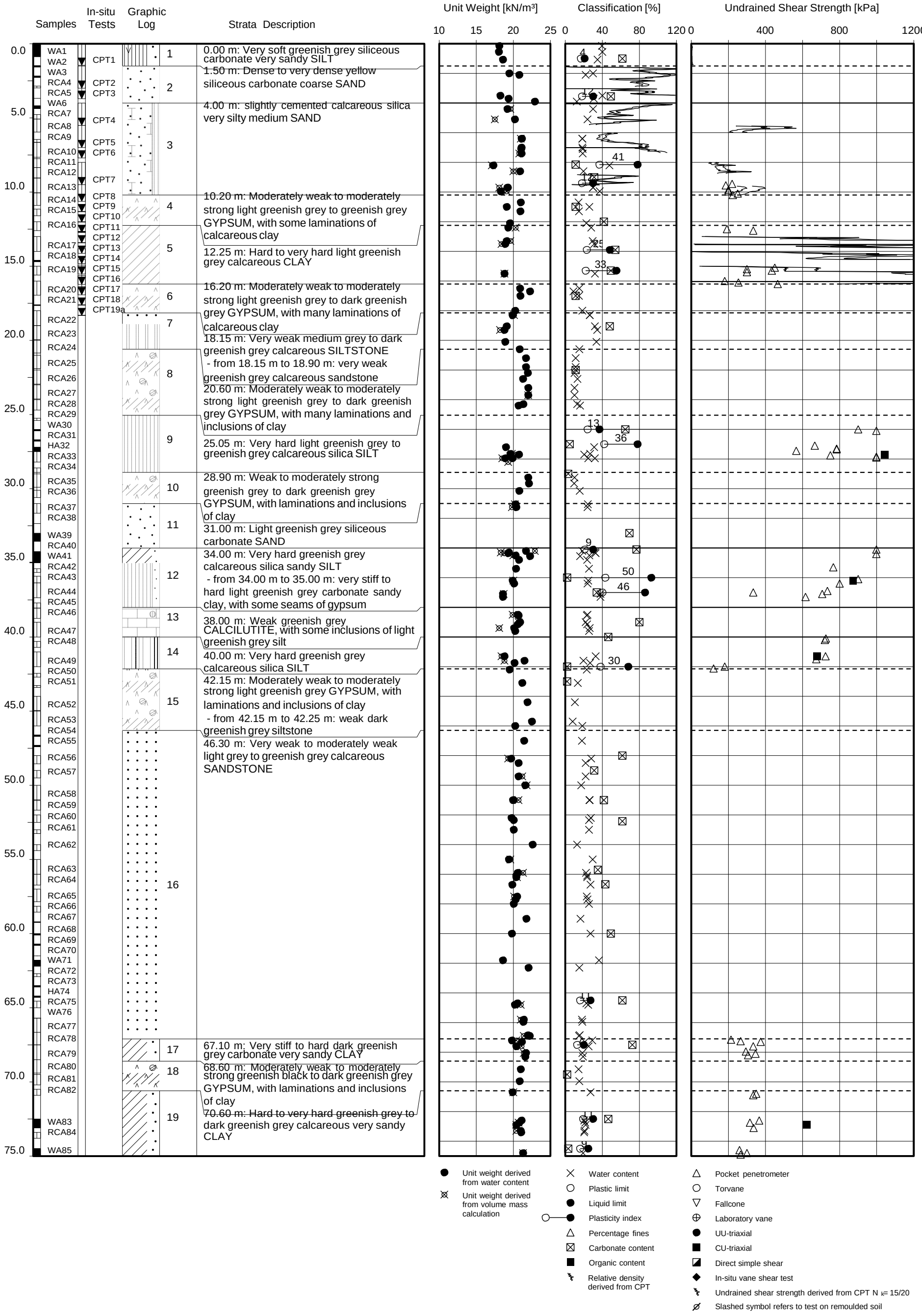

Figure 4: Typical geotechnical profile of soil at U offshore field, The Arabian Gulf [44]

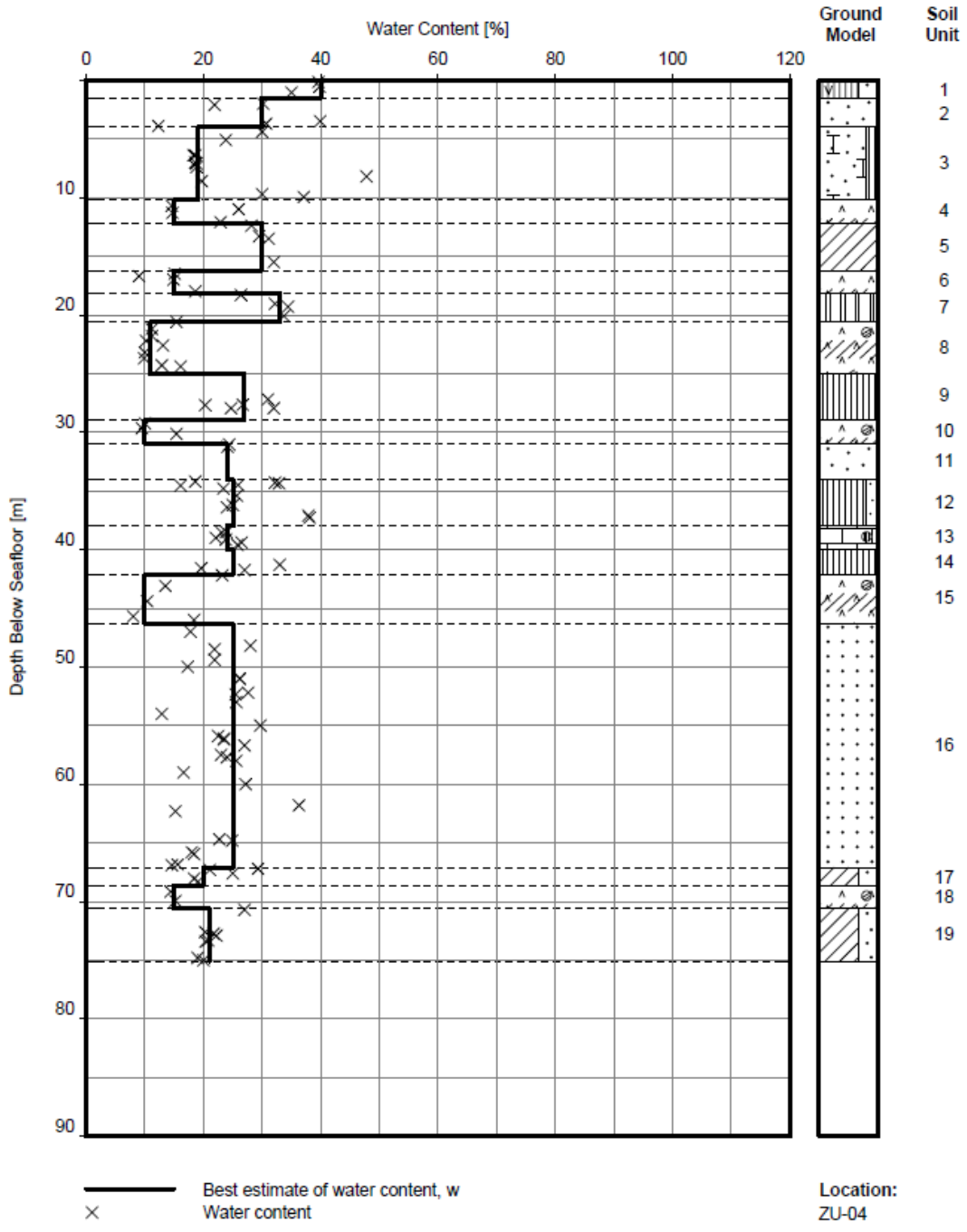

Figure 5: Water content versus depth, U field, The Arabian Gulf [43]

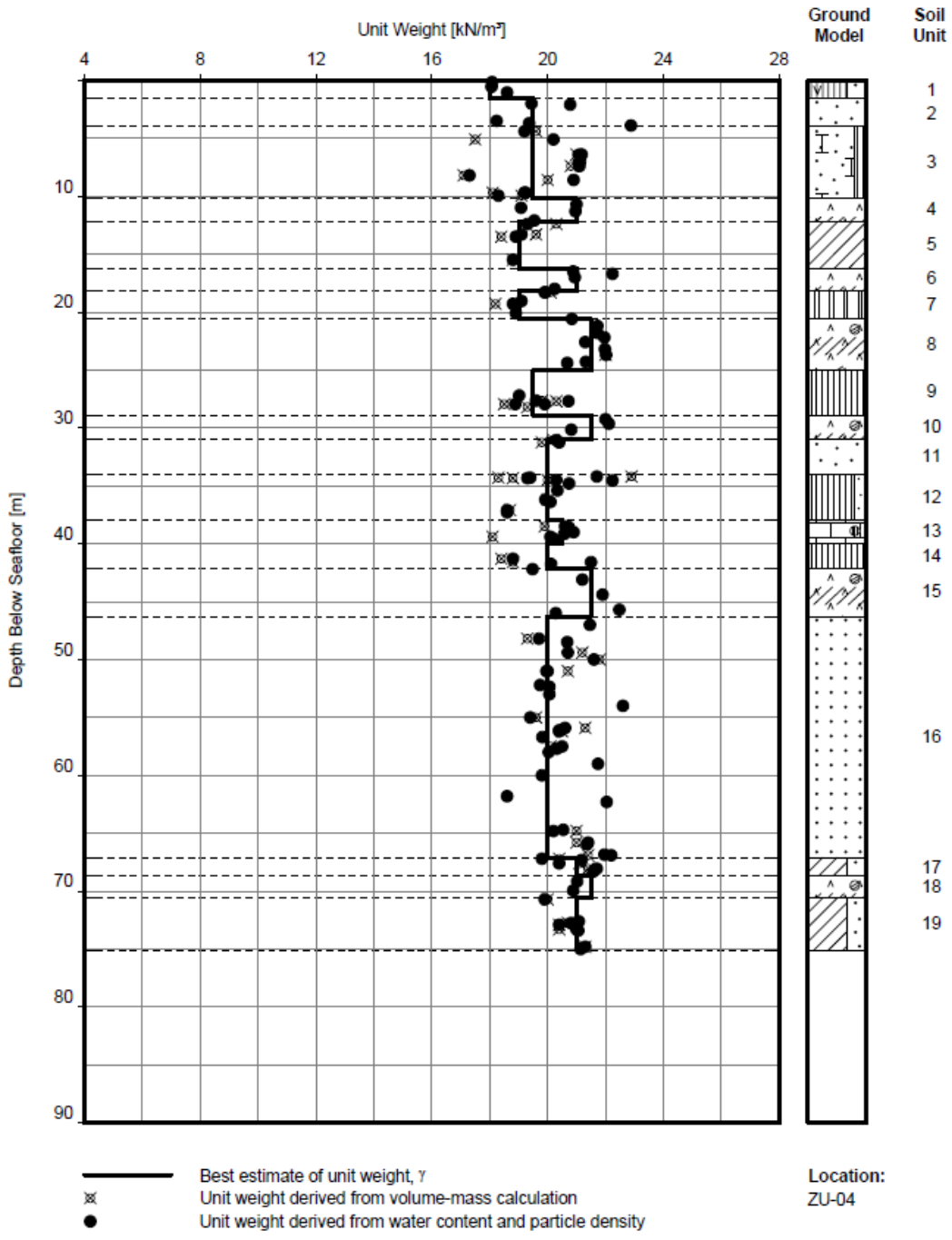

Figure 6: Unit weight versus depth, U field, The Arabian Gulf [43]

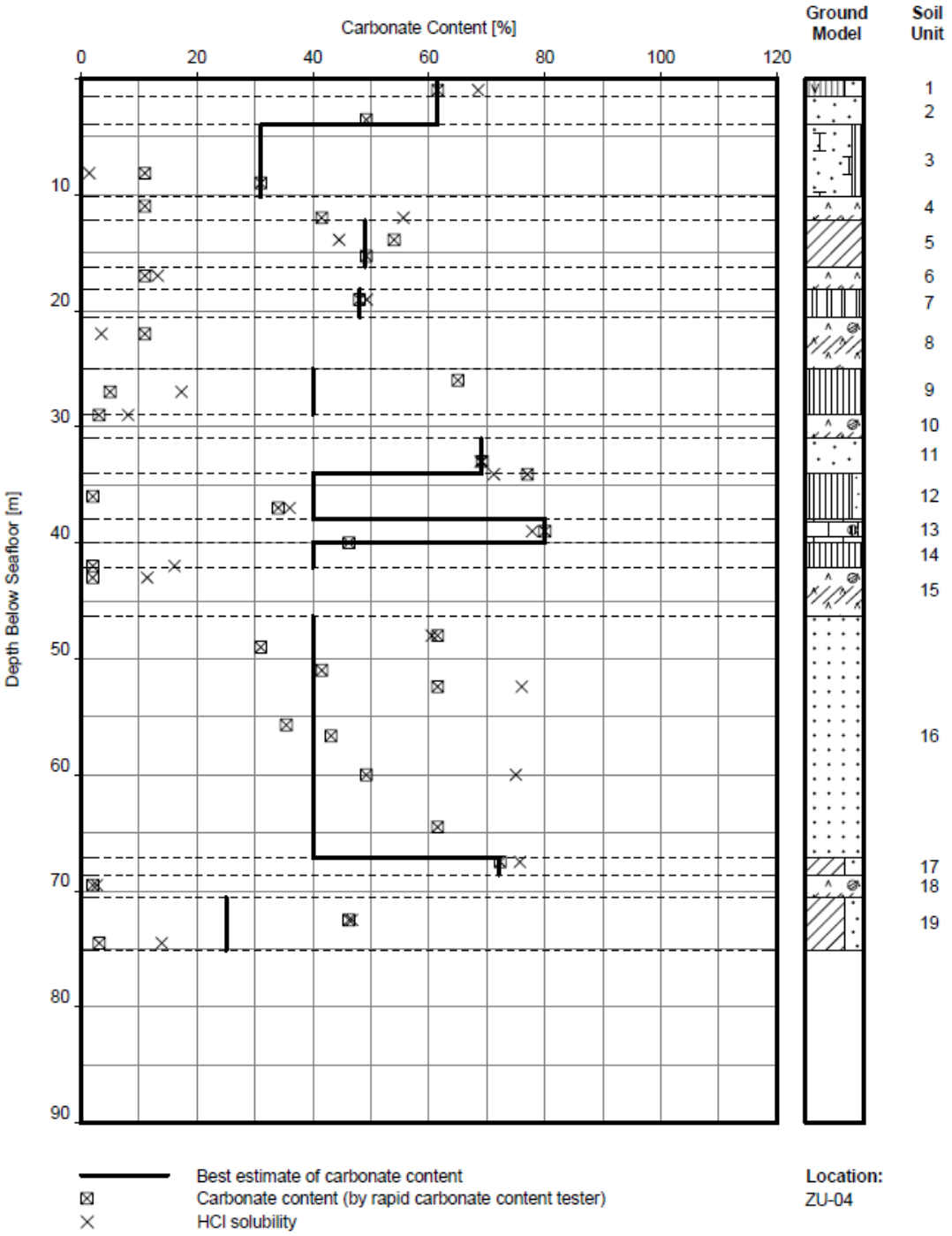

Figure 7: Carbonate content versus depth, U field, The Arabia Gulf [43]

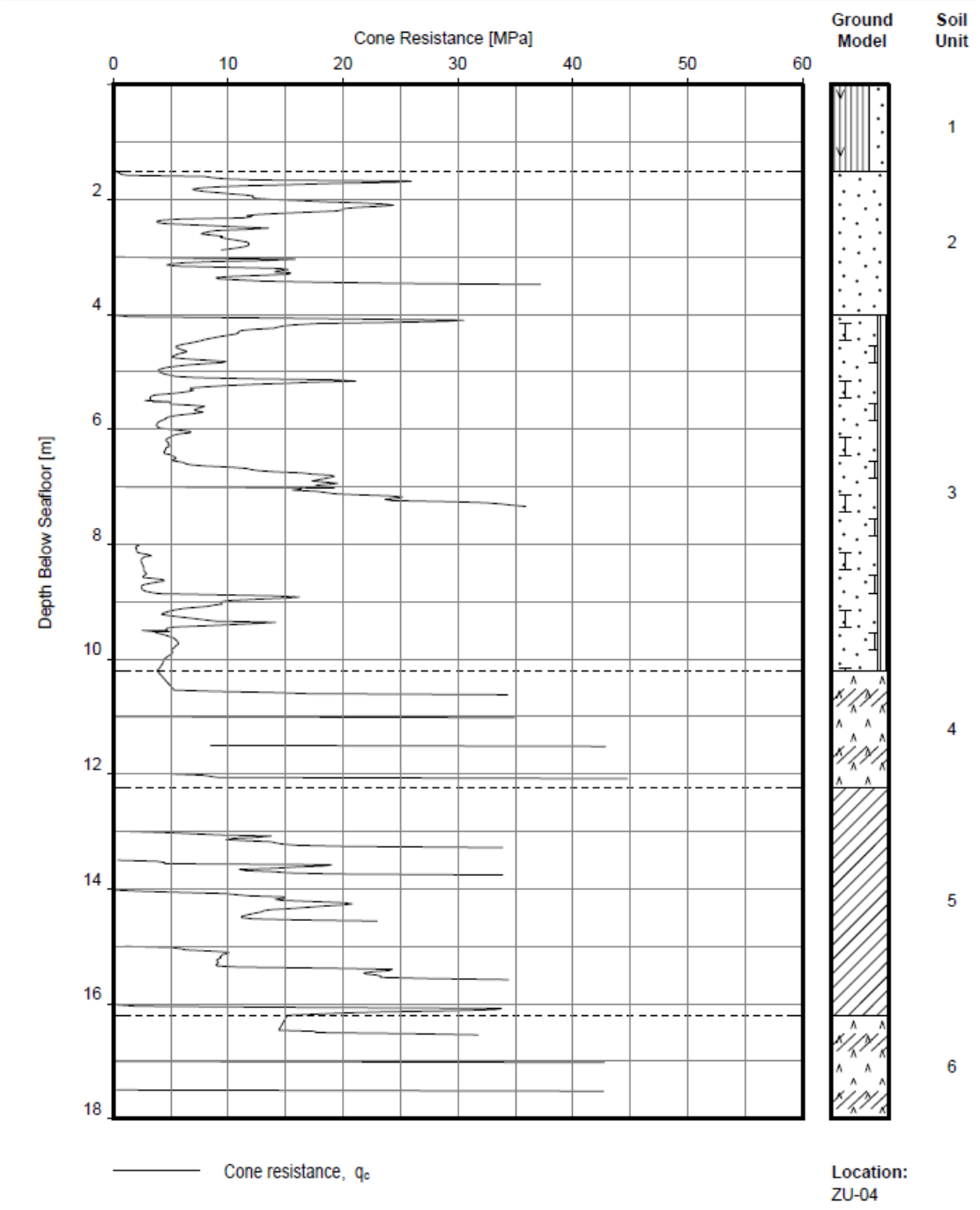

Figure 8: Cone resistance versus depth, U field, The Arabian Gulf [43]

2.5.2 Classification of Calcareous sediments

A number of systems that describe and classify calcareous sediments have been developed over the years by many researchers. Some of these systems are still being used by geotechnical engineers and sedimentary petrologists. This section briefly outlines the most commonly used classification systems for calcareous sediments.

Fookes and Higginbotham [44] developed a system that relies mainly on parameters such as grain size and post-depositional induration; although, the system takes into account the importance of other parameters like strength and mineral composition.

Clark and Walker [45] expanded the system developed by Fookes and Higginbotham to cover the entire materials range between total carbonate and total non-carbonate. The system uses three parameters for classifying the materials namely, grain size, carbonate content, and strength. In order to avoid confusion with mixed or non-carbonate materials, the authors proposed the use of new terms namely ‘cacilutite’, ‘calcarenite’, and ‘calcirudite’ instead of previous ones such as ‘carbonate claystone’, ‘carbonate siltstone’, etc. The remaining constituents between 50 – 90% carbonate content are described as ‘siliceous’. Further, the term ‘calcareous’ has been used to define the general carbonate presence below the 50% carbonate line when there is uncertainty identifying the specific carbonate type.

King et al. [46] developed a system based on Clark and Walker’s work. The authors quantified the degree of cementation/induration on the basis of cone penetration resistance. Their system has been widely adopted by geotechnical engineers for use in identifying and

describing materials in the Middle East. Nonetheless, it has some shortcomings, specifically, when it comes to description of uncemented skeletal calcareous sands [20].

A system of description as opposed to a classification system has been proposed by Datta et al. [47]. This system aimed to further describe the degree of uniformity of cementation and the propensity of constituent particles for crushing.

Golightly [20] proposed a modified classification system based on Clark and Walker system. The author described the constituent material in a more thorough manner. His system also suggests that the nature and extent of cementation should be determined qualitatively, and moreover the mineralogy of the sediment should be determined as it influences the sediments susceptibility to undergo chemical alteration. The system also proposes the use of intra-particle porosity to further define the crushability.

A summary of the previously discussed classification systems for calcareous sediments is shown in Table 2.

2.5.3 Crushing of Calcareous Sands

Several researchers have proposed different methods to quantitatively express the degree of crushing. Lee and Farhoomand [48] investigated the crushing of granular material under anisotropic compression. The authors proposed a "relative crushing" parameter defined by $\frac{(D_{15})_i}{(D_{15})_a}$, where $(D_{15})_i$ is the diameter through which 15% of the original material particles pass and $(D_{15})_a$ is the diameter through which 15% of particles pass after undergoing anisotropic compression. The degree of crushing has been quantitatively been expressed by Ramamurthy and Lal [49] as the area between the grain size distribution curves of sand

Table 2: Summary of calcareous soil classification systems

System	Year	Main parameters
Fookes and Higginbotham [44]	1975	• Grain size • Post-depositional induration
Clark and Walker [45]	1977	• Grain size • Carbonate content • Strength
King et al. [46]	1980	• Grain size • Name of base material • Degree of induration or cementation • Bedding and lamination • Origin of carbonate • Colour and minor fractions
Golightly [20]	1988	• Colour • Strength • Origin • Particle composition • Grain size and shape • Nature and extent of cementation • Mineralogy • Intraparticle porosity • Minimum void ratio

before and after it has been subjected to shear. Datta et al. [50] suggested expressing the magnitude of crushing by means of a crushing coefficient C_c which is defined as $\frac{(D_{10})_i}{(D_{10})_a}$, where:

$(D_{10})_i$ is the percentage of particles of the sand after being subjected to stress finer than D_{10} of the original sand, and $(D_{10})_a$ is the percentage of particles of the original sand finer than D_{10} of the original sand.

Miao and Airey [51] studied the difference between particle breakage of carbonate sand caused by one-dimensional compression test and ring shear test. The authors discussed the void collapse, grading properties and particle shape evolution. They concluded that

compression and shear produce basically different mechanism of breakage and reported that changes breakage induced by shear was more predominant than that caused by compression in agreement with what Datta et al.[50] have also confirmed.

Several case histories were reported in the literature that demonstrate how troublesome calcareous soils are. The engineers involved in the petroleum industry working offshore Australian coasts, both Bass Strait and the Northern Shelf, were unwelcomely surprised. Notwithstanding, the high angle of internal friction they could measure for the calcareous sand, very small skin frictional resistance was observed. Unfortunately, earlier geotechnical investigations did not reveal this behaviour. Samples had the same superficial look as if they were conventional sand. The drillers on the Kingfish platform in Bass Strait were the first to encounter the surprise, when they attached a hold-down line to a 50.8 cm diameter steel conductor casing. The conductor casing exhibited absolutely no resistance other than its own weight when pulled out. The design engineers soon adopted some measures to maintain the safety of the platform's piles during storm events. Primarily, a drilling was made down inside the existing pin piles, a concrete plug was placed, and the lower end of the pile was filled with high-density iron sand [52].

Similar serious problem was encountered a few years later at the North Rankin platform on the Northwest Shelf. Dense sand with angle of internal friction of 38° had been discovered by the geotechnical borings. This called for using the largest possible pile hammer to drive the steel pipe piles to the designed depth of 260 m. But when the hammering process began, the driving resistance was of order of 1 – 5 blows/m. The pipe pile was likened to a cookie cutter" cutting through the soil. The reason had been explained later by performing extensive geotechnical investigations including microscopic

examination. The microscopic results showed the tiny diatom shells which comprise these calcareous sediments [52].

CHAPTER 3

RESEARCH METHODOLOGY

3.1 General

This chapter presents details of the methodology and work tasks performed to fulfil the objective of the research. Basically, the work is divided into two main parts namely, analytical and experimental. The analytical part involves collecting, organising, and compiling field data and its preparation for calculation stage. This part also includes performing back-calculation of soil parameters and further statistically analysing these parameters. On the other hand, the experimental programme involves investigating the degree of crushing of marine carbonate sand samples collected from different offshore locations in the Arabian Gulf, and compare that with crushing potential of quartz sand, in attempt to explain the reduced shaft friction values of the piles that penetrate these soils.

3.2 Collecting, Organising, and Compiling Analysis Data

Early stages of this research involved communications with the Consulting Services Department (CSD) of Saudi ARAMCO to obtain relevant engineering data for offshore platforms installed in different locations within the Arabian Gulf, to be used for analysis and evaluation purposes. Engineering database used in this research was compiled from

multitude of offshore geotechnical investigation and dynamic pile monitoring reports provided by Saudi ARAMCO.

The data acquisition stage in this research has involved collecting over 100 offshore geotechnical investigation and dynamic pile monitoring reports (DMS) between 1984 and 2016. These reports cover a number of marine platforms installed at 5 major fields within the Arabian Gulf. The author is not authorised to disclose the real names of these fields. Hence, they are referred to by the following letters namely, F, J, N, U, and Y. The reports have been classified based on their date and further named according to the specific platform project they are issued for (e.g., F-10, J-1, etc.). Only those reports issued after the last Millennium were considered. Table 3 shows a summary of these reports and their relevant details.

Each geotechnical investigation report prepared for a specific platform project at any of the offshore field named above, has a corresponding dynamic pile monitoring report for the same platform and location as can be noticed in Table 3. General practice is that pile capacity is estimated based on geotechnical investigations and in accordance with API standard recommendations, and when the pile is being driven in the field, the capacity is also measured using PDA and CAPWAP (DMS) in order to be compared with that of API and geotechnical reports as a way of check and evaluation. Should the DMS capacity record a smaller number than that of API, a larger penetration or any other proper adjustment may be required which translates into cost and time.

The state of stress of soil surrounding a pile changes dramatically while driving. Therefore,

Table 3: Details of marine geotechnical investigation and dynamic pile monitoring reports which data are compiled from

Sr.	Field	Platform	Report type	Year	Issuing company	Report type	Year	Issuing company
1	N	N-1	O.G.I.R[1]	2016	HSC	DMS[2]	2010	GRL Engineers
2	F	F-1	O.G.I.R	2014	HSC	DMS	2015	GRL Engineers
3	F	F-2	O.G.I.R	2014	HSC	DMS	2015	GRL Engineers
4	F	F-3	O.G.I.R	2014	HSC	DMS	2015	GRL Engineers
5	F	F-4	O.G.I.R	2015	HSC	DMS	2015	GRL Engineers
6	F	F-5	O.G.I.R	2014	Fugro	DMS	2014	GRL Engineers
7	F	F-6	O.G.I.R	2014	HSC	DMS	2015	GRL Engineers
8	F	F-7	O.G.I.R	2014	HSC	DMS	2014	GRL Engineers
9	F	F-8	O.G.I.R	2007	OEO	DMS	2009	GRL Engineers
10	F	F-9	O.G.I.R	2007	OEO	DMS	2008	GRL Engineers
11	F	F-10	O.G.I.R	2007	OEO	DMS	2009	GRL Engineers
12	F	F-11	O.G.I.R	2007	OEO	DMS	2009	GRL Engineers
13	F	F-12	O.G.I.R	2007	OEO	DMS	2008	GRL Engineers
14	F	F-13	O.G.I.R	2007	OEO	DMS	2008	GRL Engineers
15	J	J-1	O.G.I.R	2014	FSME	DMS	2015	GRL Engineers
16	J	J-2	O.G.I.R	2012	Fugro	DMS	2015	GRL Engineers
17	J	J-3	O.G.I.R	2013	HSC	DMS	2015	GRL Engineers
18	J	J-4	O.G.I.R	2014	FSME	DMS	2015	GRL Engineers
19	Y	Y-1	O.G.I.R	2014	HSC	DMS	2014	GRL Engineers
20	Y	Y-2	O.G.I.R	2013	HSC	DMS	2014	GRL Engineers

Table 3 continued

21	Y	Y-3	O.G.I.R	2014	Fugro	DMS	2014	GRL Engineers
22	Y	Y-4	O.G.I.R	2005	RGME	DMS	2006	GRL Engineers
23	Y	Y-5	O.G.I.R	2007	Fugro	DMS	2009	GRL Engineers
24	Y	Y-6	O.G.I.R	2007	Fugro	DMS	2009	GRL Engineers
25	Y	Y-7	O.G.I.R	2007	Fugro	DMS	2009	GRL Engineers
26	Y	Y-8	O.G.I.R	2008	Fugro	DMS	2009	GRL Engineers
27	Y	Y-9	O.G.I.R	2008	Fugro	DMS	2009	GRL Engineers
28	Y	Y-10	O.G.I.R	2009	Fugro	DMS	2014	GRL Engineers
29	Y	Y-11	O.G.I.R	2007	Fugro	DMS	2009	GRL Engineers
30	U	U-1	O.G.I.R	2005	RGME	DMS	2009	GRL Engineers
31	U	U-2	O.G.I.R	2007	Fugro	DMS	2009	GRL Engineers
32	U	U-3	O.G.I.R	2007	Fugro	DMS	2008	GRL Engineers
33	U	U-4	O.G.I.R	2007	Fugro	DMS	2009	GRL Engineers
34	U	U-5	O.G.I.R	2008	Fugro	DMS	2010	GRL Engineers
35	U	U-6	O.G.I.R	2008	Fugro	DMS	2010	GRL Engineers
36	U	U-7	O.G.I.R	2013	HSC	DMS	2015	GRL Engineers

[1] O.G.I.R stands for Offshore Geotechnical Investigation Report

[2] DMS stands for Dynamic Monitoring System (dynamic pile monitoring report)

restrikes are often implemented after initial installation (typically 12 hours) to assess the long-term changes in the pile bearing capacity, due to time-dependent changes in soil strength.

Blow count during restrike often referred to as beginning of restrike (BOR), is always compared to that of the end of initial driving (EOD) so as to evaluate pile behaviour over time.

Consequently, necessary relevant information and details of all piles which restrike was performed on have been compiled in Excel files having the same name of the platform project as shown earlier in Table 3. Examples of such details are pile outside diameter, total capacity, factors of safety, blow count, and waiting time of restrike. The tables in the Appendix illustrate a summary of these details. Blow counts are always reported per 0.25 m or per 1 m. When the penetration is less than 0.25 m, it is reported in units of cm to specifically show that it did not penetrate by 0.25 m. For the sake of simplifying compiled data for later use, all values were converted to per 0.25 m and reported that way. Piles are divided into segments typically 2 m long each, and shaft friction values corresponding to each segment at a certain depth below the grade are also reported in kN and kPa and labelled "SF_{DMS}" as shown in the tables in the Appendix. At the other end of the spectrum, shaft friction values from the geotechnical reports (labelled SF_{API}) are also tabulated alongside other relevant details and parameters that correspond to the soil layer within which a pile segment lies and DMS measurements were taken.

3.3 Back-Calculation of Soil Parameters

3.3.1 General

Setup value is calculated for each pile by dividing the ultimate capacity at the beginning of restrike by that at the end of initial driving as the following equation shows:

$$\text{Setup} = \frac{(Q_c)_{BOR}}{(Q_c)_{EOD}} \tag{3.1}$$

For example, the ultimate capacity for the pile at location F-1 was measured as 8.4 MN at the end of initial drive (EOD), and 10.1 MN at the beginning of restrike/redrive. So, the setup is $\frac{10.1}{8.4} = 1.2$. The waiting time before restrike was 12 hours for this pile as shown in Table A-1 in the Appendix.

All tables in the Appendix were organised in such a way that details and information collected from both DMS and geotechnical reports are segregated under three main titles namely, general information and specifics, sand layers' information, and clay layers' information.

3.3.2 Clay

The α-factor is the main parameter for evaluating the reliability of pile capacities driven in clay, and estimated as per API RP 2Geo recommendations. This factor is back-calculated for each clay layer using equations 2.7 and 2.8 and referred to as "α_{API}". On the other hand, the counterpart "α_{DMS}" is determined simply by dividing the shaft friction - reported in stress units - of a particular clay layer measured by PDA and CAPWAP by the undrained cohesion of that layer, as in the following equation:

$$\alpha_{DMS} = \frac{SF_{DMS}}{s_u} \tag{3.2}$$

Several factors are involved in the back-calculation of α_{API} employing equations 2.7 and 2.8 including the submerged unit weight of the soil stratum, and the calculated effective vertical stress at the corresponding depth, z. The submerged unit weight is computed by averaging out unit weight values reported at different depth increments in the geotechnical reports. The final value is then used to calculate the effective stress. This procedure, and considering the potential inaccuracy of the reported numbers of soil unit weight, resulted in a slight discrepancy between α_{API} back-calculated by equations 2.7 and 2.8 and the one estimated by directly dividing shaft friction by undrained cohesion and named $\alpha_{API\,2}$ as indicated in equation 3.3 below:

$$\alpha_{API\,2} = \frac{f(z)}{s_u} \tag{3.3}$$

The values obtained from equation 3.3 were compared with α_{API} values to check their accuracy. The $\alpha_{API\,2}$ values are considered whenever there is a noticeable discrepancy in numbers.

Compiled clay layers from all offshore fields are classified based on their OCR value into three categories; OCR = 1, $1 < OCR \leq 4.0$, and OCR > 4.0. The equation used to calculate OCR is given below [53]:

$$\frac{s_u}{p_0'(z)} = 0.24\ OCR^{1.1} \tag{3.4}$$

Holtz and Kovacs [54], and Mitchel and Saga [55] reported similar relationships between OCR and $\frac{s_u}{p_0'(z)}$.

3.3.3 Sand

As for sand layers, the evaluation process is done directly through shaft friction. Skin friction was presented in form of plots in most geotechnical reports adopted. Accordingly, a useful tool, namely PlotDigitizer was employed to digitise the curves on the plots and extract values from them. Further, a cubic spline interpolation function embedded in Excel was used to attain shaft friction values at the required depths.

Sand layers are categorised into very loose, loose, medium dense, dense, and very dense using the BS5930 [56] relationship given in Table 4 below and according to their relative density, which in turn is estimated by the following correlation with cone tip resistance [57]:

$$D_r = \frac{1}{2.93} \ln\left[\frac{q_c}{205\left(p_0'(z)\left(\frac{1+2K_0}{3}\right)\right)^{0.51}}\right] \quad (3.5)$$

where, D_r: relative density of the sand layer

q_c: cone tip resistance

K_0: coefficient of lateral earth pressure at rest

Whenever there was a borderline case, for instance MD to D, or L to MD the angle of internal friction, ∅ was sought and used to correlate the value of D_r as per Peck et al. [58] (see Table 4).

Sands are also subdivided into three categories according to their carbonate content ($CaCO_3$) as follows:

- Carbonate sands ($CaCO_3 > 80\%$)
- Calcareous sands ($20\% < CaCO_3 \leq 80\%$)
- Silica sands ($CaCO_3 < 20\%$)

This is the standard classification adopted in the geotechnical reports; nonetheless, for simplicity all sand layers with $CaCO_3 \geq 50\%$ were classified as carbonate, otherwise, they were considered silica sand.

It is important to draw attention to that a number of thick layers of clay and sand (e.g., more than 6 m thick) was encountered in some fields, and as the DMS capacity is usually measured every 2 metres, several values are reported within the same soil layer. These values are averaged out to obtain a single value for the sake of analysis and comparison with API capacity.

Table 4: Relative density classes [56], [58]

Density Classification	$\mathbf{D_r}$ (%)	**Ø (deg.)**
Very Loose (VL)	< 20	< 29
Loose (L)	20 – 40	29 – 30
Medium Dense to Dense (MD)	40 – 60	30 – 36
Dense (D)	60 – 80	36 – 41
Very Dense (VD)	> 80	> 41

3.4 Statistical Analysis

The relationship between the α-factors of DMS and API in case of clay, and shaft frictions in sand is plotted for each clay and sand category. The best-fit line is drawn and the correlation coefficient (R^2) is determined. The degree of the overconservatism expressed as a factor is determined denoted by the ratio of the slope of the best-fit line to the average line. At this stage a statistical nonparametric test is carried out on the compiled data using Minitab 17 to evaluate the difference between the calculated and measured capacities by API standard and DMS, respectively. As stated earlier in this chapter, the factor considered for capacity evaluation in clay layers is the back-calculated α, while statistical analysis is conducted directly on shaft friction in case of sand. The estimated difference in these design parameters is then utilised to adjust the API capacity, and subsequently suggest an adjusted or enhanced overconservative factor denoted by the ratio of the newly constructed best-fit line to the average line.

3.5 Experimental Work

This section discusses an experimental program intended to evaluate the crushability of some calcareous sand samples of the Arabian Gulf.

It is well-established that sands undergo particle crushing under stresses at high confinement. Stresses in the soil induced by pile driving process for marine platforms often reach magnitudes where particle crushing becomes a major concern. The crushing effect is even more predominant when pile is penetrating through calcareous sands. This is due to

either the presence of intraparticle voids that increase their crushing tendency under stresses and/or the presence of thin plate-like shell fragments which further increases their vulnerability.

3.5.1 Calcareous Sand Samples

A total number of 7 calcareous sand samples were obtained from Fugro-Suhaimi Limited. These samples were collected from different locations in the Arabian Gulf. Table 5 shows a summary of these samples and some of their relevant details.

Table 5: A summary of some relevant details of calcareous sand samples tested

Sample ID	Depth (m)	$CaCO_3$ (%)	W.C. (%)	Min. dry density (g/cm^3)	G_s
AB-1	14.5	81.8	23.34	1.474	2.67
AB-2	9.5	75.4	18.13	1.445	2.64
AB-3	27.0	73.8	11.35	1.861	2.62
AB-4	10.5	75.4	1.44	1.756	2.64
AB-5	7.1	87.3	20.97	1.643	2.67
AB-6	6.0 – 6.4	67.7	23.19	1.379	2.68
AB-7	4.0 – 4.3	81.8	18.05	1.478	2.68

3.5.2 Programme of Testing the Samples

Sieve analysis is performed on each sample before crushing. All crushing tests are carried out for a selected portion consisting of the coarse particles sized 0.425 – 2 mm to allow for large particle breakage and ease observing the crushing effect on soil gradation.

A one-dimensional compression cylinder test is conducted on the seven samples having the same grading using the oedometer ring having a diameter of 68.7 mm and height of 20 mm. Each soil sample is placed loosely in the ring and compacted by slightly tapping on it, and then loaded under a constant displacement rate of 1.3 mm/min. All samples are compressed to a maximum load of about 10 kN which translates approximately into 2700 kPa, and the stress-deformation behaviour is observed. This value is selected based on the maximum value of the earlier calculated effective overburden pressure at the piles tip, $p'_{0,\ tip}$ at each offshore field as summarised in the Appendix to simulate the stress state in the calcareous sand at these locations. The maximum vertical stress is found to be 1428.0 kPa, at a depth of penetration equal to 68.0 m below the mudline, for the Y-10 platform. Figures 9 and 10 show samples preparation stage while Figure 11 shows the compression test setup.

Post-test samples are sieved again to assess the gradation evolution. SEM and XRD are used to identify the constituent minerals and compounds of the calcareous sand. For comparison purpose, quartzitic silica sand sample of similar gradation is also tested.

Figure 9: Initial sieve analysis during preparation stage for calcareous sand samples

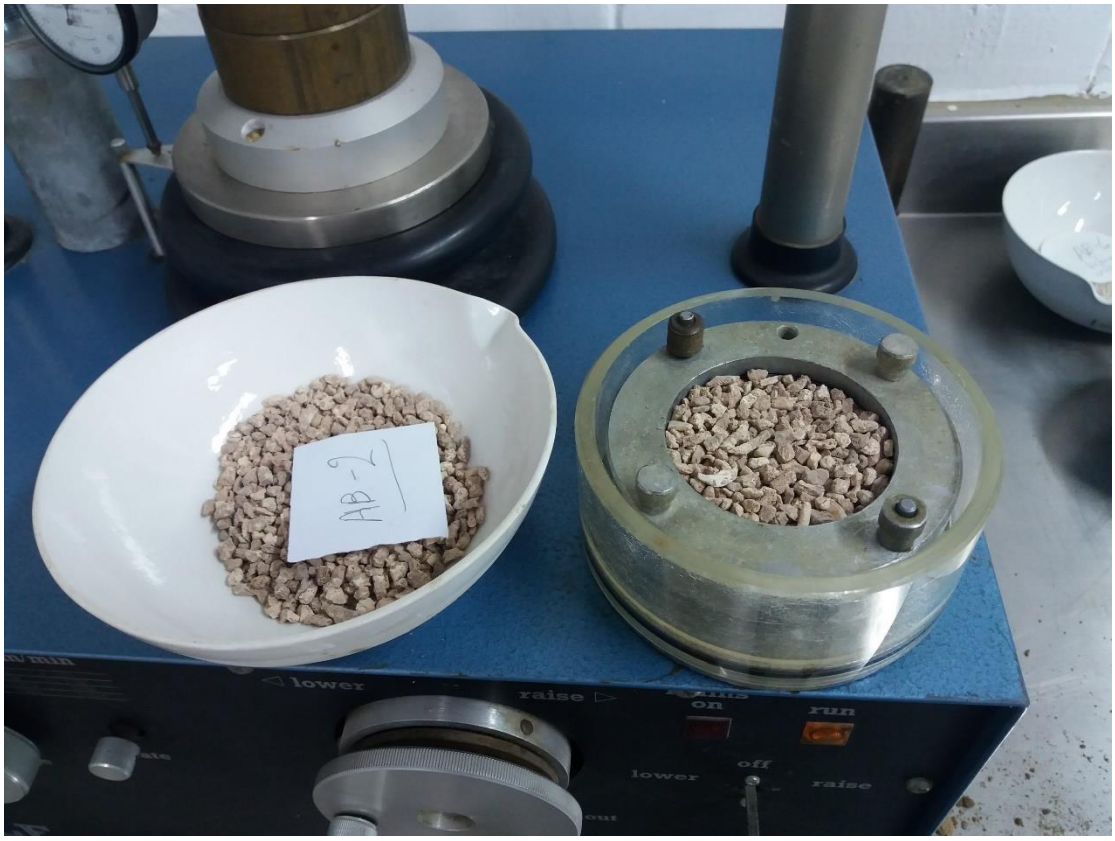

Figure 10: Sample AB-2 ready for crushing test

Figure 11: One dimensional compression test setup

CHAPTER 4

RESULTS AND DISCUSSION

4.1 General

This chapter presents and discusses the results of the statistical analysis and experimental work conducted. The statistical analysis was performed on compiled sand and clay layers using Minitab 17. The experimental programme was conducted on a few marine calcareous sand samples.

4.2 Evaluation of Pile Capacity

For all statistical tests and where applicable, the level of significance (α_α) is set at 0.05 (i.e., confidence level = 95%). Sand and clay data are reported separately and statistical tests are done on each group.

4.2.1 Statistical Analysis of Compiled Sand Layers

Tables 6 to 11 illustrate a summary of sand layers used in the analysis, which are classified into silica and carbonate sand. The silica sand layers were further categorised into 5 groups based on the relative density as explained in chapter 3. The tables show only summary of necessary parameters and details for analysis sake, the complete compiled information can be found in the Appendix.

The (SF_{DMS}) is plotted against (SF_{API}) for carbonate sand and all silica sand categories. The best-fit line is drawn with and without y-intercept and the coefficient of determination, R^2 is displayed to assess the correlation of the two value sets. Best-fit lines are shown in Figure 12 and 13 for the two scenarios, with and without y-intercept, respectively. Most of statistical textbooks and articles tend to caution against dropping the constant term from a regression, on the grounds that imposing any such restriction can diminish the model's fit to the data. There are, however, some articles in the literature that discussed situations in which regression through the origin (RTO) would be appropriate. For instance, RTO may be inevitable if transformations of the ordinary least-squares regression (OLS) are needed. Even without such transformations, however, there are sometimes strong reasons for believing that the response (y) equals zero when the predictor (x) is zero. Generally, the R^2 of the no-intercept model must not be compared to that of the model which includes an intercept [59]. In this thesis, RTO is favoured over OLS since the DMS shaft friction is likely to be zero when API shaft friction is zero. Nevertheless, OLS models are shown for illustration.

As can be seen in Figure 12, the coefficients of determination are relatively low in most silica sand categories, ranging between 0.18 to 0.59 for Loose and Very Dense groups, respectively. The carbonate sand is no different having an adjusted R^2 of 0.21.

Considering the two fitted line plot scenarios discussed above, the small values of the coefficient of determination indicate that DMS and API shaft frictions are not correlated, with the exception of the Very Loose category in silica sand which has an almost equal adjusted R^2 as high as 0.81 in the two models.

Table 6: Compiled very loose sand layers' details from different locations

Sand category: Very Loose											
Location	**Depth range (m)**		**Layer thickness (m)**	**$CaCO_3$, (%)**	**SF_{DMS}, (kPa)**	**SF_{API}, (kPa)**	**γ, (kN/m^3)**	**W.C, (%)**	**D_r, (%)**	**Sand type**	**$p_0'(z)$, (kPa)**
N-1	26.80	28.00	1.20	13.80	111.47	83.50	10.00	23.00	14.90	Silica sand	257.35
F-10	0.00	3.00	3.00	38.83	0.00	0.62	9.67	51.21	-ve	Calcareous sand	14.77
F-10	6.00	7.50	1.50	NR	14.28	9.72	9.50	42.10	-ve	NA	60.60
F-11	0.00	3.00	3.00	39.00	0.00	0.28	7.50	47.20	-ve	ML	7.50
F-11	4.50	6.00	1.50	38.00	0.00	4.84	7.50	52.30	-ve	Calcareous sand	38.25
F-12	3.00	4.50	1.50	43.00	24.15	4.46	7.50	36.94	NA	Calcareous sand	27.00
J-1	33.00	34.80	1.80	35.00	360.53	95.91	20.50	20.00	14.30	Calcareous sand	669.37
J-2	2.40	3.60	1.20	46.00	2.98	6.68	18.50	30.00	-ve	Calcareous sand	55.50
J-2	4.70	5.40	0.70	39.00	4.47	15.12	19.00	25.00	1.25	Calcareous sand	93.50
J-3	50.00	51.00	1.00	37.00	257.00	125.00	10.00	24.00	22.94	Calcareous sand	513.25
Y-2	1.30	3.00	1.70	30.00	6.23	1.24	10.00	23.00	7.26	Calcareous sand	17.00
Y-3	6.50	8.10	1.60	5.00	35.97	20.33	20.00	20.00	7.25	Silica sand	147.00
Y-10	1.40	2.50	1.10	10.00	8.23	1.78	18.50	32.00	-ve	Silica sand	33.30

Table 7: Compiled information of loose sand layers from different locations

Sand category: Loose											
Location	**Depth range (m)**		**Layer thickness (m)**	**$CaCO_3$, (%)**	**SF_{DMS}, (kPa)**	**SF_{API}, (kPa)**	**γ, (kN/m^3)**	**W.C, (%)**	**D_r, (%)**	**Sand type**	**$p_0'(z)$, (kPa)**
F-3	2.25	6.00	3.75	20.00	31.15	12.50	11.00	17.95	NA	Silica sand	41.80
F-3	6.00	9.75	3.75	16.00	97.92	26.00	11.00	18.68	NA	Silica sand	86.35
F-4	12.80	15.25	2.45	34.00	40.72	27.00	10.50	20.32	NA	Calcareous sand	104.20
F-5	7.50	11.70	4.20	6.00	69.70	26.10	20.00	21.00	26.66	Silica sand	188.55
F-5	28.50	30.00	1.50	6.00	201.58	46.70	20.00	17.00	24.55	Silica Sand	575.23
F-6	2.45	7.50	5.05	21.00	54.60	15.83	11.00	17.93	NA	Calcareous sand	55.07
F-8	4.50	12.00	7.50	7.80	83.16	28.84	8.00	17.94	26.68	Silica Sand	84.80
F-9	3.70	10.20	6.50	15.00	80.59	22.09	10.00	21.16	28.20	Silica sand	78.00
F-13	6.00	10.50	4.50	19.67	2.19	23.43	10.00	17.60	29.07	Silica sand	74.25
J-1	39.10	41.30	2.20	38.00	390.58	97.04	19.70	24.00	28.01	Calcareous sand	788.77
J-1	43.50	46.00	2.50	33.00	240.36	191.52	19.50	26.00	30.85	Calcareous sand	887.27
J-2	10.00	10.40	0.40	39.00	35.92	44.10	19.00	25.00	34.20	Calcareous sand	188.00
J-2	29.30	32.80	3.50	46.00	125.46	95.76	20.00	20.00	34.56	Calcareous sand	626.00
J-2	54.00	55.50	1.50	30.00	185.72	210.47	18.00	25.00	27.95	Calcareous sand	1048.00
J-2	24.10	25.30	1.20	34.00	57.71	79.73	19.00	20.00	27.40	Calcareous sand	488.50
Y-1	4.50	7.10	2.60	44.00	62.12	12.45	10.50	24.02	NA	Calcareous sand	57.75
Y-10	59.50	63.90	4.40	2.00	223.12	99.49	21.00	18.00	25.00	Silica sand	1241.45
U-4	4.00	10.20	6.20	31.00	174.40	19.23	19.50	19.00	31.92	Calcareous sand	187.20
U-5	21.50	24.50	3.00	15.00	88.07	80.03	20.00	25.00	24.94	Silica sand	458.00
U-6	1.40	6.20	4.80	45.00	258.85	6.25	20.50	23.00	33.95	Calcareous sand	86.10

Table 8: Compiled information of medium dense sand layers from different locations

Sand category: Medium Dense											
Location	**Depth range (m)**		**Layer thickness (m)**	**$CaCO_3$, (%)**	**SF_{DMS}, (kPa)**	**SF_{API}, (kPa)**	**γ, (kN/m^3)**	**W.C, (%)**	**D_r, (%)**	**Sand type**	**$p_0'(z)$, (kPa)**
N-1	0.90	2.50	1.60	21.40	34.48	0.96	8.50	28.00	57.41	Calcareous sand	14.45
N-1	7.70	8.80	1.10	40.00	14.41	32.04	10.00	22.00	62.02	Calcareous sand	66.85
N-1	17.50	18.50	1.00	27.10	48.33	73.46	9.80	26.00	53.12	Calcareous sand	159.35
N-1	33.30	36.50	3.20	36.00	111.31	47.62	10.20	25.00	42.01	Calcareous sand	326.95
N-1	52.50	55.60	3.10	0.00	162.82	81.21	10.00	23.31	53.95	Gypsum	521.00
F-1	7.00	8.50	1.50	20.00	14.55	30.00	9.00	29.46	NA	Calcareous sand	72.00
F-1	9.45	12.65	3.20	6.00	83.14	42.50	10.00	21.75	NA	Silica Sand	102.00
F-90	16.75	18.50	1.75	8.00	101.81	45.00	10.50	20.41	NA	Silica Sand	126.25
F-5	4.30	7.50	3.20	9.00	37.76	24.40	20.50	20.00	63.17	Silica Sand	138.55
F-6	9.75	12.75	3.00	6.00	184.28	36.80	10.00	22.37	NA	Silica Sand	118.80
F-6	26.45	62.60	36.15	4.00	102.38	121.10	10.00	24.58	NA	Silica Sand	297.10
F-8	0.00	3.00	3.00	34.00	11.29	0.31	8.00	25.75	59.52	Calcareous sand	12.80
F-8	4.50	12.00	7.50	7.80	57.33	15.62	8.00	17.94	35.05	Silica sand	52.80
F-9	3.70	10.20	6.50	15.00	49.81	9.97	10.00	21.16	36.88	Silica sand	47.00
F-9	13.40	16.50	3.10	10.50	178.74	63.86	11.00	27.05	50.62	Silica sand	155.10
F-10	7.50	9.00	1.50	6.00	22.06	22.71	10.00	22.10	35.10	Silica sand	80.60
F-11	12.00	15.00	3.00	8.50	84.31	37.74	9.50	14.70	45.33	Silica sand	112.98
F-12	4.50	12.00	7.50	4.50	70.43	25.10	9.50	17.20	NA	Silica sand	72.50
F-12	12.00	19.00	7.00	5.25	198.98	53.10	11.00	22.84	NA	Silica sand	147.60
F-12	19.00	21.00	2.00	NR	193.49	92.15	12.50	NR	NA	Rock core	205.60
J-2	27.00	28.30	1.30	32.00	101.89	98.33	19.00	20.00	53.14	Calcareous sand	546.00
J-2	29.30	32.80	3.50	46.00	108.73	95.80	20.00	20.00	35.71	Calcareous sand	586.00
J-2	35.20	38.00	2.80	43.00	201.21	99.34	19.50	27.00	47.31	Calcareous sand	706.00
J-2	39.10	48.00	8.90	30.00	323.09	94.90	19.00	27.00	55.52	Calcareous sand	838.00
J-2	27.00	28.30	1.30	32.00	89.83	109.35	19.00	20.00	53.77	Calcareous sand	526.50
J-2	29.30	32.80	3.50	46.00	300.94	95.74	20.00	20.00	35.11	Calcareous sand	606.50
J-2	35.20	38.00	2.80	43. 00	395.29	95.58	19.50	27.00	46.79	Calcareous sand	727.50

Table 8 continued

J-2	39.10	48.00	8.90	30.00	331.22	94.93	19.00	27.00	55.08	Calcareous sand	859.50
J-3	37.50	43.50	6.00	48.00	422.75	41.10	11.00	21.50	61.81	Calcareous sand	408.20
J-3	46.00	47.20	1.20	46.00	411.23	125.00	10.50	22.00	63.09	Calcareous sand	473.25
J-3	37.50	43.50	6.00	48.00	305.31	44.60	11.00	21.50	61.19	Calcareous sand	423.05
Y-1	7.10	13.55	6.45	20.00	107.53	38.10	10.50	20.94	NA	Silica sand	100.80
Y-1	21.20	25.65	4.45	16.00	227.76	96.01	11.00	20.55	NA	Silica sand	241.90
Y-2	1.30	3.00	1.70	30.00	8.49	5.05	10.00	23.00	46.52	Calcareous sand	27.00
Y-2	3.00	7.40	4.40	8.00	37.63	25.17	11.00	20.40	62.43	Silica sand	65.50
Y-3	3.30	4.00	0.70	29.00	23.12	7.26	20.00	20.00	51.71	Calcareous sand	78.00
Y-3	8.10	9.00	0.90	11.00	54.85	34.79	20.00	20.00	58.91	Silica sand	177.00
Y-4	1.50	10.00	8.50	12.00	19.93	19.99	10.00	17.64	49.87	Silica sand	63.72
Y-4	29.00	32.50	3.50	15.00	318.94	48.19	9.70	22.80	44.64	Silica sand	303.50
Y-5	1.50	8.20	6.70	25.00	46.24	20.41	20.50	24.00	53.65	Calcareous sand	112.22
Y-7	10.50	12.00	1.50	2.50	51.99	45.76	23.00	NR	64.92	Sandstone	242.30
Y-7	21.00	23.00	2.00	2.50	157.44	78.46	23.00	NR	60.40	Sandstone	442.30
Y-7	29.50	36.60	7.10	2.50	210.08	145.55	20.00	23.00	53.48	Silica sand	659.72
Y-7	40.50	44.50	4.00	2.50	171.14	99.09	20.25	22.00	41.14	Silica sand	863.50
Y-7	49.80	59.55	9.75	18.20	173.17	178.11	21.00	19.00	38.36	Silica sand	1012.75
Y-8	5.50	6.60	1.10	30.00	56.12	20.27	21.00	19.00	60.08	Calcareous sand	115.70
Y-8	13.50	15.50	2.00	19.00	62.91	52.48	22.00	15.00	44.29	Silica sand	286.70
Y-8	18.40	20.50	2.10	2.00	240.22	75.64	21.00	22.00	44.34	Silica sand	408.70
Y-8	20.50	26.00	5.50	2.00	273.30	179.60	20.00	25.00	64.20	Silica sand	508.70
Y-8	26.00	31.50	5.50	2.00	171.18	98.81	20.50	21.00	60.16	Silica sand	590.20
Y-8	31.50	42.00	10.50	10.00	170.85	179.36	21.00	18.00	59.85	Silica sand	652.70
Y-9	8.00	10.30	2.30	19.00	36.94	29.34	21.00	18.00	64.67	Silica sand	172.00
Y-9	13.50	15.50	2.00	15.00	131.64	67.42	20.50	24.00	60.31	Silica sand	287.00
Y-10	33.10	46.70	13.60	3.00	145.03	149.45	20.00	25.00	62.97	Silica sand	868.35
Y-10	46.70	49.30	2.60	3.00	178.49	101.35	20.00	25.00	52.98	Silica sand	968.35
Y-10	50.30	58.30	8.00	8.00	200.81	99.83	21.00	18.00	60.35	Silica sand	1115.45
Y-11	13.50	17.10	3.60	5.00	165.78	56.76	20.00	30.00	63.10	Sandstone	308.00
U-4	4.00	10.20	6.20	31.00	97.21	13.31	19.50	19.00	38.64	Calcareous sand	128.70
U-4	16.20	18.15	1.95	NR	494.03	62.06	21.00	15.00	64.61	Gypsum	347.20

Table 8 continued

U-4	20.60	25.05	4.45	NR	489.22	76.91	21.50	11.00	60.96	Gypsum	428.20
U-5	29.50	32.30	2.80	27.00	262.37	139.23	19.50	26.00	54.68	Calcareous sand	614.50
U-5	35.50	37.50	2.00	15.00	324.63	149.62	19.50	26.00	52.11	Silica sand/Gypsum	712.00
U-5	37.50	40.10	2.60	15.00	302.97	100.13	20.50	22.00	50.68	Sandstone	773.50
U-6	1.40	6.20	4.80	45.00	56.34	3.00	20.50	23.00	45.21	Calcareous sand	45.10
U-7	15.00	17.20	2.20	24.00	64.96	82.14	10.50	26.57	60.20	Calcareous sand	164.30
U-7	38.50	39.60	1.10	24.00	303.18	119.57	10.00	26.00	59.13	Calcareous sand	370.30

Table 9: Compiled information of dense sand layers from different locations

Sand category: Dense											
Location	**Depth range (m)**		**Layer thickness (m)**	**$CaCO_3$, (%)**	**SF_{DMS}, (kPa)**	**SF_{API}, (kPa)**	**γ, (kN/m^3)**	**W.C, (%)**	**D_r, (%)**	**Sand type**	**$p_0'(z)$, (kPa)**
N-1	19.80	22.40	2.60	13.10	57.36	72.69	10.00	20.00	84.76	Silica sand	199.35
F-1	18.10	20.50	2.40	3.00	218.23	95.00	10.00	21.52	NA	Silica Sand	192.00
F-1	20.50	22.25	1.75	3.00	218.23	100.00	10.00	20.70	NA	Silica Sand	213.00
F-2	5.40	8.30	2.90	8.00	62.18	32.00	10.50	20.58	NA	Silica sand	67.00
F-2	10.45	12.80	2.35	8.00	124.36	55.00	10.00	22.27	NA	Silica sand	127.00
F-2	13.90	17.50	3.60	13.00	124.36	70.00	10.00	22.11	NA	Silica sand	157.50
F-2	17.50	21.00	3.50	10.00	129.54	89.00	10.00	19.51	NA	Silica sand	198.00
F-2	21.00	25.20	4.20	11.00	145.08	103.00	10.50	21.17	NA	Silica sand	229.00
F-3	9.75	13.80	4.05	18.00	167.49	57.00	10.50	24.23	NA	Silica sand	129.40
F-3	18.00	21.00	3.00	14.00	206.14	98.00	11.00	18.54	NA	Silica sand	204.95
F-4	22.40	29.15	6.75	7.00	101.81	80.00	11.00	19.27	NA	Silica sand	192.35
F-5	4.30	7.50	3.20	9.00	23.34	20.00	20.50	20.00	67.80	Silica sand	106.78
F-5	15.00	16.00	1.00	5.00	95.37	55.60	20.50	19.00	67.13	Silica sand	300.43
F-5	17.00	17.50	0.50	5.00	109.40	62.20	20.50	19.00	80.95	Silica sand	341.43
F-5	30.00	31.00	1.00	6.00	201.58	46.70	21.00	17.00	71.18	Silica sand	598.33
F-6	12.75	23.45	10.70	10.00	192.47	87.36	11.00	19.03	NA	Silica sand	186.56
F-7	9.75	10.65	0.90	9.90	57.44	53.41	10.00	24.63	NA	Silica sand	106.00
F-7	11.75	14.75	3.00	12.57	88.77	65.91	10.00	26.43	NA	Calcareous sand	136.00
F-7	14.75	22.05	7.30	1.30	167.09	91.74	10.00	21.41	NA	Silica sand	186.00
F-7	22.45	25.00	2.55	1.30	308.06	96.59	11.00	21.36	NA	Silica sand	239.00
F-7	26.35	27.75	1.40	1.30	313.28	100.00	11.00	24.10	NA	Silica sand	272.00
F-9	21.00	32.90	11.90	3.57	156.28	114.87	11.00	20.79	82.60	Silica sand	310.93
F-9	42.10	50.90	8.80	4.00	153.85	115.41	11.00	25.15	75.48	Silica sand	467.50
F-11	24.00	27.00	3.00	19.00	183.49	80.56	11.00	20.65	77.62	Silica sand	235.15
F-13	22.50	28.50	6.00	10.50	177.16	81.42	11.00	23.35	81.16	Silica sand	260.25
F-13	28.50	34.50	6.00	6.67	261.56	96.20	11.00	25.87	81.76	Silica sand	326.25
F-13	34.50	37.50	3.00	5.50	179.98	80.84	11.00	25.00	79.53	Silica sand	370.25

Table 9 continued

F-13	37.50	42.00	4.50	5.33	169.07	95.77	11.00	19.70	78.01	Silica sand	404.35
F-13	42.00	56.50	14.50	6.50	123.73	93.61	11.00	21.66	73.90	Silica sand	514.35
F-13	57.00	67.00	10.00	10.17	97.54	96.36	12.50	17.87	74.68	Silica sand	616.35
J-1	1.70	5.00	3.30	45.00	3.01	13.67	19.50	23.00	70.24	Calcareous sand	69.72
J-4	6.20	12.00	5.80	30.00	14.92	44.92	20.00	23.00	76.85	Calcareous sand	177.50
J-4	27.00	32.00	5.00	35.00	208.83	155.45	20.00	25.00	71.95	Calcareous sand	572.90
Y-1	13.55	16.50	2.95	1.00	207.06	66.64	10.50	22.46	NA	Silica sand	153.30
Y-2	3.00	7.40	4.40	8.00	16.02	14.71	11.00	20.40	69.64	Silica sand	43.50
Y-2	9.00	12.00	3.00	6.00	54.18	57.23	11.00	20.00	75.98	Silica sand	117.00
Y-2	12.00	13.50	1.50	31.00	107.80	54.64	11.00	14.33	72.93	Calcareous sand	139.00
Y-2	13.50	18.20	4.70	3.00	144.53	74.29	11.50	17.00	76.76	Silica sand	173.50
Y-2	20.00	21.50	1.50	1.00	189.44	102.01	11.50	21.00	82.20	Silica sand	231.00
Y-2	21.50	24.00	2.50	1.00	204.31	133.42	11.50	23.00	76.29	Silica sand	254.00
Y-2	30.00	33.50	3.50	15.00	263.06	192.47	12.00	14.33	74.67	Silica sand	356.10
Y-3	9.00	10.00	1.00	11.00	76.60	38.09	20.00	20.00	80.70	Silica sand	197.00
Y-3	13.00	15.00	2.00	10.00	81.51	43.93	20.00	20.00	69.07	Silica sand	269.00
Y-3	19.00	25.00	6.00	2.00	133.53	100.69	20.00	20.00	80.97	Silica sand	431.00
Y-4	13.00	18.00	5.00	36.00	30.15	36.81	10.00	22.05	83.77	Calcareous sand	173.32
Y-4	20.50	23.00	2.50	30.00	101.66	61.68	9.90	15.00	73.19	Calcareous sand	212.12
Y-4	25.50	29.00	3.50	11.00	286.18	144.65	9.90	21.40	76.70	Silica sand	264.50
Y-4	32.50	48.70	16.20	20.00	295.94	149.25	9.60	21.35	83.25	Silica sand	361.20
Y-5	1.50	8.20	6.70	25.00	7.72	3.03	20.50	24.00	67.11	Calcareous sand	49.90
Y-5	22.75	32.00	9.25	5.00	207.23	173.21	20.50	21.00	81.24	Silica sand	470.23
Y-6	4.10	27.00	22.90	2.00	371.39	162.80	20.50	21.00	83.73	Silica sand	450.90
Y-8	20.50	26.00	5.50	2.00	252.11	160.07	20.00	25.00	66.37	Silica sand	448.70
Y-9	24.50	29.20	4.70	5.00	251.49	139.05	20.00	26.00	73.59	Silica sand	522.00
Y-9	29.70	37.50	7.80	2.00	192.72	148.27	20.00	25.00	69.12	Silica sand	622.00
Y-10	27.50	31.10	3.60	8.00	44.63	66.71	20.50	20.00	66.94	Silica sand	587.85
Y-10	33.10	46.70	13.60	3.00	111.56	95.39	20.00	25.00	66.02	Silica sand	728.35
Y-10	66.80	73.10	6.30	7.00	223.12	95.13	21.00	17.00	65.23	Silica sand	1304.45
Y-11	17.10	35.00	17.90	2.00	252.00	172.07	21.00	23.00	71.87	Silica sand	518.47
U-4	10.20	12.25	2.05	NR	198.39	46.98	21.00	15.00	71.84	Gypsum	229.20

Table 9 continued

U-5	7.50	8.60	1.10	23.00	28.30	31.67	20.50	22.00	80.29	Calcareous sand	164.00
U-5	15.60	16.50	0.90	35.00	71.02	73.55	20.50	22.00	79.30	Calcareous sand	322.00
U-5	41.50	44.00	2.50	8.00	296.78	81.02	20.50	22.00	73.00	Silica sand	835.00
U-5	47.60	50.00	2.40	23.00	223.12	150.14	19.00	35.00	66.55	Calcareous sand	941.00
U-6	6.20	6.80	0.60	NR	295.82	28.31	21.00	10.00	74.07	Gypsum	130.20
U-7	11.80	13.00	1.20	30.00	28.88	46.74	9.50	23.00	81.10	Calcareous sand	124.30
U-7	19.50	21.40	1.90	30.00	64.96	84.91	10.00	24.00	73.76	Calcareous sand	205.30
U-7	21.40	27.30	5.90	32.00	46.92	69.53	11.00	22.60	70.94	Calcareous sand	249.30
U-7	30.50	34.40	3.90	27.00	126.32	107.00	10.50	20.50	71.17	Calcareous sand	318.80

Table 10: Compiled very dense sand layers from different locations

Sand category: Very Dense											
Location	**Depth range (m)**		**Layer thickness (m)**	**$CaCO_3$, (%)**	**SF_{DMS}, (kPa)**	**SF_{API}, (kPa)**	**γ, (kN/m^3)**	**W.C, (%)**	**D_r, (%)**	**Sand type**	**$p_0'(z)$, (kPa)**
N-1	19.80	22.40	2.60	13.10	55.86	65.92	10.00	20.00	86.60	Silica sand	179.35
F-1	12.65	18.10	5.45	4.00	198.83	83.33	10.00	21.41	NA	Silica Sand	152.00
F-2	3.75	5.40	1.65	27.00	41.45	20.00	11.00	16.30	NA	Calcareous sand	46.00
F-3	13.80	18.00	4.20	13.35	205.11	90.00	10.50	21.76	NA	Silica sand	171.93
F-4	18.50	20.85	2.35	7.00	162.90	83.00	10.50	23.32	NA	Silica sand	147.25
F-5	11.70	15.00	3.30	4.00	87.03	71.13	19.80	22.00	102.38	Silica sand	258.81
F-5	16.00	17.00	1.00	5.00	109.40	60.00	20.50	19.00	95.86	Silica sand	320.93
F-5	17.50	20.00	2.50	4.00	109.40	104.45	19.50	23.00	93.36	Silica sand	370.68
F-5	24.00	28.50	4.50	6.00	201.58	119.12	20.00	22.00	87.65	Silica sand	515.23
F-6	9.00	9.75	0.75	4.00	174.05	27.60	10.50	21.84	NA	Silica sand	98.80
F-6	23.45	26.45	3.00	8.00	163.81	134.20	11.00	NR	NA	Silica sand	265.10
F-8	3.00	4.50	1.50	34.00	19.27	3.93	8.00	26.40	100.33	Calcareous sand	28.80
F-8	13.50	15.00	1.50	4.00	112.33	38.67	11.00	24.70	103.94	Silica sand	114.80
F-8	15.00	18.00	3.00	5.00	189.64	70.30	11.00	22.00	99.46	Silica sand	148.90
F-9	21.00	32.90	11.90	3.57	102.55	113.76	11.00	20.79	86.83	Silica sand	244.20
F-10	9.00	43.50	34.50	4.83	231.79	72.12	11.00	24.00	96.79	Silica sand	180.70
F-11	16.50	18.00	1.50	NR	153.46	60.79	11.00	17.20	95.86	NA	144.95
F-11	18.00	24.00	6.00	5.75	199.15	80.92	11.00	20.65	91.26	Silica sand	189.68
F-11	27.00	36.00	9.00	5.60	177.58	96.16	11.00	23.33	85.88	Silica sand	257.15
F-13	10.50	22.50	12.00	9.67	40.76	69.31	11.00	24.60	94.50	Silica sand	161.25
J-1	7.80	10.80	3.00	33.00	45.71	42.74	20.00	23.00	99.45	Calcareous sand	191.72
J-3	6.55	12.00	5.45	41.00	18.12	36.90	10.50	23.55	112.26	Calcareous sand	96.13
Y-1	16.50	21.20	4.70	1.00	227.76	107.81	11.00	21.78	NA	Silica sand	197.35
Y-1	25.65	30.90	5.25	1.00	262.27	103.94	11.00	17.88	NA	Silica sand	297.27
Y-2	7.40	9.00	1.60	24.00	47.05	39.19	12.00	15.50	92.21	Calcareous sand	89.00
Y-2	18.20	20.00	1.80	14.00	189.44	109.61	11.50	11.00	99.97	Silica sand	213.75

Table 10 continued

Y-2	24.00	30.00	6.00	5.00	258.16	165.39	12.00	17.80	93.05	Silica sand	307.50
Y-3	17.00	19.00	2.00	2.00	123.55	97.63	20.00	20.00	94.31	Silica sand	351.00
Y-4	13.00	18.00	5.00	36.00	18.17	29.51	10.00	22.05	87.12	Calcareous sand	143.32
Y-5	8.20	13.50	5.30	22.00	110.31	77.25	20.00	67.50	107.03	Calcareous sand	214.85
Y-5	13.50	21.60	8.10	2.70	239.74	123.74	20.00	60.00	94.65	Calcareous sand	347.20
Y-6	0.80	4.10	3.30	2.00	12.26	8.14	21.00	20.30	112.04	Silica sand	50.40
Y-6	4.10	27.00	22.90	2.00	262.99	93.11	20.50	21.00	94.93	Silica sand	256.15
U-1	0.40	3.00	2.60	22.00	5.03	2.85	10.20	25.44	100.13	Calcareous sand	17.34
U-2	0.00	3.50	3.50	30.00	63.23	0.17	19.00	32.00	111.18	Calcareous sand	34.20
U-2	3.50	5.00	1.50	30.00	66.53	8.98	21.00	NR	106.62	Siltstone	76.20
U-5	0.00	7.50	7.50	23.00	28.30	8.32	20.50	22.00	94.66	Calcareous sand	82.00
U-6	9.60	14.60	5.00	NR	473.32	47.89	22.00	5.00	96.68	Gypsum	214.20
U-7	3.05	5.00	1.95	17.00	7.22	20.70	10.00	25.67	106.67	Silica sand	44.30
U-7	5.00	9.00	4.00	31.00	25.27	26.13	10.50	23.29	103.72	Calcareous sand	75.80

Table 11: Compiled parameters of carbonate sand from different locations

Carbonate sand ($CaCO_3$ > 50%)										
Location	**Depth range (m)**		**Layer thickness (m)**	**$CaCO_3$, (%)**	**SF_{DMS}, (kPa)**	**SF_{API}, (kPa)**	**γ, (kN/m^3)**	**W.C, (%)**	**Sand type**	**$p_0'(z)$, (kPa)**
F-1	4.50	7.00	2.50	57.00	4.16	10.00	9.00	39.51	Calcareous sand	54.00
F-5	0.00	1.50	1.50	90.00	4.11	0.00	20.00	26.00	Carbonate sand	18.00
F-5	1.50	4.30	2.80	50.00	8.91	8.80	19.00	34.00	Calcareous sand	75.00
F-6	0.00	2.45	2.45	74.00	0.00	0.00	8.00	31.49	Calcareous sand	9.60
J-2	0.00	2.00	2.00	50.00	2.98	1.28	18.50	30.00	Calcareous sand	18.50
Y-11	0.00	3.00	3.00	66.00	1.89	0.00	18.00	40.00	Calcareous sand	18.00
F-1	0.00	4.50	4.50	71.00	4.25	4.50	9.00	35.01	Calcareous sand	26.10
F-5	1.50	4.30	2.80	51.00	6.19	5.50	19.00	34.00	Calcareous sand	46.50
F-5	21.00	22.70	1.70	85.00	156.38	46.65	18.00	35.00	Carbonate sand	425.83
J-4	50.00	51.50	1.50	90.00	199.88	17.75	19.00	30.00	Carbonate sand	992.30
Y-8	9.10	12.60	3.50	87.00	69.39	15.77	22.00	15.00	Siliceous Calcarenite	220.70
N-1	71.80	73.50	1.70	100.00	50.27	86.70	10.00	89.00	Calcisiltite	703.60
N-1	73.50	76.15	2.65	94.00	50.27	145.01	10.00	21.67	Calcisiltite	733.60
F-2	1.50	3.75	2.25	61.00	8.88	5.00	10.00	14.92	Calcareous sand	24.00
F-5	22.70	24.00	1.30	85.00	178.68	13.30	19.50	25.00	Carbonate sand	455.23
J-4	1.80	2.40	0.60	90.00	0.00	5.58	19.00	30.00	Carbonate sand	39.90
Y-1	0.50	4.50	4.00	92.00	20.71	2.39	10.50	21.16	Carbonate sand	26.25
Y-2	0.50	1.30	0.80	94.00	5.62	0.38	10.00	29.50	Carbonate sand	7.00
Y-3	0.00	3.30	3.30	88.00	16.68	5.02	20.00	20.00	Carbonate Sand	58.00
Y-8	0.20	2.00	1.80	54.00	53.12	6.68	21.00	22.00	Calcareous sand	35.70
Y-8	16.80	18.40	1.60	70.00	78.53	14.56	21.50	14.00	Siliceous Calcarenite	366.70
Y-9	17.20	19.70	2.50	50.00	138.78	79.37	21.00	19.00	Calcarenite	368.00
N-1	77.50	81.50	4.00	65.00	50.27	81.08	10.50	24.17	Limestone/ Calcilutite	775.10
N-1	81.50	82.50	1.00	99.00	261.57	14.62	10.00	29.00	Silt	805.60

Table 11 continued

N-1	82.50	85.55	3.05	99.00	338.17	16.57	9.80	25.00	Carbonate sand	825.20
Y-3	0.00	3.30	3.30	88.00	7.48	0.80	20.00	20.00	Carbonate Sand	28.00
Y-9	2.00	3.00	1.00	71.00	5.48	11.48	20.00	30.00	Calcareous sand	54.00
Y-11	3.00	5.50	2.50	74.00	8.35	13.14	21.00	22.00	Calcareous sand	81.00
U-4	1.50	4.00	2.50	61.50	32.13	5.49	19.50	30.00	Calcareous sand	70.20
Y-3	10.50	12.00	1.50	67.00	76.60	23.82	20.00	20.00	Calcareous sand	227.00
Y-4	0.00	1.50	1.50	86.00	49.25	1.30	9.80	21.00	Calcarenite	13.72
Y-4	11.30	13.00	1.70	77.00	107.31	15.32	9.80	11.50	Calcarenite	113.32
Y-5	0.00	1.50	1.50	85.00	3.02	0.00	21.00	75.00	Carbonate sand	18.90
U-4	1.50	4.00	2.50	61.50	4.20	3.42	19.50	30.00	Calcareous sand	31.20

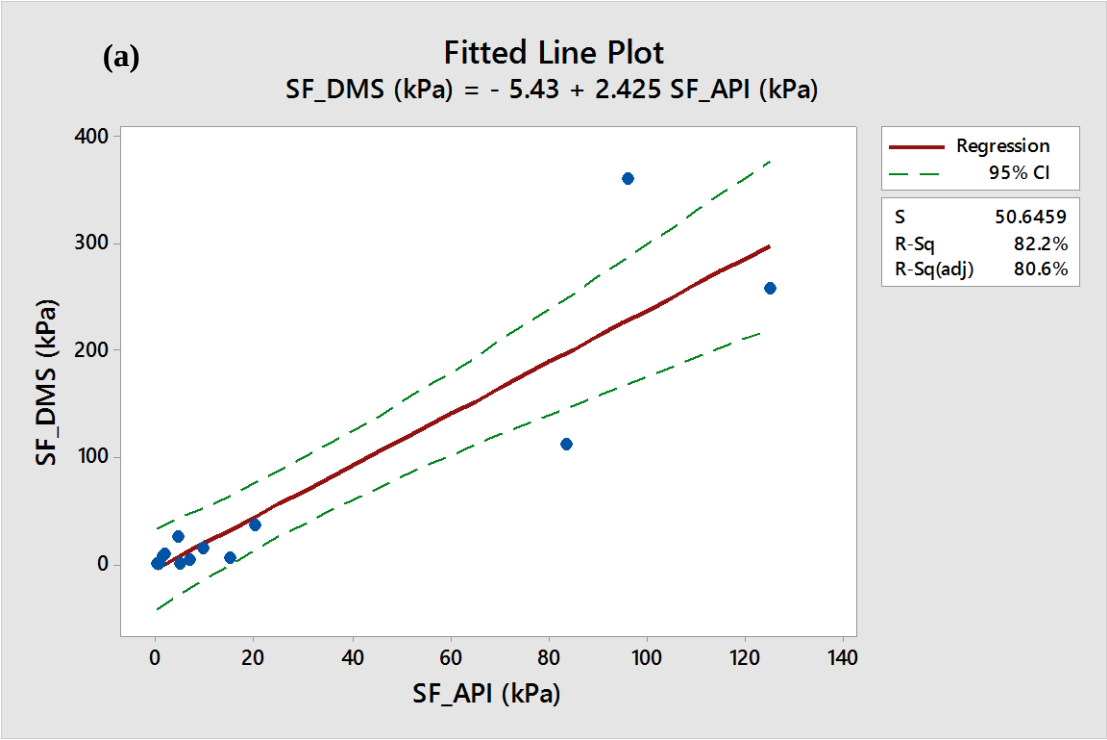

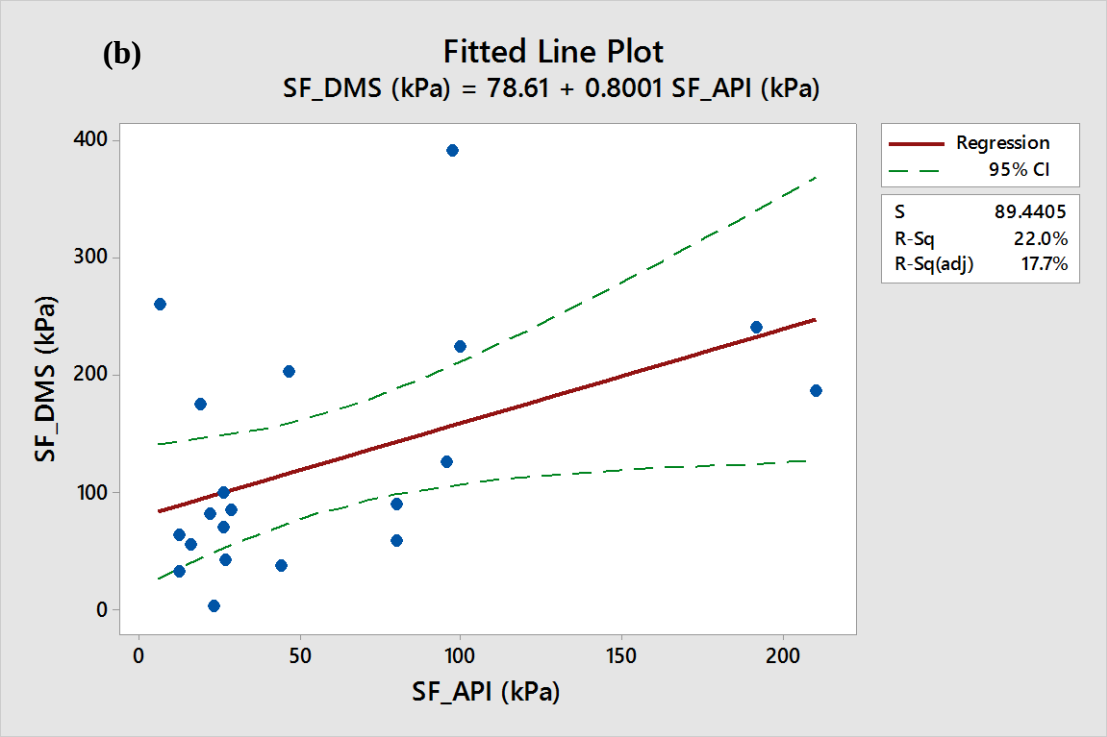

Figure 12: Best-fit line plot of DMS vs API shaft friction with 95% confidence interval coefficients for sand: (a) Very Loose, (b) Loose, (c) Medium Dense, (d) Dense, (e) Very Dense, and (f) Carbonate Sand

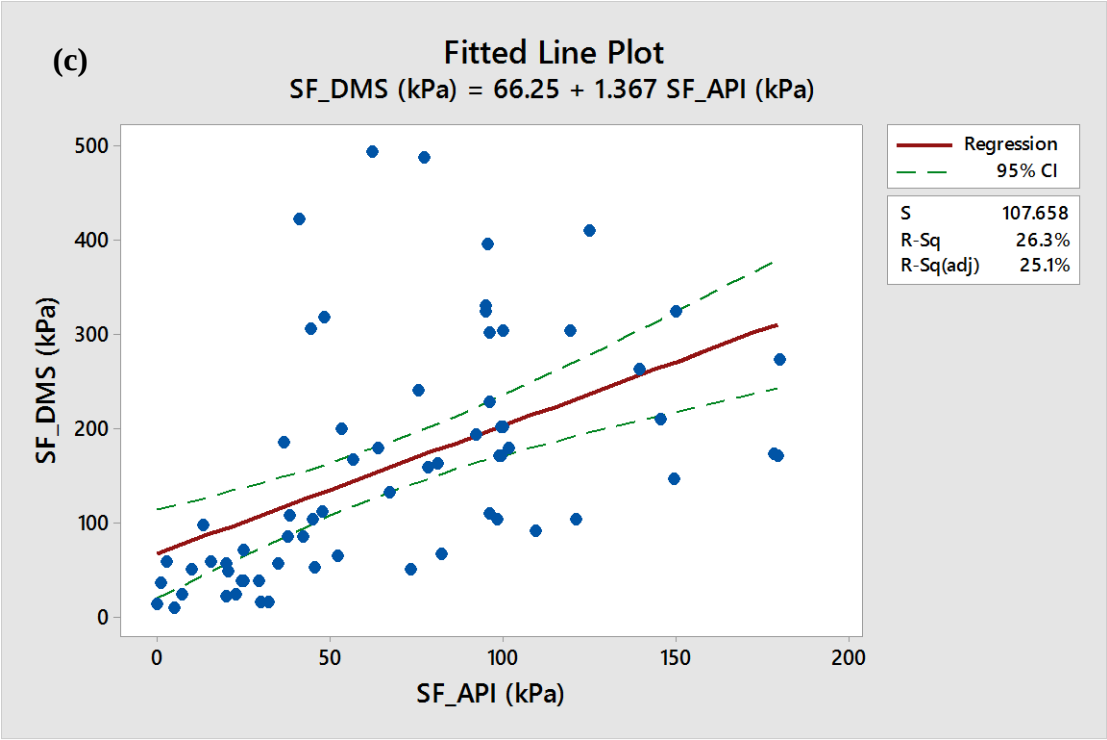

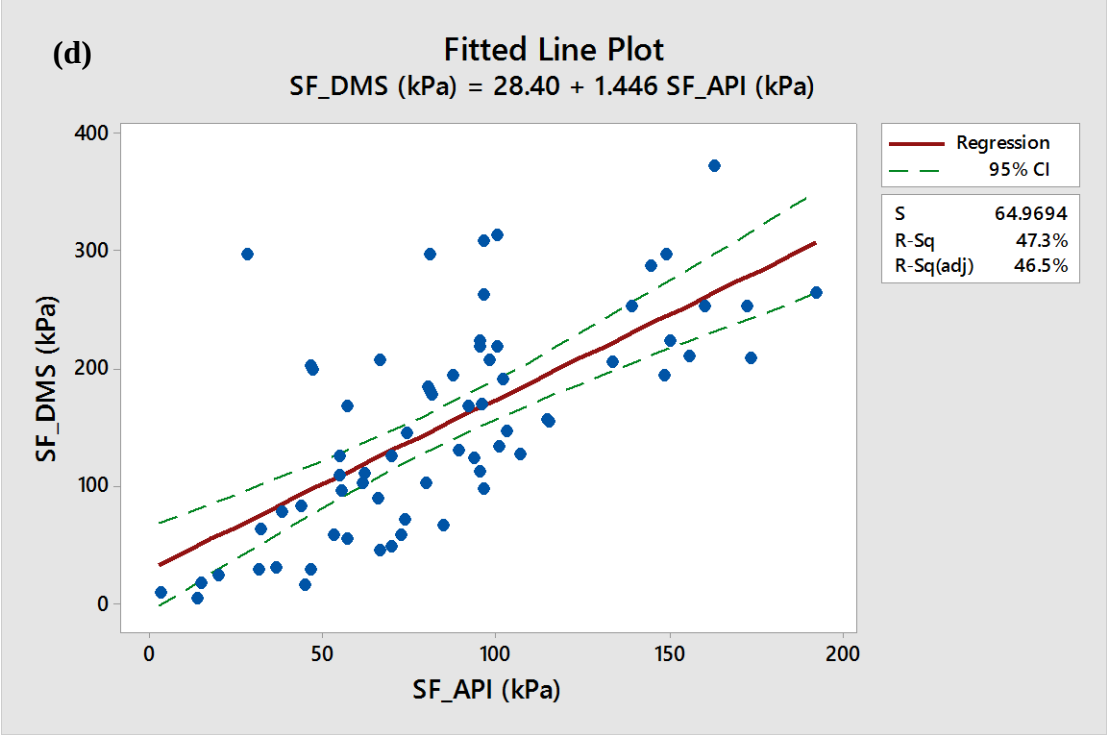

Figure 12 continued

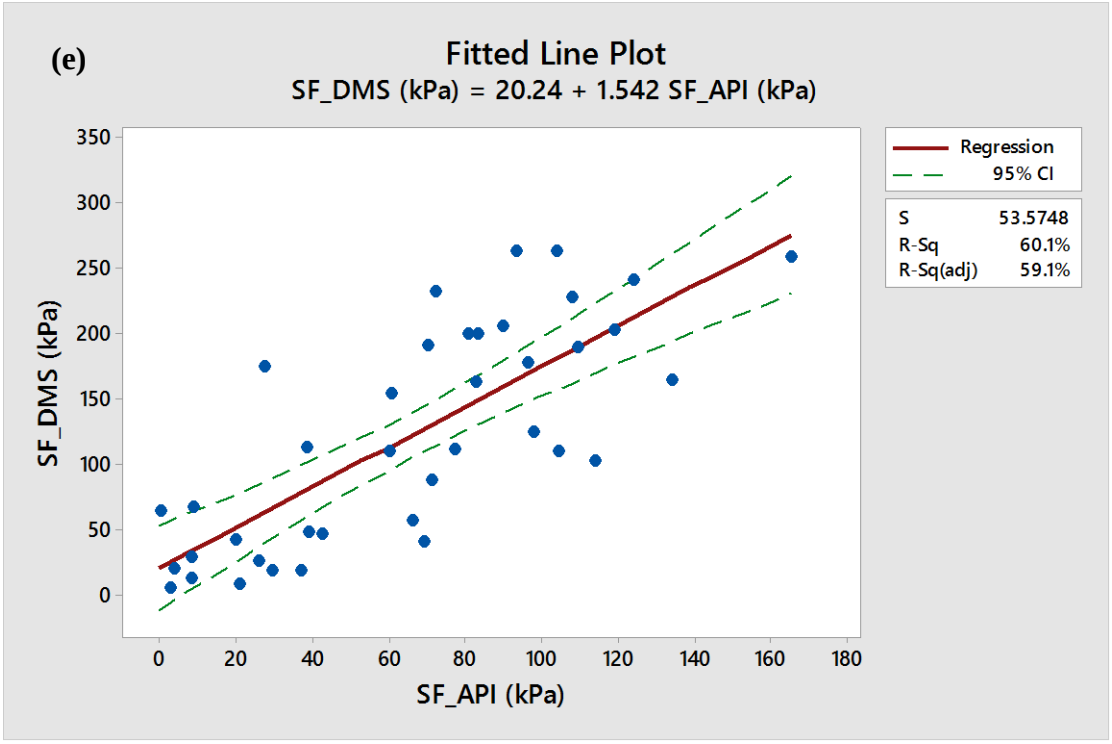

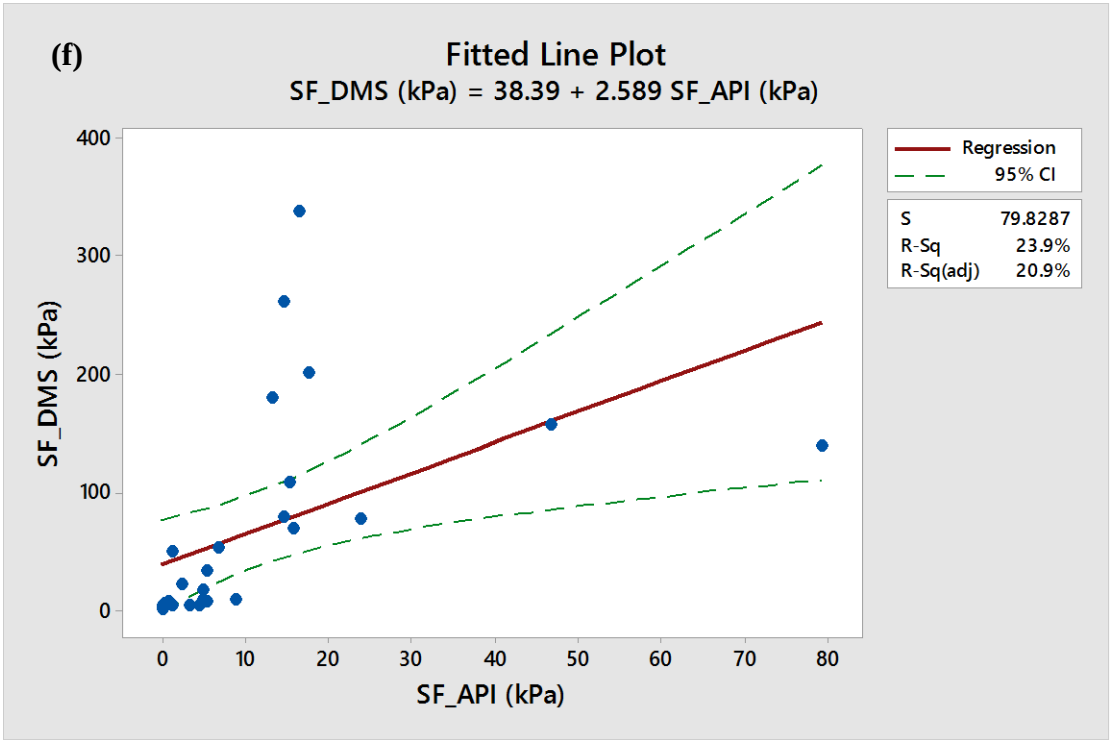

Figure 12 continued

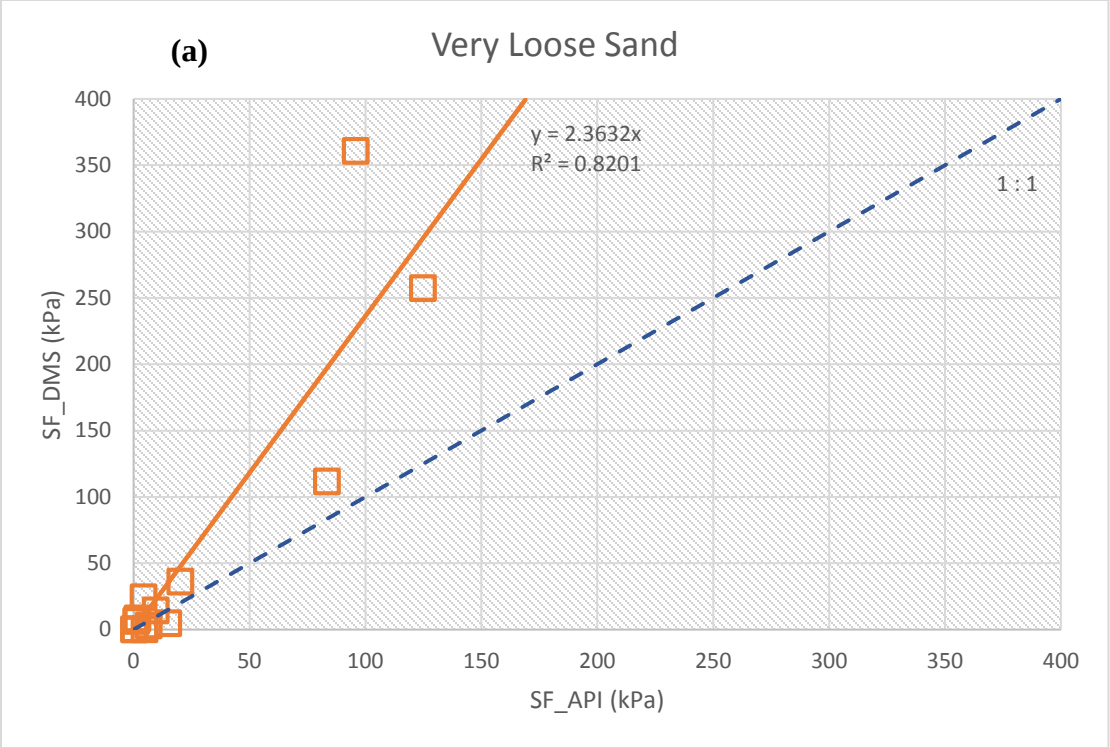

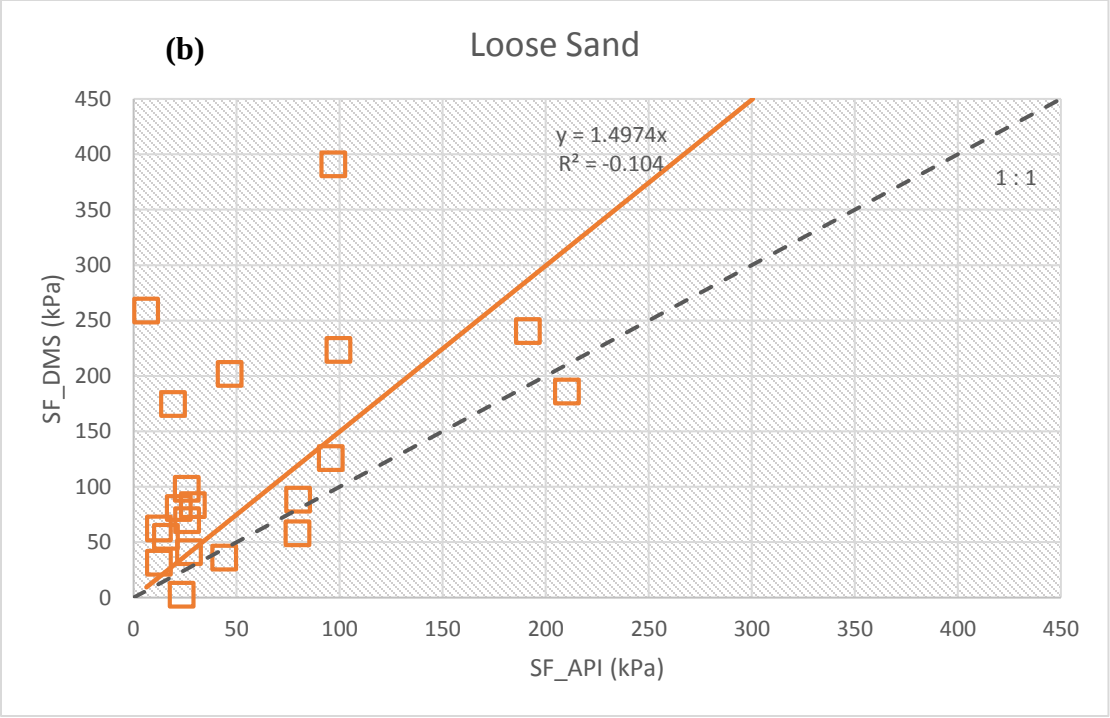

Figure 13: Best-fit line plot of DMS vs API shaft friction drawn through the origin for sand: (a) Very Loose, (b) Loose, (c) Medium Dense, (d) Dense, (e) Very Dense, and (f) Carbonate Sand

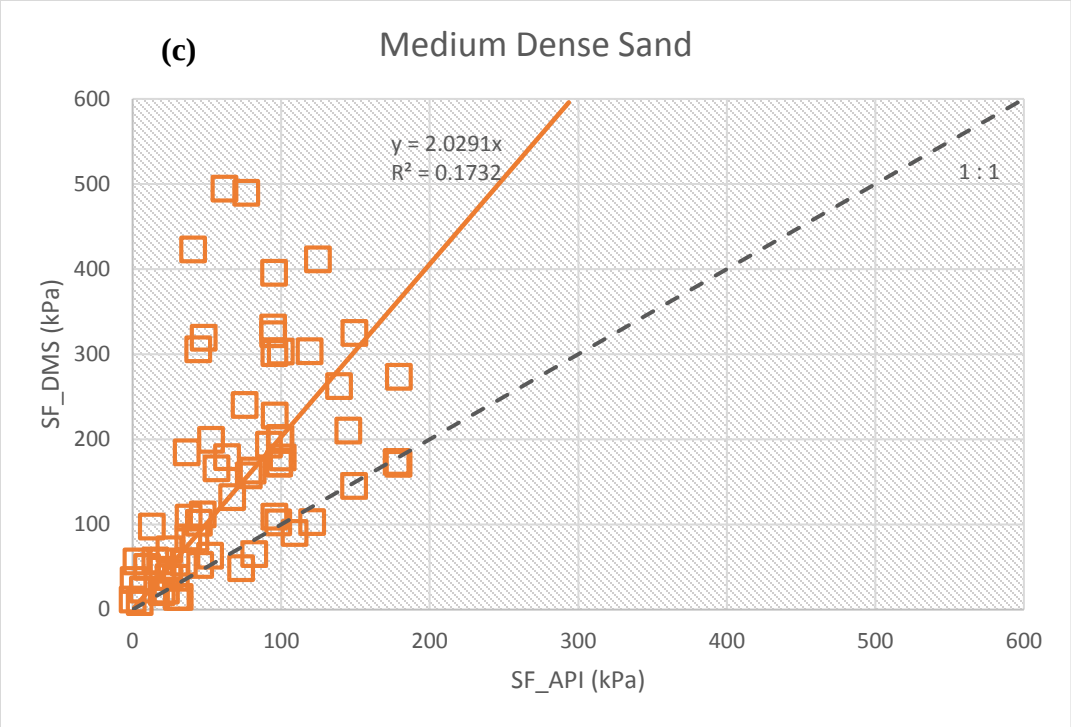

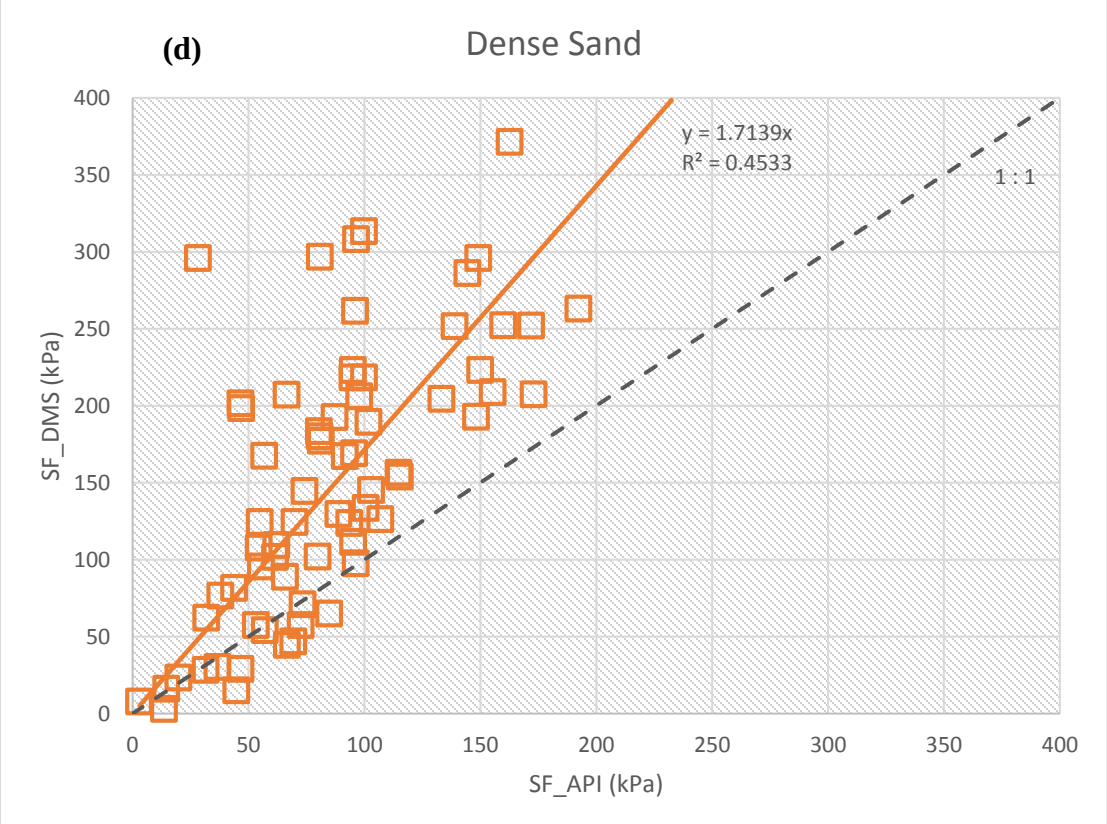

Figure 13 continued

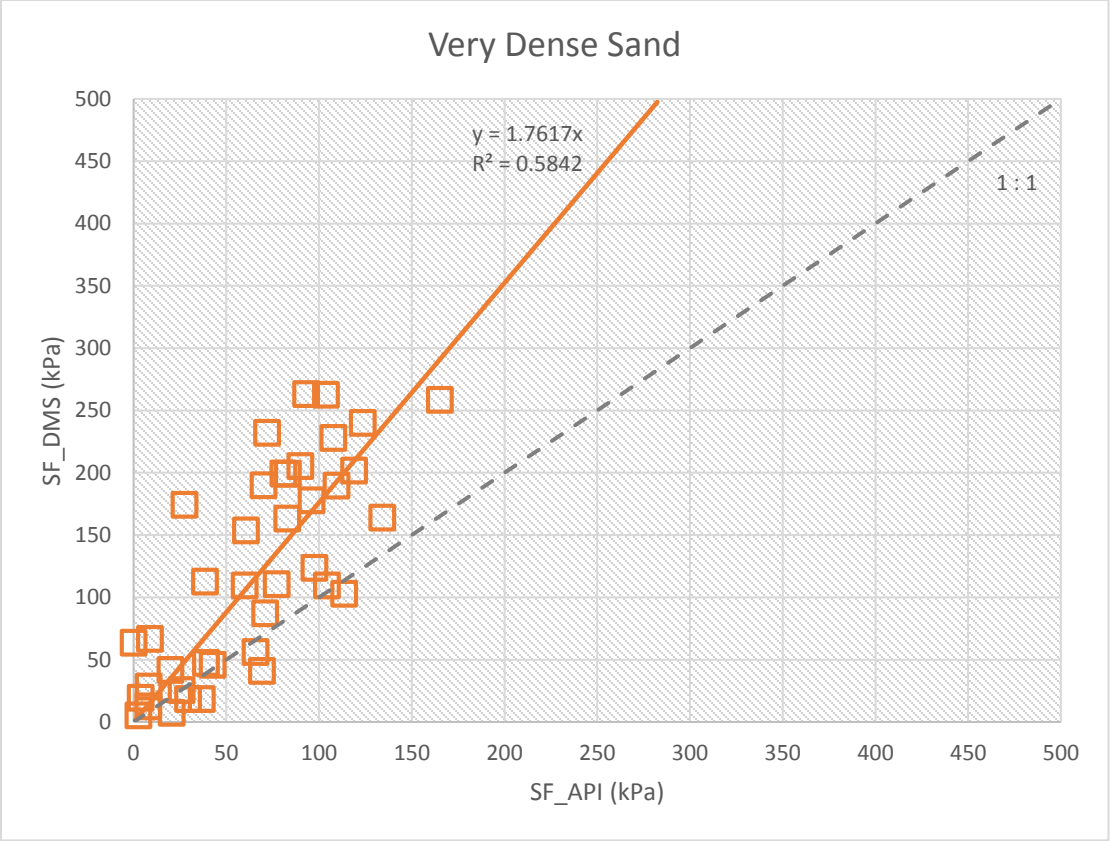

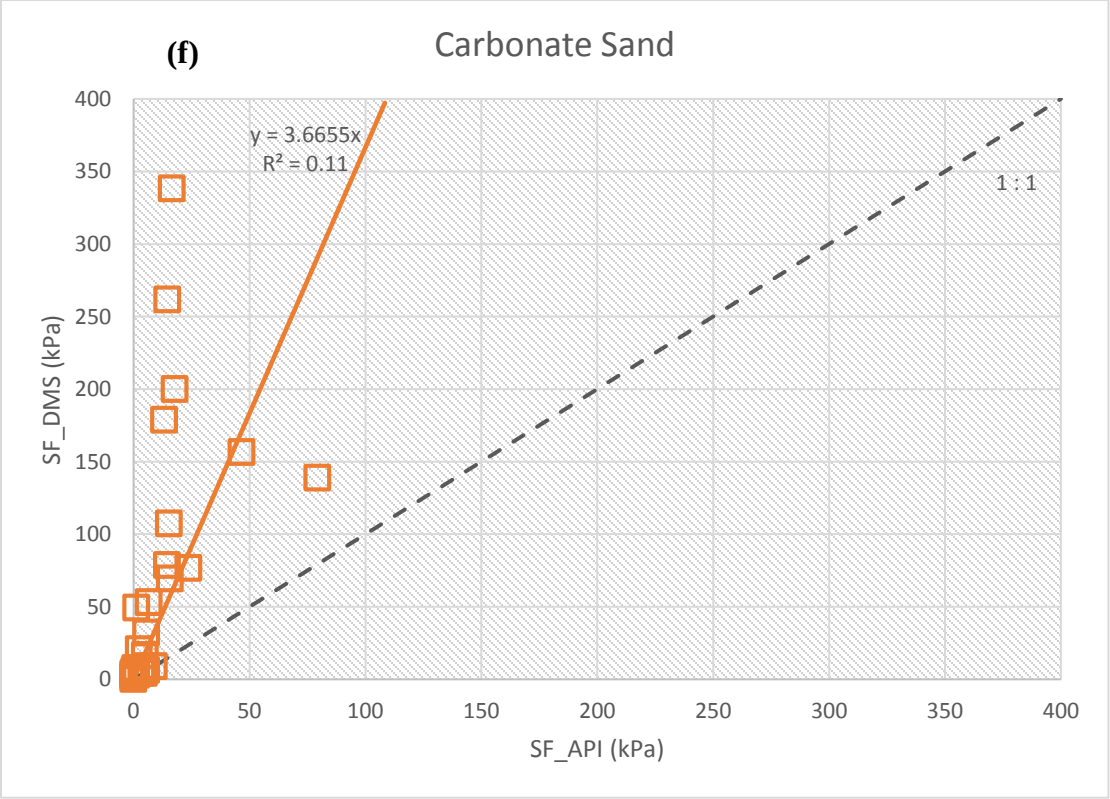

Figure 13 continued

Furthermore, in order to evaluate the difference between DMS and API shaft capacities, a nonparametric test is performed on the collected shaft friction data. Statistical nonparametric tests have been commonly employed as an alternative to parametric procedures whenever the distribution of the data being dealt with is unknown. The data (DMS and API shaft frictions) are not expected to follow a normal distribution because they depend upon several factors such as depth, unit weight, relative density, carbonate content, etc., which differ considerably from layer to another. Hence, parametric tests are not a relaiable option for analysis. This is the practice the author has adopted; although, some researchers like [60]–[63] reported that parametric procedures can be used even when the normality assumption is violated given that the number of observations is large (hundreds).

Subsequently, a 2-sample rank test (known also as the Mann-Whitney test) of the equality of the two population medians (DMS and API shaft capacities) is performed to estimate the difference between the two capacities. The test hypotheses are as follows:

H_0: $\eta_1 = \eta_2$ versus H_1: $\eta_1 \neq \eta_2$

The Mann-Whitney test has an assumption that data are independent random samples from two populations that have the same shape and a scale that is continuous or ordinal. Results of Mann-Whitney test on sand are summarised in Tables 12.

The results in Table 12 denoted by the attained levels of significance being smaller than α_α of 0.05, demonstrate that apart from the Very Loose silica sand there is sufficient evidence to reject the null hypothesis, H_0, and hence the data supports the alternative hypothesis, H_1 that the DMS and API shaft capacities are not equal.

Table 12: Results of Mann-Whitney test on DMS and API shaft capacities

Sand group	Population	N	η	Point estimate of SF_{DMS} - SF_{API} (kPa)	95 % CI	Sig. level	Sig. level adjusted for ties
Very Loose	SF_{DMS}	13	8.2	1.5	(-9.70,23.80)	0.8777	0.8776
	SF_{API}	13	6.7				
Loose	SF_{DMS}	20	85.61	47.98	(13.71,99.46)	0.0071	–
	SF_{API}	20	27.92				
Medium Dense	SF_{DMS}	66	138.33	67.16	(33.63,102.39)	0.00	0.00
	SF_{API}	66	62.96				
Dense	SF_{DMS}	68	149.47	63.55	(35.64,92.72)	0.00	0.00
	SF_{API}	68	81.22				
Very Dense	SF_{DMS}	39	110.31	50.13	(14.18,93.29)	0.005	0.005
	SF_{API}	39	70.30				
Carbonate	SF_{DMS}	27	20.70	14.29	(2.61,60.02)	0.0046	0.0045
	SF_{API}	27	5.49				

The estimate for difference between the two capacity medians are 47.98, 67.16, 63.55, and 50.13 kPa for silica sand groups namely, Loose, Medium Dense, Dense, and Very Dense, respectively. The test on carbonate sand yielded a difference of 14.29 kPa. As for the Very Loose silica the attained significance level of 0.88 being larger than 0.05 indicates that the data does not support the hypothesis that there is difference between the capacity medians. Figure 14 displays the best fitted line plots of DMS versus API shaft friction after enhancement by the addition of the estimated difference shown in Table 13. It can be noticed in the figure how the new fitted lines have approached the average line. The overconservatism expressed as a factor (OCF) can be deduced from the figures as the ratio of the slope of the two fitted lines. Obviously, for the Very Loose silica sand, no adjusted

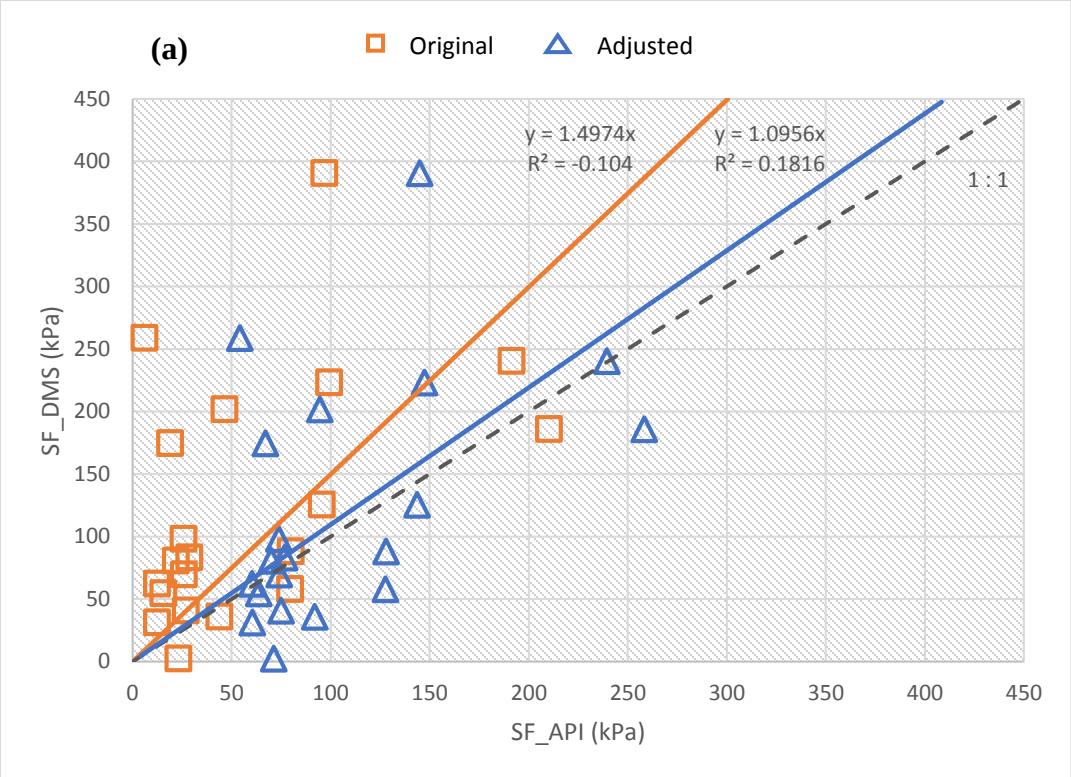

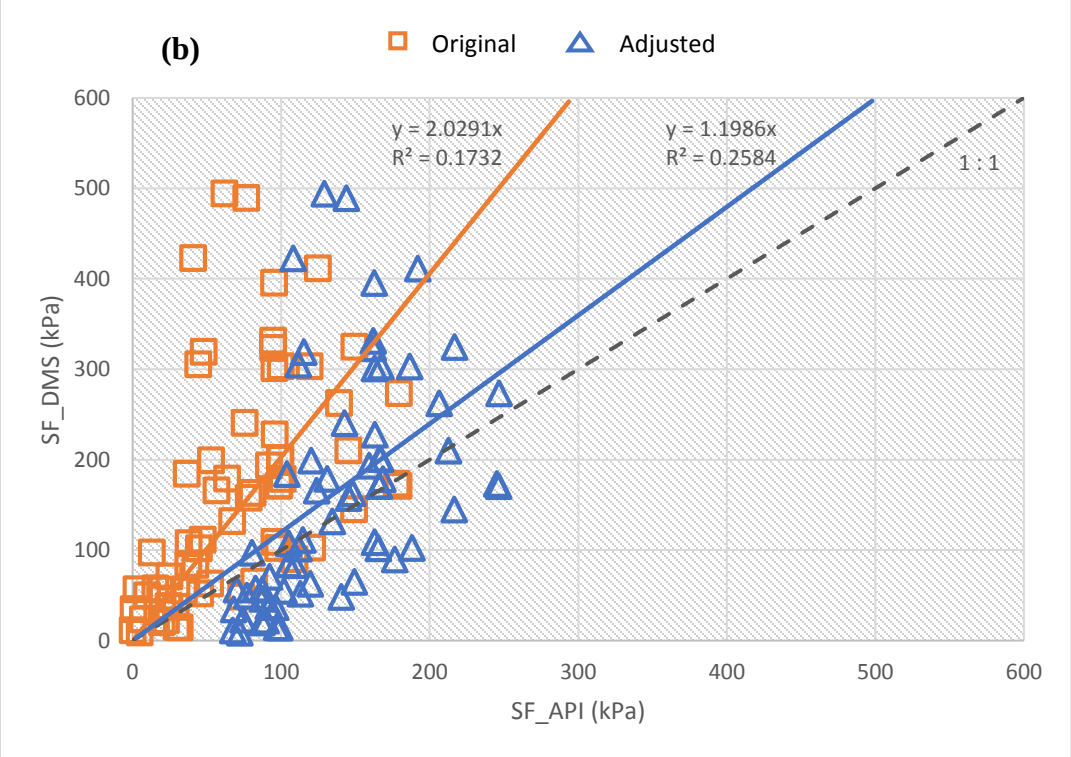

Figure 14: Best-fit line plot of DMS vs enhanced API shaft friction drawn through the origin for sand: (a) Loose, (b) Medium Dense, (c) Dense, (d) Very Dense, and (e) Carbonate Sand

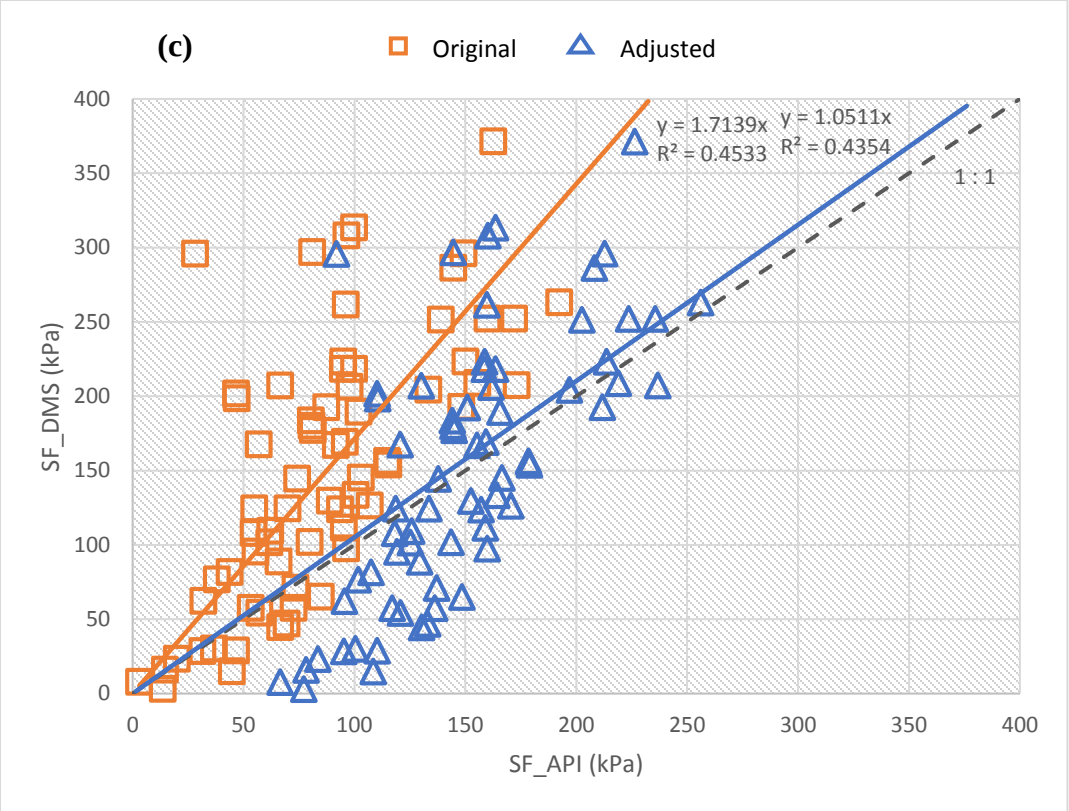

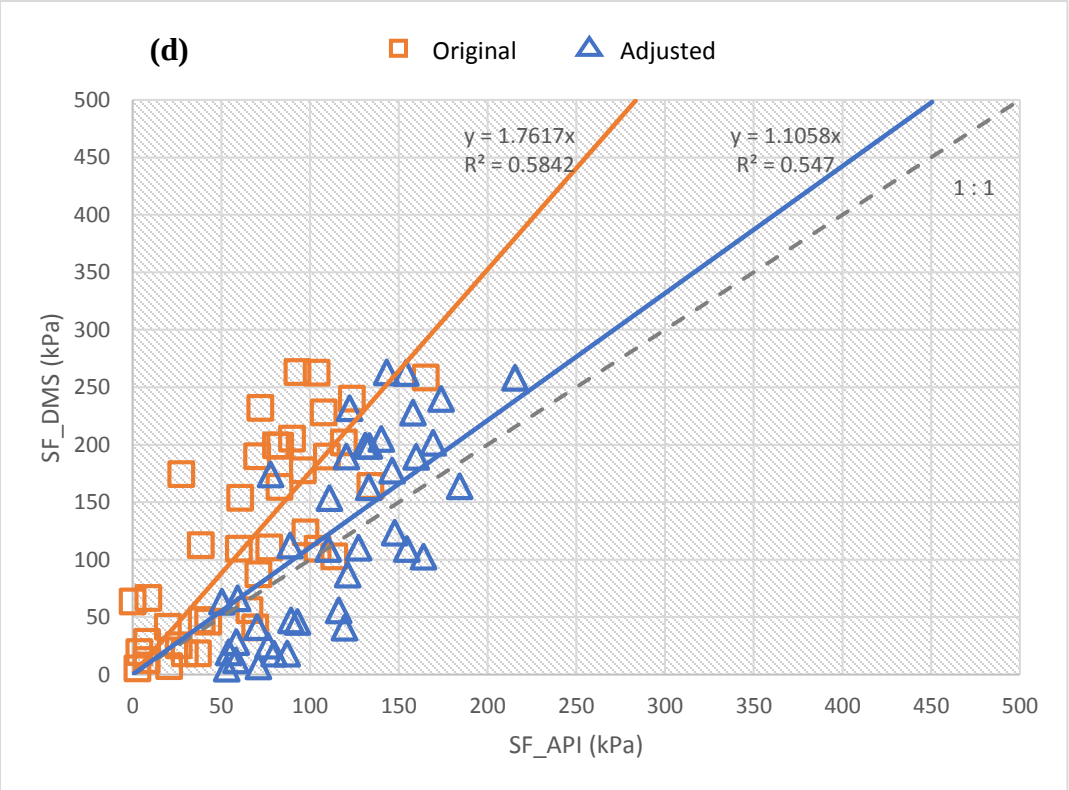

Figure 14 continued

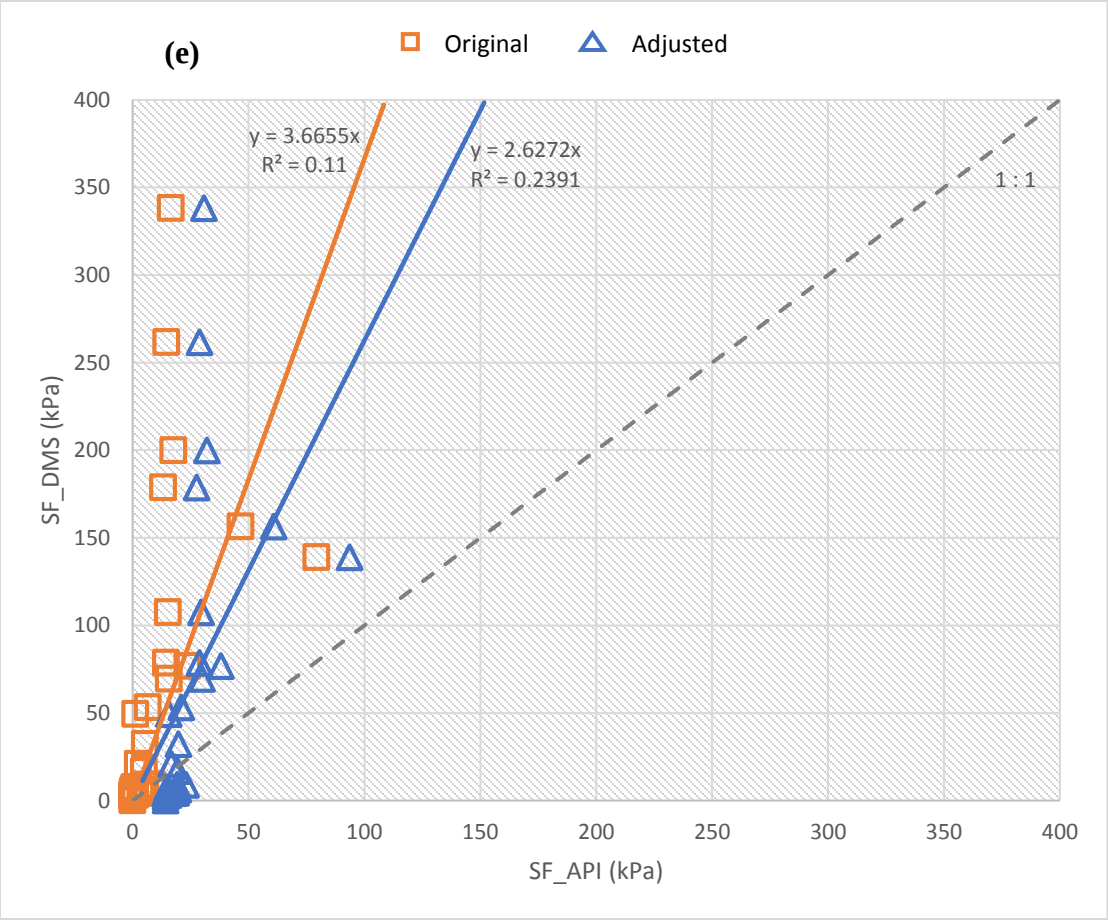

Figure 14 continued

overconservative factor (OCF) can be concluded as the nonparametric test results showed approximate equivalency of the two capacities. A summary of findings of the statistical analysis on silica and carbonate sand including the obtained and adjusted OCF is presented in Table 13.

Table 13: Summary of shaft friction evaluation results for silica and carbonate sand

Sand category	Statistical test	Test type	Result	Estimate for difference (kPa)	OCF	Adjusted OCF
Very Loose	Mann-Whitney	Nonparametric	$SF_{DMS} \approx SF_{API}$	–	2.36	–
Loose	Mann-Whitney	Nonparametric	$SF_{DMS} > SF_{API}$	47.98	1.50	1.10
Medium Dense	Mann-Whitney	Nonparametric	$SF_{DMS} > SF_{API}$	67.16	2.03	1.20
Dense	Mann-Whitney	Nonparametric	$SF_{DMS} > SF_{API}$	63.55	1.71	1.05
Very Dense	Mann-Whitney	Nonparametric	$SF_{DMS} > SF_{API}$	50.13	1.76	1.11
Carbonate	Mann-Whitney	Nonparametric	$SF_{DMS} > SF_{API}$	14.29	3.67	2.63

4.2.2 Statistical Analysis of Compiled Clay Layers

Tables 14 to 16 summarise the data of the three clay categories used in the analysis, namely OCR = 1, $1 < OCR \leq 4$, and $OCR > 4$. The α_{DMS} values are plotted against α_{API} for the three clay groups. Best-fit lines and R^2 are displayed on the plots as shown in Figure 15.

The α_{DMS} values that are smaller than 0.3 and greater than 3.0 are considered extreme or outliers, and therefore have been excluded from the plots and statistical analyses.

Figure 15 shows that alpha factors data are scattered and no sound correlation is observed between the two parameters. This is evidenced by the small value of R^2 attained in the three groups, with the third category (i.e., OCR > 4) having the least value. The presence of sand layers in the five offshore fields studied is predominant compared to clay strata; and therefore, compiled data of the clay is much less than that of the sand. This fact might as well have slightly affected the reliability of results of the statistical analyses performed on this category.

Similarly, the 2-sample rank test is carried out on the two datasets of α_{DMS} and α_{API} so as to evaluate the difference. The results are illustrated in Table 17. The attained level of significance shown in the table for clay layers with $1 < OCR \leq 4$, and OCR > 4, indicates that the null hypothesis is rejected, hence the two alpha factors are not equal. The difference is estimated at 0.1239 and 0.103 for the two groups, respectively. In contrast, for the first group with OCR = 1, the test yielded a significance level greater than 0.05, therefore, there is not sufficient evidence to reject the null hypothesis. In other words, the data do not support the hypothesis that there is difference between the two alpha factors.

Subsequently, the estimated difference is used to adjust the best-fit line of the α_{DMS} vs α_{API} relationship as presented in Figure 17. The obtained and adjusted overconservative factors are shown in Table 18.

Table 14: Analysis data of clay group with OCR = 1

Clay group: OCR = 1									
Location	**Depth range**		**Layer thickness (m)**	α_{DMS}	α_{API}	$\alpha_{API\ 2}$	$\alpha_{DMS}/\alpha_{API}$	$\alpha_{DMS}/\alpha_{API\ 2}$	**OCR**
F-4	0.00	12.80	12.80	1.20	1.46	1.39	0.85	0.96	1.00
F-5	20.00	21.00	1.00	1.07	0.89	0.89	1.20	1.21	1.43
F-7	0.00	3.10	3.10	1.66	1.41	0.91	1.18	1.83	1.00
F-9	3.00	3.70	0.70	2.11	1.16	0.33	1.82	6.42	1.00
F-9	37.50	42.10	4.60	1.10	0.85	0.97	1.30	1.14	1.36
F-8	6.00	12.00	6.00	3.27	2.05	1.19	1.59	2.74	1.00
F-13	3.00	6.00	3.00	0.11	0.95	0.85	0.11	0.14	1.16
J-1	41.30	43.50	2.20	1.37	0.87	0.48	1.57	2.86	1.33
J-2	2.00	2.40	0.40	0.97	1.34	0.44	0.72	2.21	1.00
J-2	38.00	39.10	1.10	2.67	1.44	1.06	1.86	2.52	1.00
J-2	55.50	66.00	10.50	0.40	1.12	0.77	0.36	0.53	1.00
J-2	38.00	39.10	1.10	4.44	1.46	1.07	3.05	4.17	1.00
J-4	62.80	65.00	2.20	0.13	0.84	0.59	0.16	0.23	1.41
Y-3	5.50	6.50	1.00	3.58	1.71	1.03	2.09	3.48	1.00
Y-7	44.50	49.80	5.30	0.57	0.89	0.63	0.64	0.90	1.20
Y-10	31.10	33.10	2.00	0.74	1.04	0.73	0.72	1.02	1.00

Table 15: Analysis data of clay group with 1 < OCR ≤ 4

Clay group: 1 < OCR ≤ 4									
Location	**Depth range**		**Layer thickness (m)**	α_{DMS}	α_{API}	$\alpha_{API\ 2}$	$\alpha_{DMS}/\alpha_{API}$	$\alpha_{DMS}/\alpha_{API\ 2}$	**OCR**
F-4	20.85	22.40	1.55	1.09	0.53	0.51	2.04	2.14	2.47
F-8	20.50	27.00	6.50	0.59	0.49	0.48	1.20	1.22	3.54
F-8	27.00	28.50	1.50	1.04	0.52	0.50	2.00	2.06	3.06
F-8	28.50	31.50	3.00	1.08	0.54	0.53	2.00	2.06	2.86
F-9	16.50	21.00	4.50	0.59	0.49	0.27	1.20	2.20	3.63
F-9	32.90	36.00	3.10	0.88	0.68	0.64	1.30	1.37	2.04
F-9	37.50	42.10	4.60	1.17	0.82	0.90	1.43	1.30	1.45
F-12	21.00	27.00	6.00	1.32	0.56	0.55	2.36	2.42	2.78
J-1	10.80	12.50	1.70	0.32	0.58	0.44	0.55	0.73	2.87
J-1	29.20	33.00	3.80	0.78	0.71	0.47	1.09	1.61	1.94
J-1	34.80	39.10	4.30	0.79	0.59	0.45	1.35	1.75	2.66
J-2	32.80	35.20	2.40	0.30	0.61	0.46	0.50	0.66	2.46
J-2	48.00	51.60	3.60	0.94	0.77	0.52	1.22	1.80	1.66
J-2	51.60	54.00	2.40	0.91	0.80	0.55	1.14	1.65	1.57
J-2	28.30	29.30	1.00	0.55	0.61	0.44	0.89	1.25	2.46
J-2	32.80	35.20	2.40	0.85	0.61	0.37	1.39	2.39	2.46
J-2	48.00	51.60	3.60	0.29	0.78	0.54	0.37	0.53	1.63
J-3	43.50	46.00	2.50	0.91	0.50	0.47	1.84	1.96	3.65
J-3	47.20	50.00	2.80	0.83	0.57	0.58	1.45	1.42	2.96
J-3	51.00	60.05	9.05	0.35	0.55	0.51	0.65	0.69	2.94
J-3	51.00	60.05	9.05	0.31	0.56	0.54	0.55	0.57	2.84
J-3	51.00	60.05	9.05	0.27	0.57	0.58	0.47	0.46	2.71
J-3	19.40	30.00	10.60	0.32	0.49	0.52	0.66	0.62	4.03
J-3	43.50	46.00	2.50	0.73	0.50	0.50	1.45	1.47	3.56
J-3	47.20	50.00	2.80	0.98	0.57	0.35	1.71	5.03	2.95
J-3	51.00	60.05	9.05	0.87	0.55	0.45	1.58	1.98	2.93
J-4	23.80	27.00	3.20	0.47	0.59	0.45	0.79	1.04	2.64

Table 15 continued

J-4	32.00	36.00	4.00	0.60	0.64	0.47	0.93	1.28	2.28
J-4	38.00	43.00	5.00	0.41	0.60	0.46	0.68	0.89	2.60
J-4	45.90	46.50	0.60	0.42	0.68	0.50	0.62	0.84	2.13
J-4	46.50	50.00	3.50	0.35	0.63	0.47	0.55	0.74	2.42
Y-3	4.80	5.50	0.70	0.74	0.78	0.55	0.94	1.33	1.65
Y-3	15.00	17.00	2.00	0.55	0.67	0.45	0.82	1.21	2.07
Y-4	23.00	25.50	2.50	1.35	0.62	0.60	2.17	2.26	3.50
Y-7	12.00	21.00	9.00	0.50	0.55	0.43	0.91	1.15	3.27
Y-7	23.00	24.00	1.00	0.87	0.78	0.54	1.12	1.59	1.72
Y-7	25.50	29.50	4.00	1.11	0.82	0.56	1.36	1.98	1.54
Y-7	36.60	40.50	3.90	0.51	0.81	0.52	0.63	0.99	1.52
Y-8	15.50	16.80	1.30	0.27	0.52	0.42	0.51	0.63	3.72
Y-9	20.20	24.00	3.80	0.36	0.51	0.40	0.71	0.90	3.65
Y-10	49.30	50.30	1.00	0.36	0.71	0.50	0.50	0.72	1.94
Y-10	63.90	66.80	2.90	0.41	0.76	0.55	0.54	0.74	1.60
Y-11	10.00	13.50	3.50	0.38	0.55	0.44	0.68	0.86	3.12
U-2	11.60	14.20	2.60	1.87	0.56	0.40	3.34	4.66	3.21
U-5	8.60	15.60	7.00	0.38	0.66	0.48	0.57	0.79	2.29
U-5	16.50	19.00	2.50	0.43	0.67	0.48	0.64	0.89	2.25
U-5	24.50	29.50	5.00	0.58	0.73	0.51	0.79	1.12	1.86
U-5	32.30	35.50	3.20	1.03	0.75	0.52	1.38	1.97	1.78
U-5	44.00	47.60	3.60	0.67	0.74	0.52	0.89	1.27	2.03
U-5	50.00	50.50	0.50	0.51	0.78	0.40	0.66	1.27	1.67
U-7	34.40	35.50	1.10	1.75	0.71	0.68	2.48	2.57	1.78
U-7	35.50	38.50	3.00	0.71	0.48	0.49	1.48	1.46	3.83
U-7	39.60	43.00	3.40	1.59	0.58	0.53	2.73	3.04	2.67
U-7	46.50	51.00	4.50	1.54	0.70	0.65	2.22	2.45	2.12
U-7	52.00	60.15	8.15	0.44	0.63	0.54	0.71	0.82	2.16

Table 16: Analysis data of clay group with OCR > 4

Clay group: OCR > 4									
Location	**Depth range**		**Layer thickness (m)**	α_{DMS}	α_{API}	$\alpha_{API\ 2}$	$\alpha_{DMS}/\alpha_{API}$	$\alpha_{DMS}/\alpha_{API\ 2}$	**OCR**
F-2	8.30	10.45	2.15	0.83	0.45	0.37	1.85	2.34	5.65
F-8	18.00	20.50	2.50	0.96	0.46	0.45	2.08	2.12	4.17
F-9	10.20	13.40	3.20	0.74	0.44	0.41	1.67	1.83	5.25
J-3	19.40	30.00	10.60	0.26	0.47	0.45	0.55	0.57	4.74
J-3	30.00	37.50	7.50	0.38	0.47	0.46	0.80	0.81	4.52
J-3	30.00	37.50	7.50	0.41	0.47	0.47	0.86	0.84	4.49
Y-4	18.00	20.50	2.50	0.58	0.58	0.57	1.01	1.03	4.30
Y-5	21.60	22.75	1.15	0.44	0.49	0.38	0.89	1.15	57.16
Y-7	12.00	21.00	9.00	0.45	0.49	0.41	0.91	1.10	4.09
Y-8	6.60	8.10	1.50	0.27	0.44	0.35	0.61	0.77	5.73
Y-9	10.30	13.50	3.20	0.37	0.47	0.38	0.78	0.97	4.96
Y-9	15.50	17.20	1.70	0.34	0.48	0.39	0.73	0.89	4.41
U-1	3.00	3.90	0.90	0.51	0.37	0.18	1.37	2.79	23.00
U-2	5.00	8.50	3.50	0.58	0.38	0.31	1.52	1.85	10.37
U-3	1.50	3.20	1.70	0.39	0.32	0.16	1.24	2.45	18.75
U-3	12.20	14.00	1.80	0.99	0.50	0.43	2.00	2.33	4.16
U-3	16.20	21.90	5.70	0.59	0.47	0.39	1.28	1.52	5.13
U-4	12.25	16.20	3.95	0.87	0.46	0.38	1.88	2.26	5.13
U-6	7.40	8.40	1.00	1.38	0.43	0.35	3.18	3.92	6.27

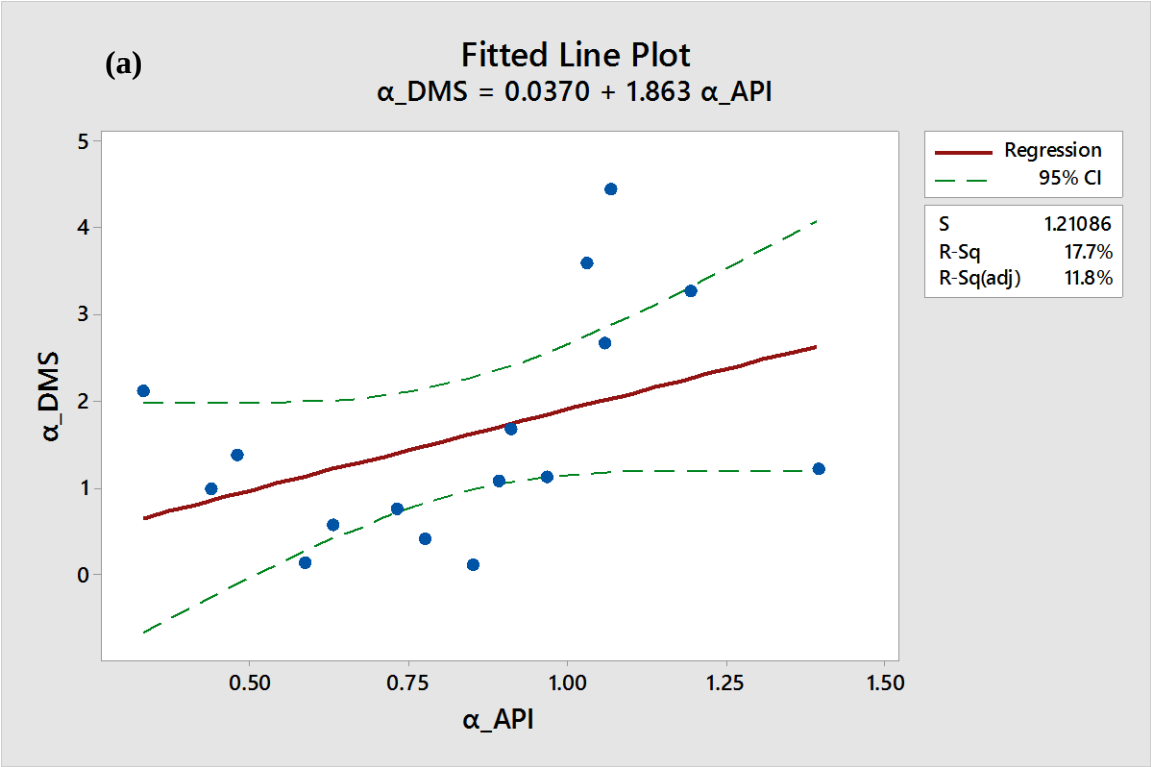

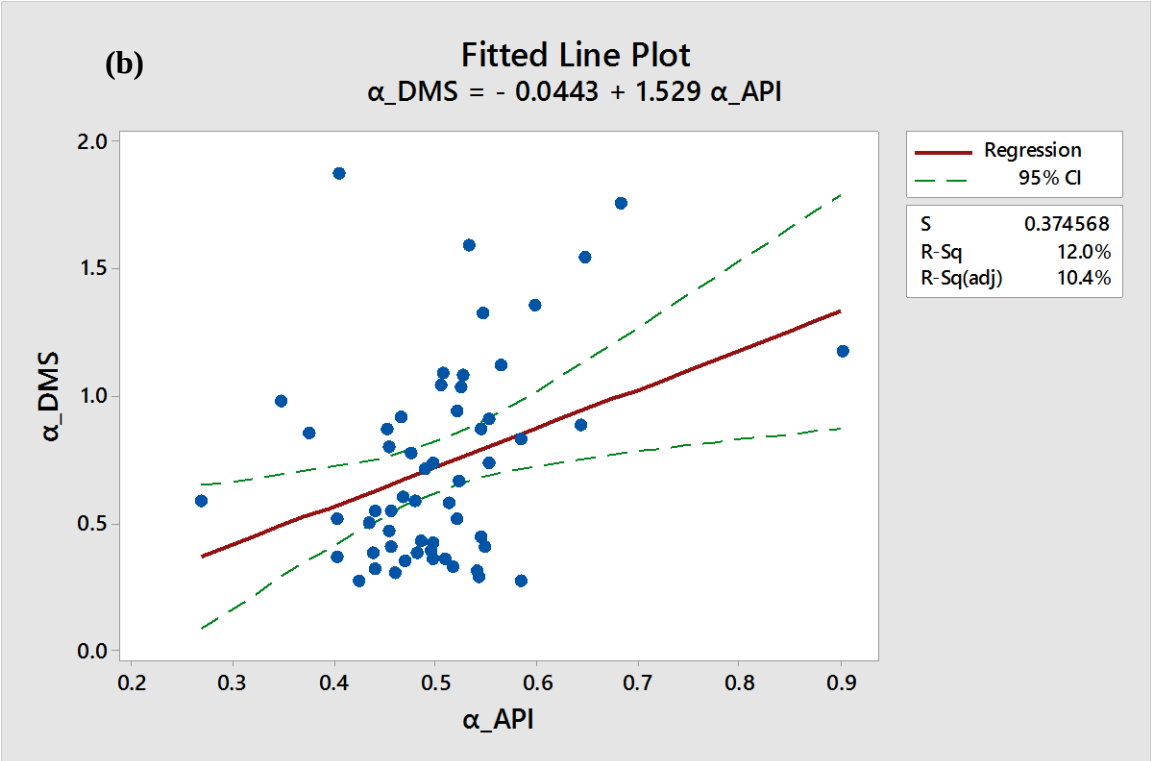

Figure 15: Best-fit line plot of α_{DMS} vs α_{API} with 95% confidence interval coefficients for clay: (a) OCR = 1, (b) 1 < OCR ≤ 4, and (c) OCR > 4

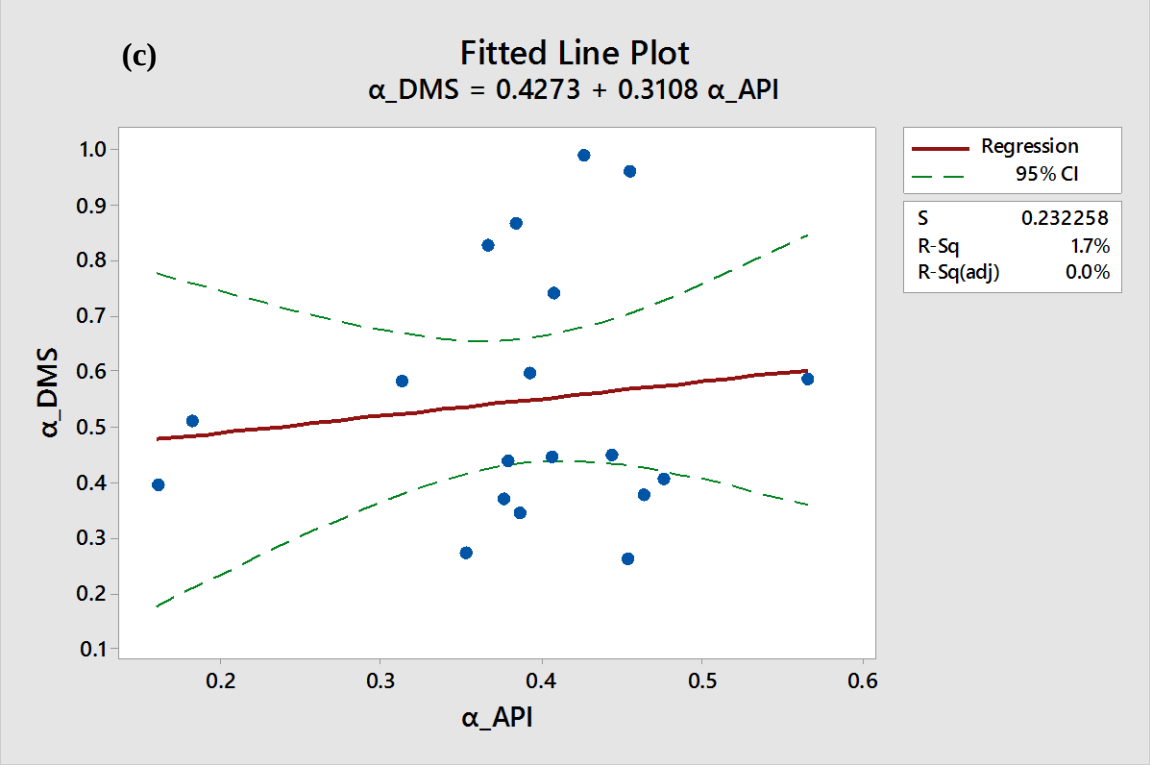

Figure 15 continued

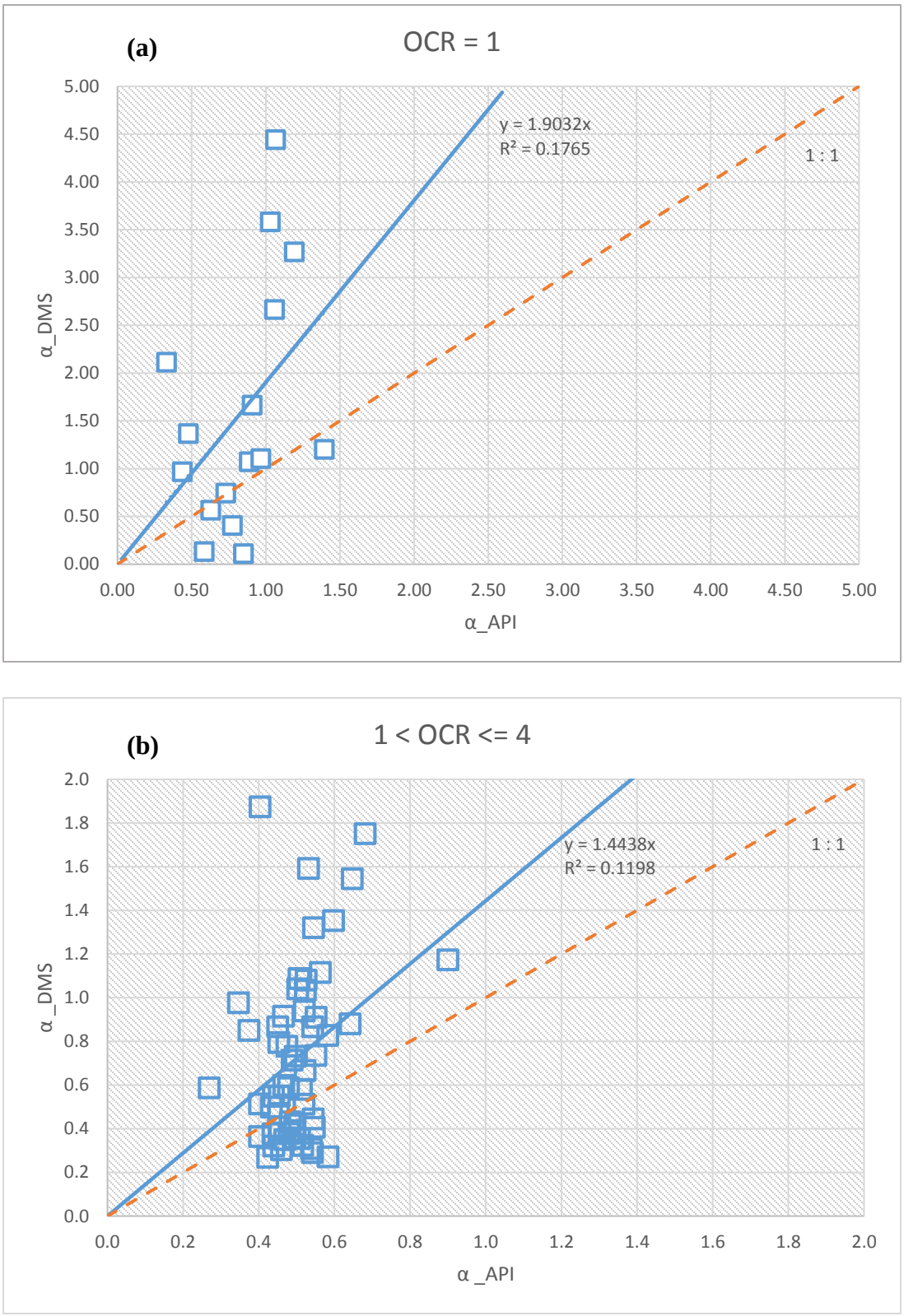

Figure 16: Fitted line plot of α_{DMS} vs α_{API} for different clay groups: (a) OCR = 1, (b) 1 < OCR ≤ 4, and (c) OCR > 4

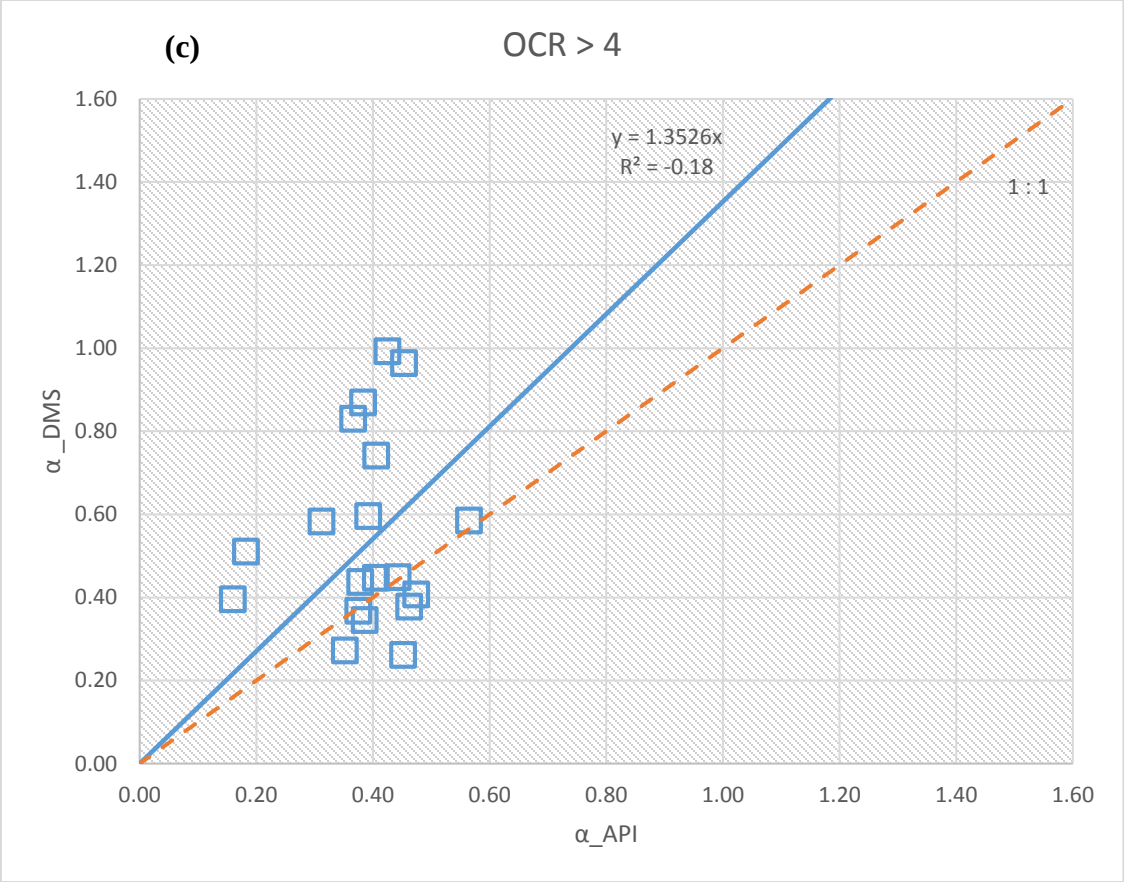

Figure 16 continued

Table 17: Summary of Mann-Whitney test results on α_{DMS} and α_{API} for clay

Clay group	Population	N	η	Point estimate of $\alpha_{DMS} - \alpha_{API}$	95 % CI	Sig. level
OCR = 1	α_{DMS}	16	1.153	0.378	(-0.063,1.206)	0.08
	α_{API}	16	0.869			
1 < OCR ≤ 4	α_{DMS}	56	0.5919	0.1239	(0.0153,0.2792)	0.021
	α_{API}	56	0.4969			
OCR > 4	α_{DMS}	19	0.4477	0.103	(0.0005,0.2424)	0.044
	α_{API}	19	0.3926			

Table 18: Summary of alpha factor evaluation results for clay

Clay category	Statistical test	Test type	Result	Estimate for difference	OCF	Adjusted OCF
OCR =1	Mann-Whitney	Nonparametric	$\alpha_{DMS} \approx \alpha_{API}$	–	1.90	–
1 < OCR ≤ 4	Mann-Whitney	Nonparametric	$\alpha_{DMS} > \alpha_{API}$	0.1239	1.44	1.16
OCR > 4	Mann-Whitney	Nonparametric	$\alpha_{DMS} > \alpha_{API}$	0.103	1.35	1.09

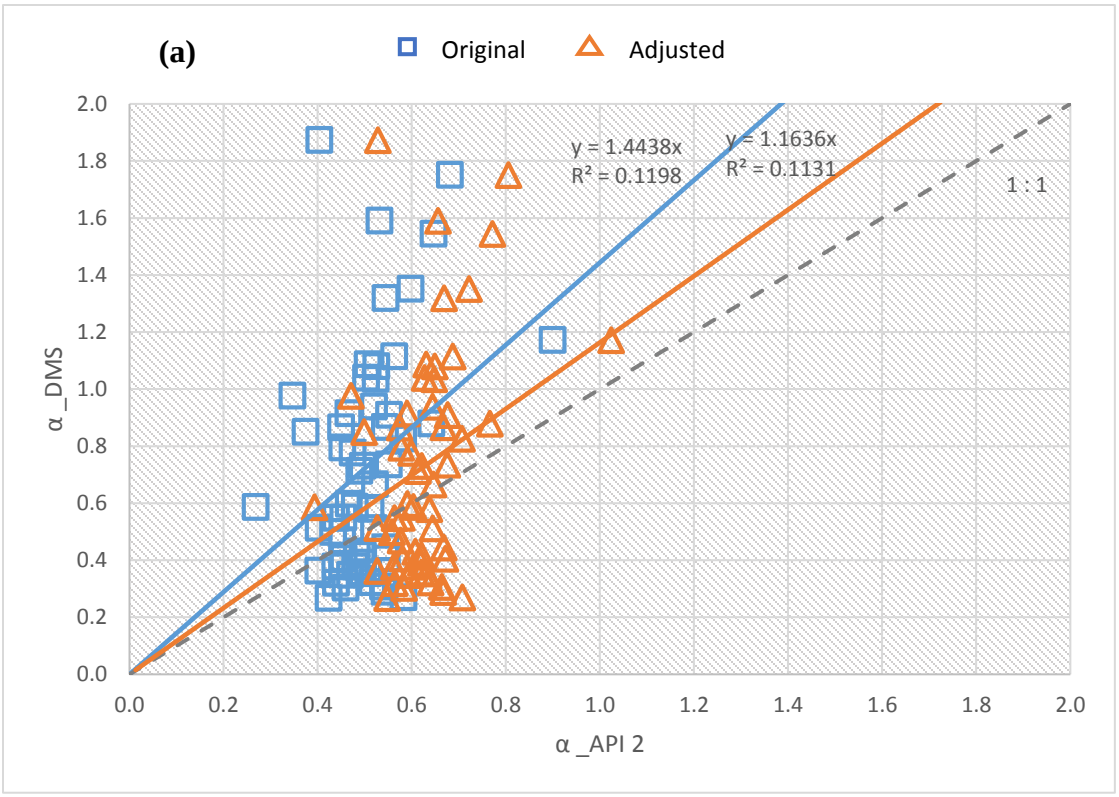

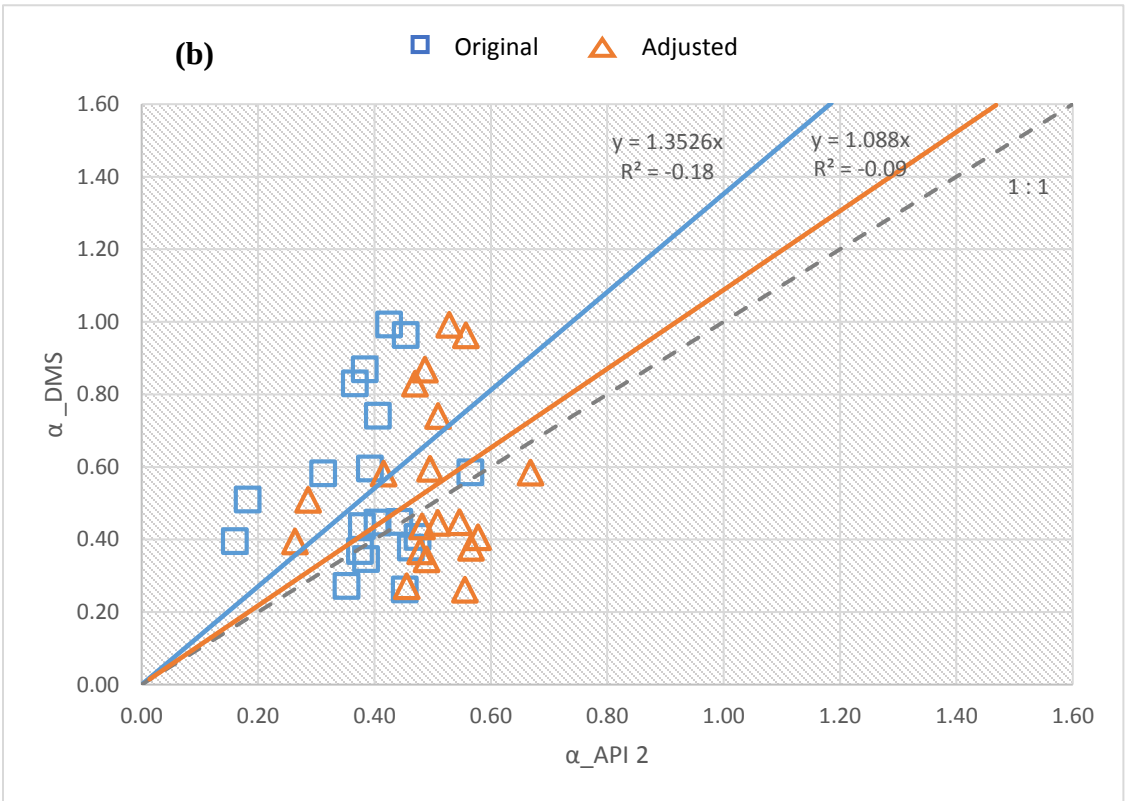

Figure 17: Best-fit line plot of α_{DMS} vs enhanced α_{API} for different clay groups: (a) 1 < OCR ≤ 4, and (b) OCR > 4

4.3 Experimental Programme

This section discusses the results obtained from the experimental programme conducted on marine calcareous sand samples.

4.3.1 Crushability of Calcareous Sand

Figure 18 shows the grain size distribution curves of the seven calcareous sand samples studied. As can be observed, samples AB-2, AB-3, and AB-4 exhibited some sort of gab gradation. In other words, they tend to have a uniform grain size.

The one-dimensional compression test is performed on a selected grading consisting of coarse particles sized 0.425 – 2 mm so that the crushing could be properly observed. Figures 19 to 25 illustrate grain size distribution curves of sand samples tested before and after crushing, and also the corresponding stress-displacement relationship curve. The stress-displacement curves demonstrate that there is no conspicuous failure point. This can be attributed to the confinement effect offered by the boundaries of the oedometer ring. The curves also show that all samples exhibited a work-hardening behaviour which is typical of loose sands as reported by Holtz and Kovacs [54]. This attained behaviour is plausible since samples were prepared by loosely placing them in the oedometer ring and perform slight tapping.

The degree of crushing, D_c, is calculated by determining the area between the two gradation curves, before and after crushing. For each sample, Microsoft Excel has been used to generate best-fit models for gradation curves and then MATLAB is employed to calculate

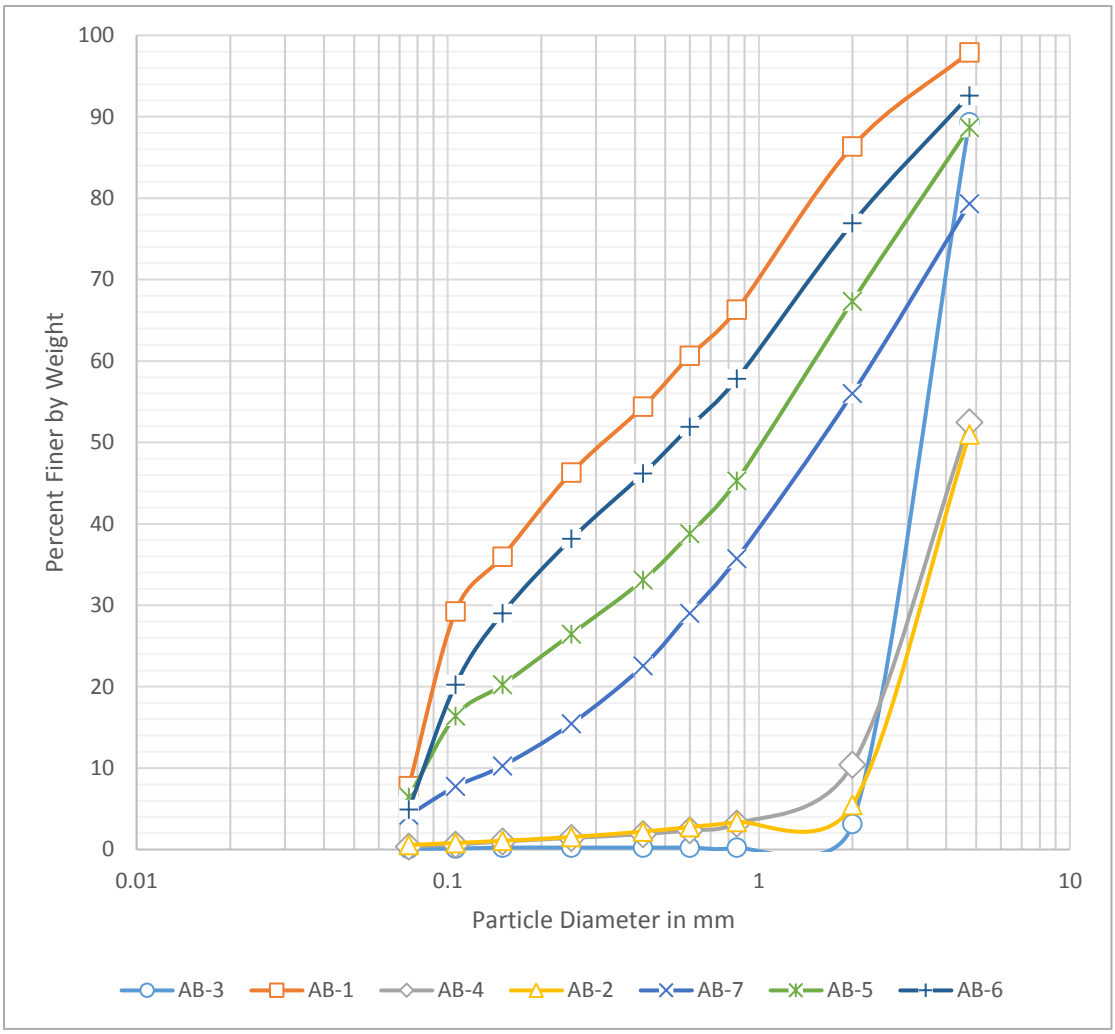

Figure 18: Grain size distribution curves of the calcareous sand samples tested

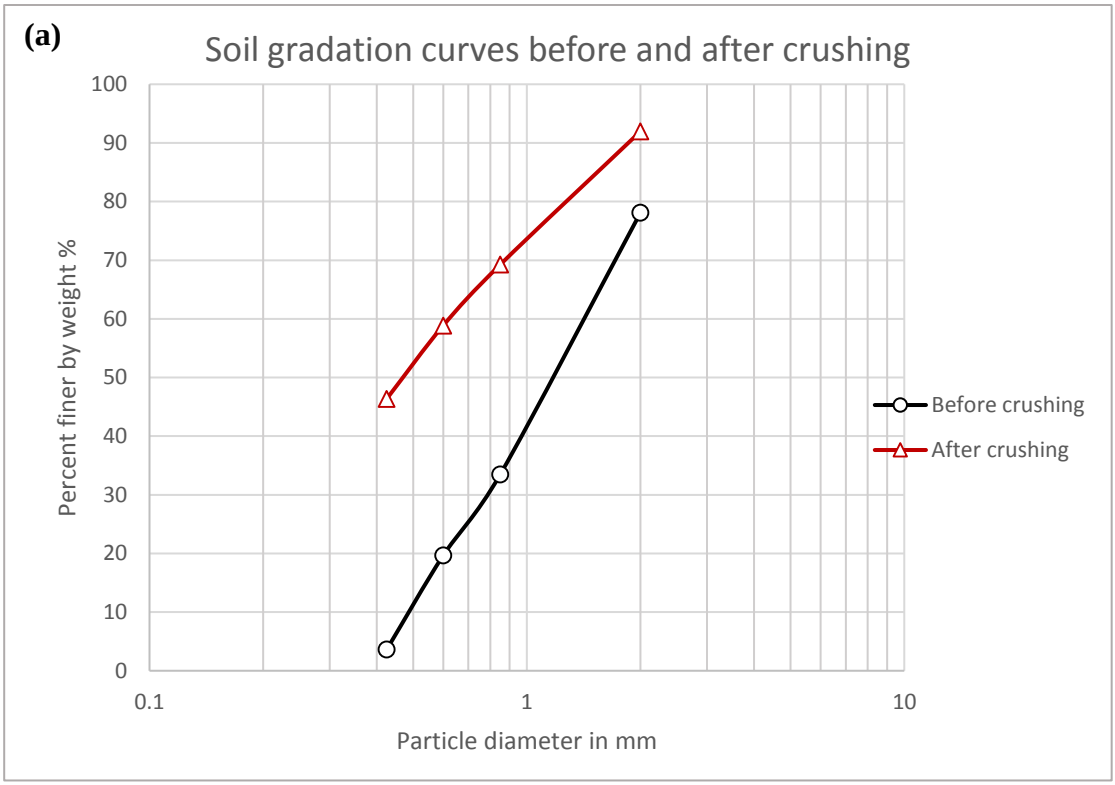

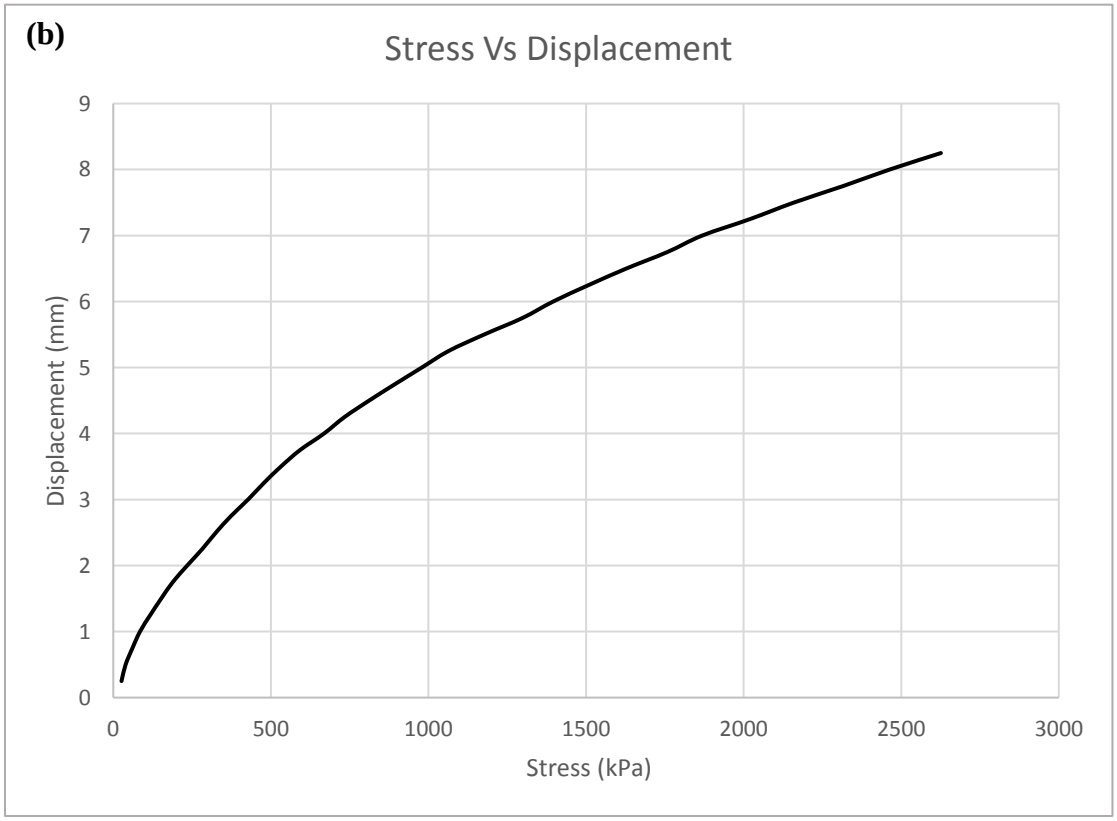

Figure 19: Crushability evaluation tests on sample AB-1 (a) Gradation curves before and after crushing, (b) stress-displacement curve

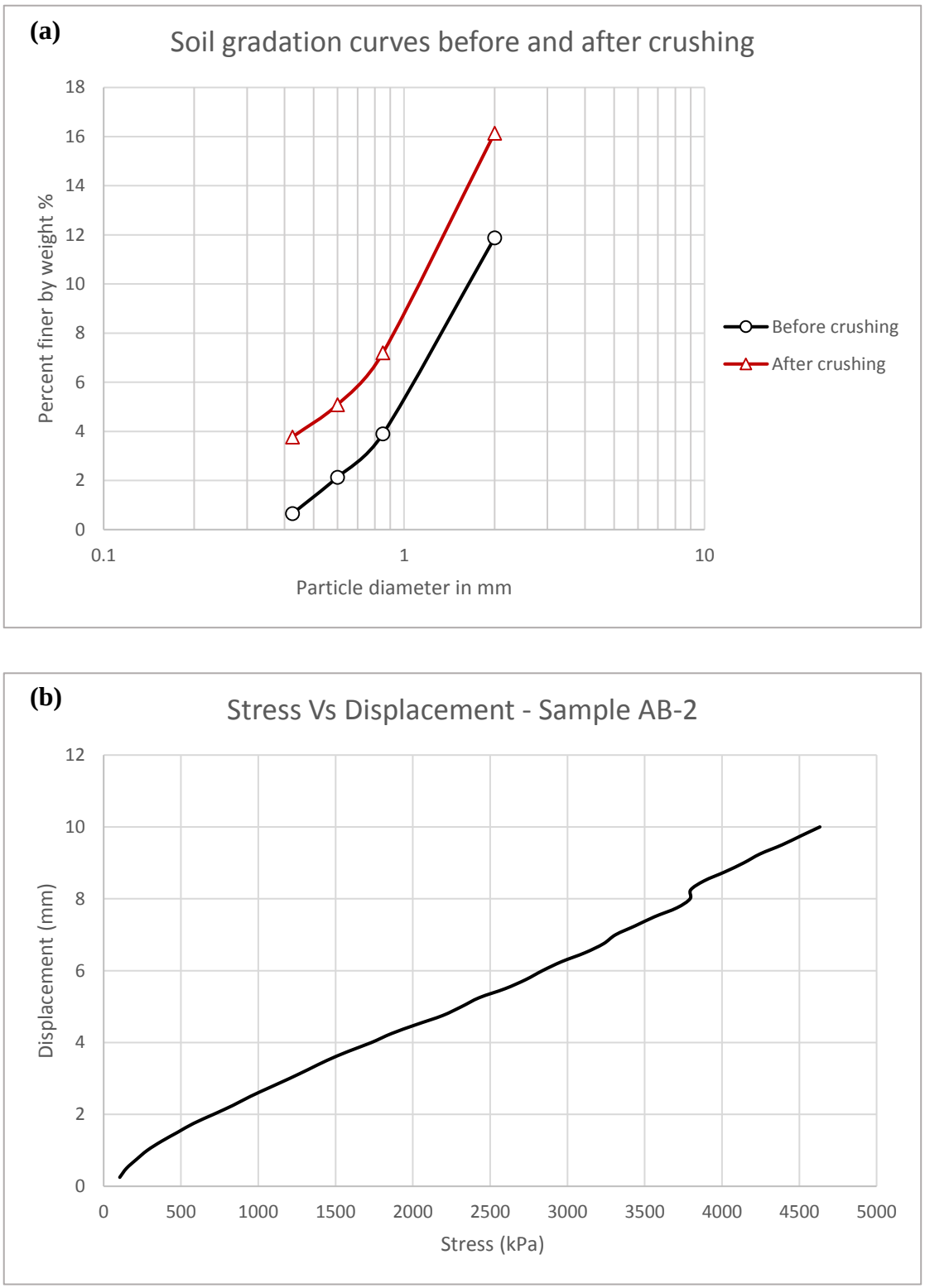

Figure 20: Crushability evaluation tests on sample AB-2 (a) Gradation curves before and after crushing, (b) stress-displacement curve

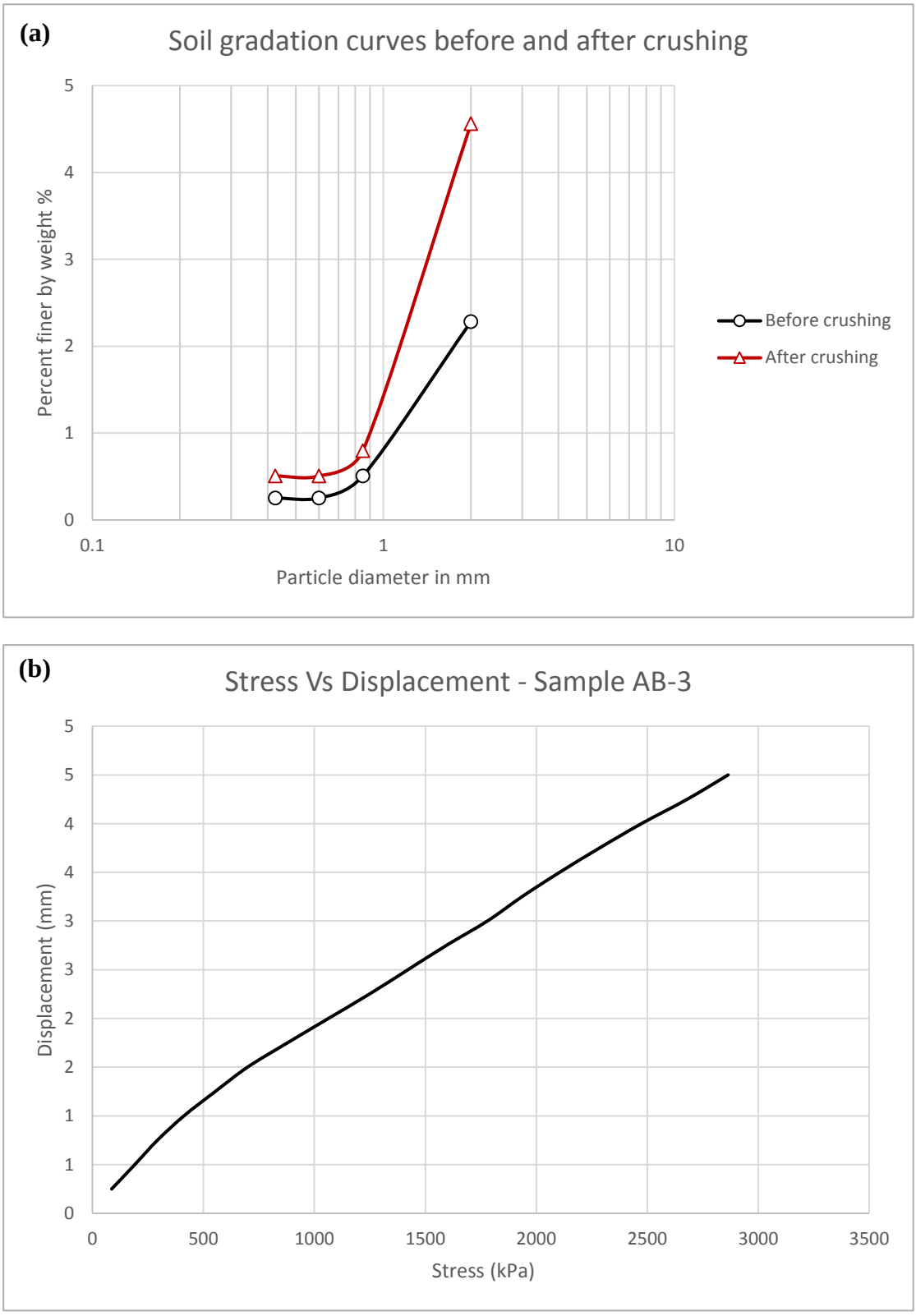

Figure 21: Crushability evaluation tests on sample AB-3 (a) Gradation curves before and after crushing, (b) stress-displacement curve

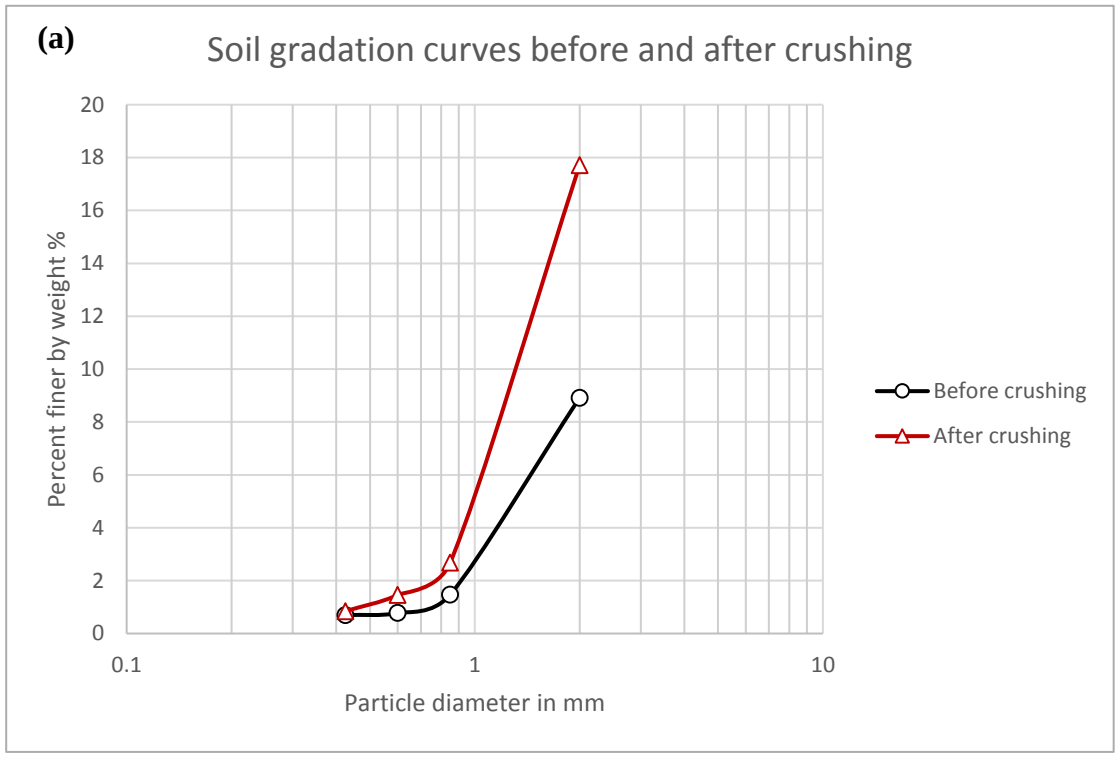

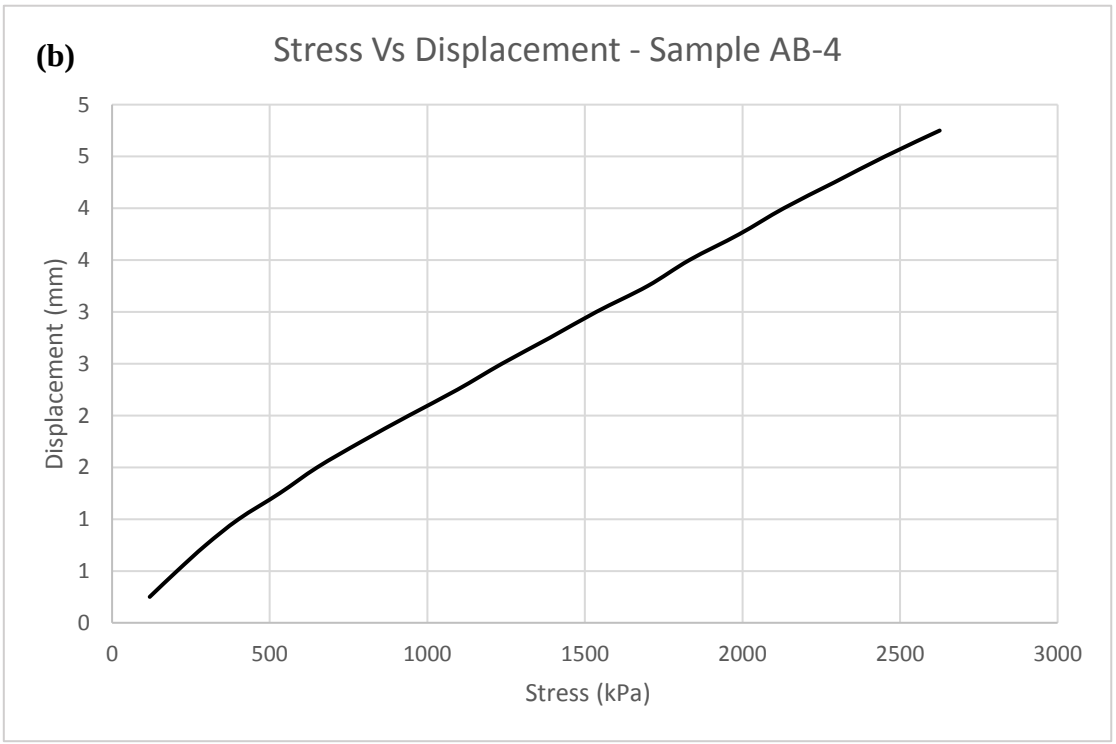

Figure 22: Crushability evaluation tests on sample AB-4 (a) Gradation curves before and after crushing, (b) stress-displacement curve

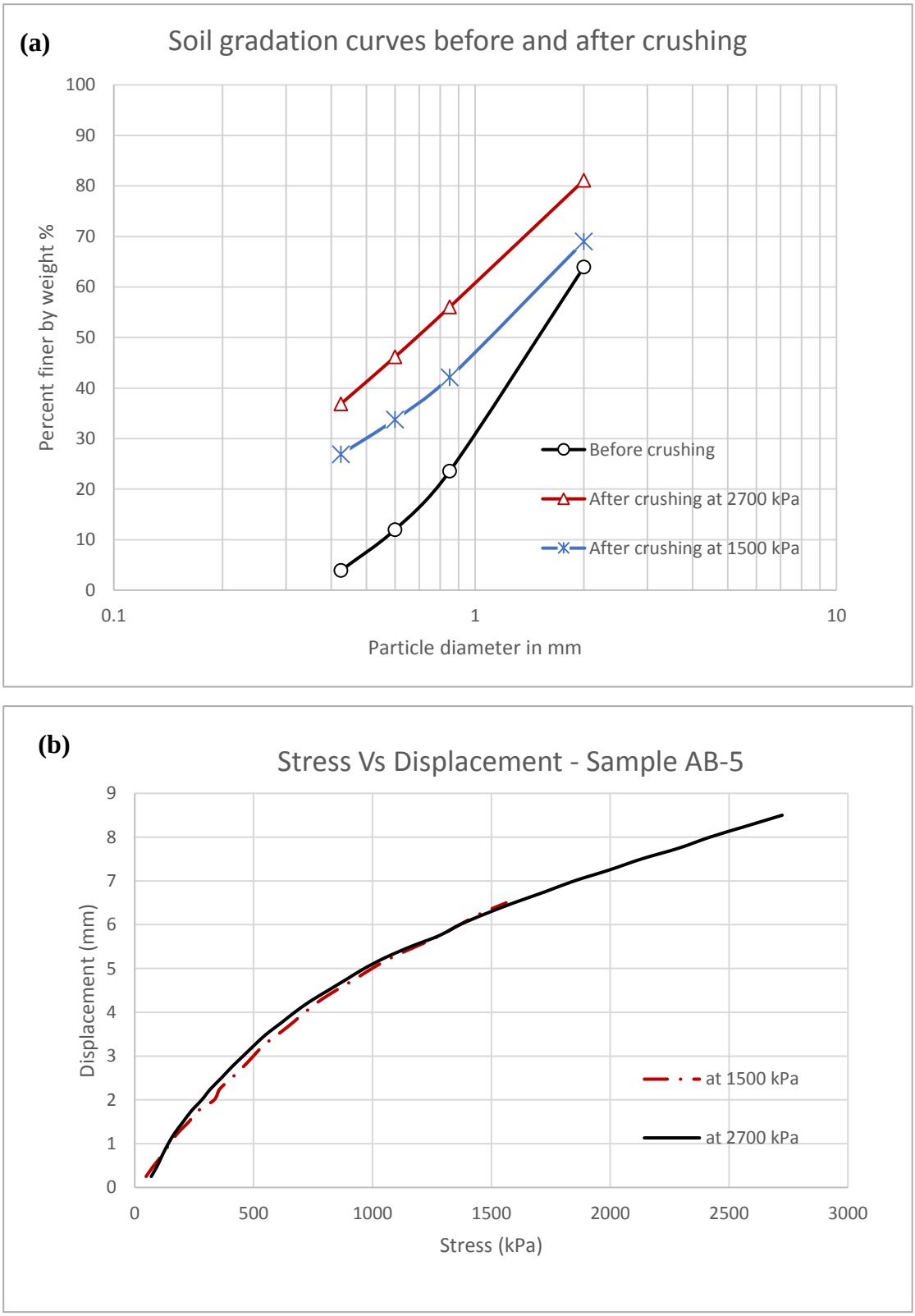

Figure 23: Crushability evaluation tests on sample AB-5 (a) Gradation curves before and after crushing at different stress levels, (b) stress-displacement curves

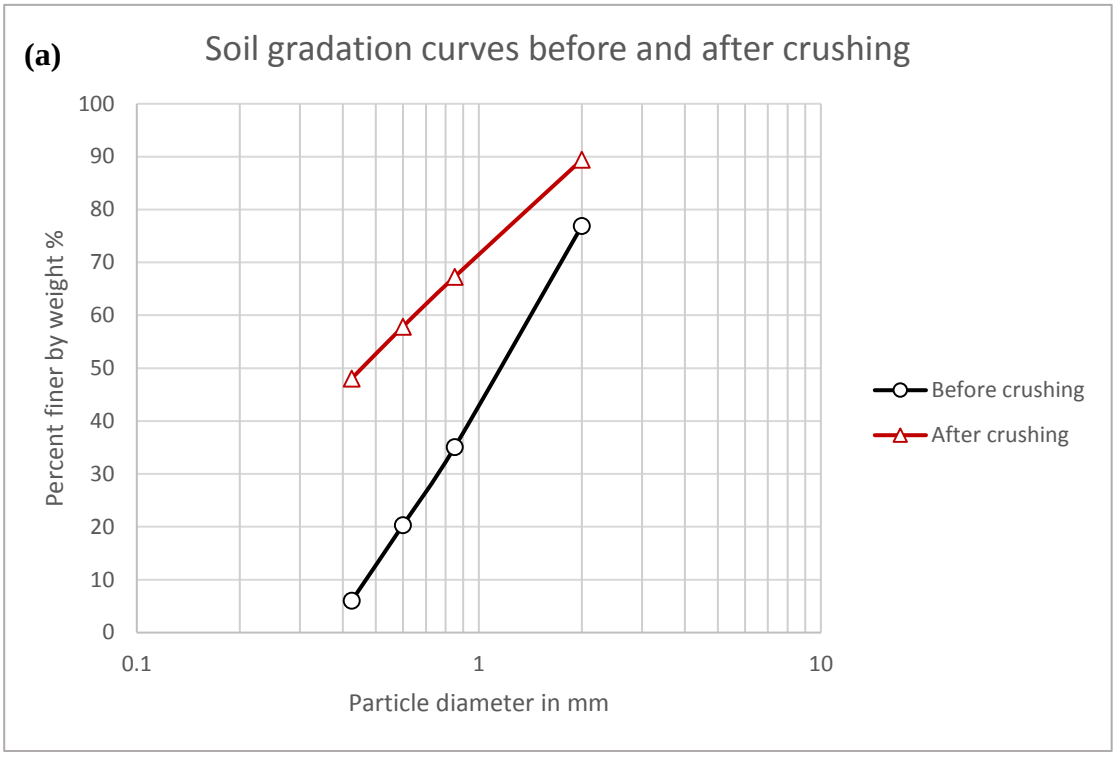

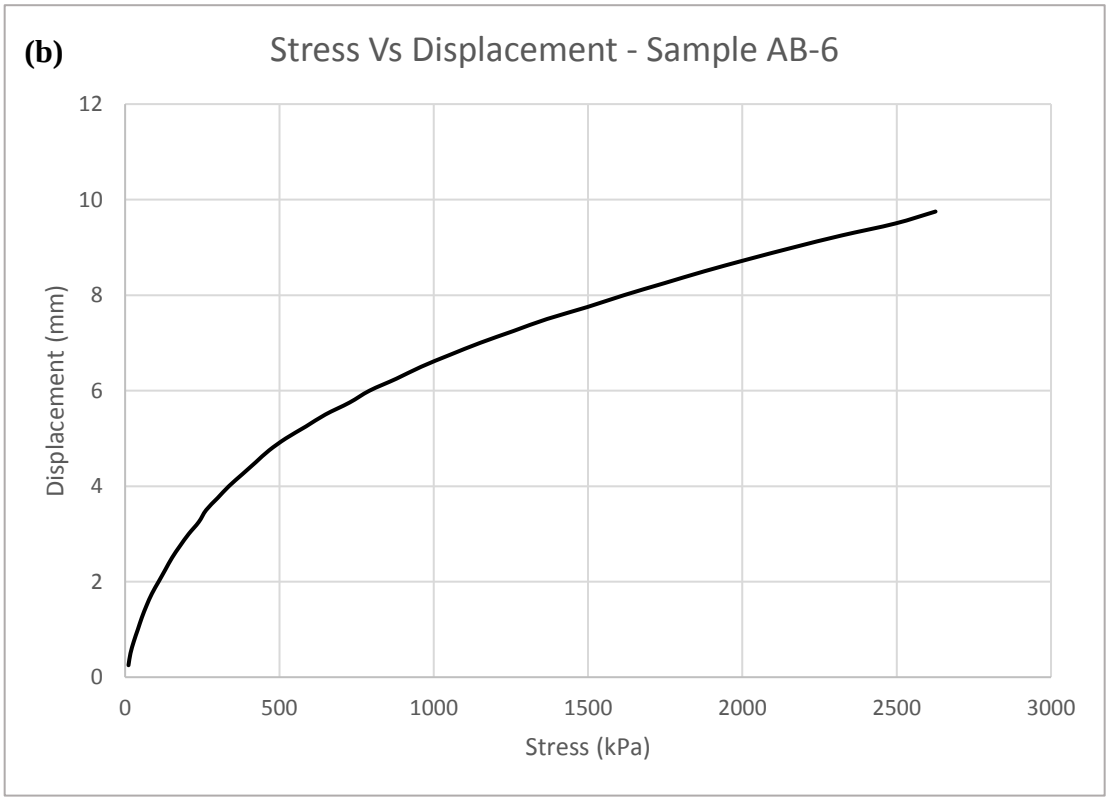

Figure 24: Crushability evaluation tests on sample AB-6 (a) Gradation curves before and after crushing, (b) stress-displacement curve

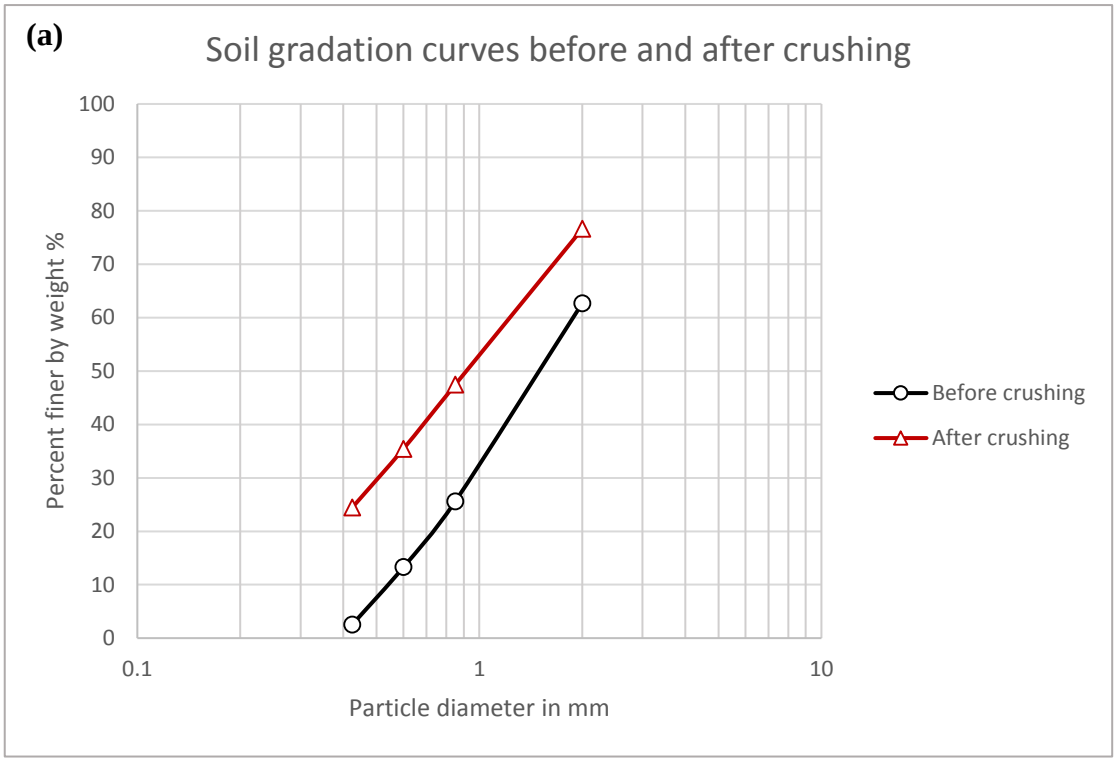

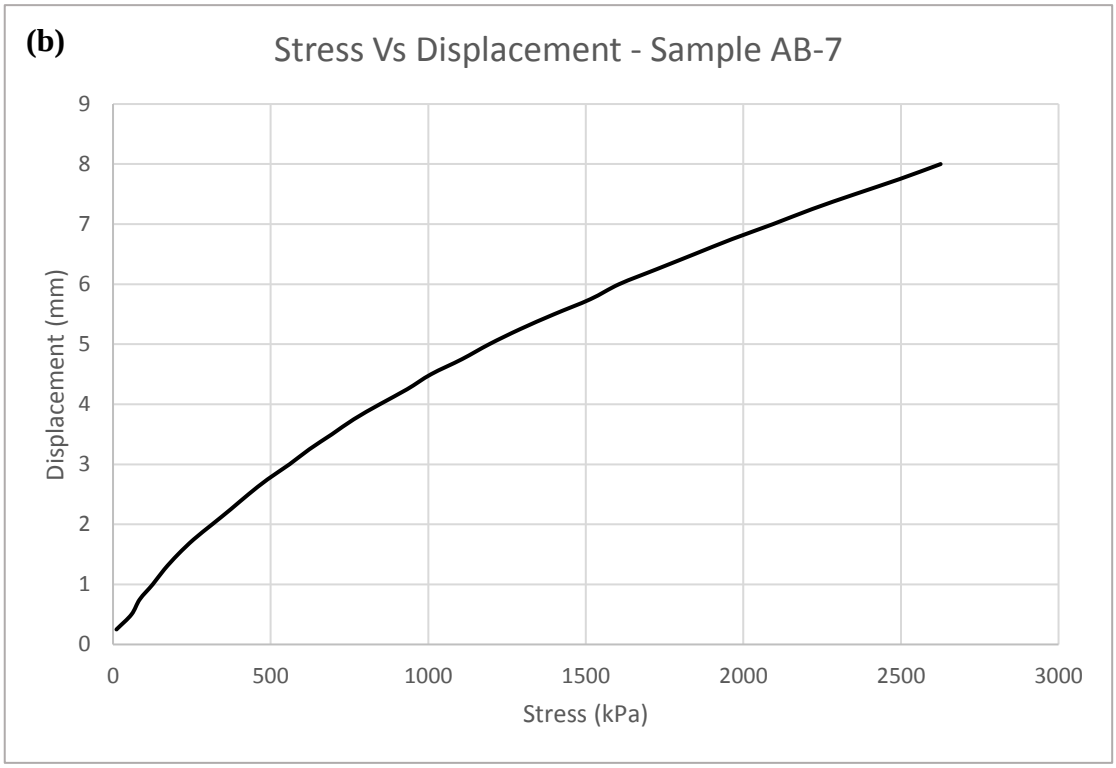

Figure 25: Crushability evaluation tests on sample AB-7 (a) Gradation curves before and after crushing, (b) stress-displacement curve

the area by integration. Other simpler approaches to evaluate the degree of crushing do exist as discussed earlier in chapter 2. Notwithstanding, their applicability are not within the realms of possibility. For instance, the crushing coefficient C_c of Datta et al. [50] utilises D_{10} which cannot be determined for both curves in most samples. For each sand sample Table 19 gives the equation for each curve, the area under the curves, A, and the area between the gradation curves designated as D_c.

Table 19: Degree of crushing, D_c expressed as the area between the gradation curves before and after crushing

Sample	Curve equations[1]	A	D_c
AB-1	$y_1 = 34.644x^3 - 135.133x^2 + 182.37x - 9.409$ $y_0 = 46.977x^3 - 173.83x^2 + 232.53x - 67.426$	114.85 66.29	48.56
AB-2	$y_1 = -1.6385x^3 + 5.1951x^2 + 3.4974x + 1.473$ $y_0 = 2.0869x^3 - 7.2806x^2 + 14.283x - 4.2663$	16.178 9.6586	6.52
AB-3	$y_1 = -0.7714x^3 + 4.1724x^2 - 3.663x + 1.3692$ $y_0 = -1.2754x^3 + 4.7781x^2 - 3.8828x + 1.139$	3.1016 1.9067	1.20
AB-4	$y_1 = 1.6068x^3 + 0.2868x^2 + 1.9333x - 0.1533$ $y_0 = -1.8382x^3 + 8.9707x^2 - 7.2895x + 2.317$	10.6221 6.0823	4.54
AB-5	$y_1 = 12.36x^3 - 55.243x^2 + 99.883x + 3.4567$ $y_0 = -4.8639x^3 + 8.888x^2 + 41.065x - 14.805$ $y_2 = 4.2742x^3 - 21.866x^2 + 58.26x + 5.762$	99.6277 59.1614 79.6457	40.47 20.48
AB-6	$y_1 = 19.079x^3 - 78.982x^2 + 121.81x + 9.0906$ $y_0 = 23.82x^3 - 98.328x^2 + 163.61x - 47.561$	114.4995 72.9197	41.58
AB-7	$y_1 = 11.935x^3 - 57.363x^2 + 112.13x - 13.761$ $y_0 = 10.692x^3 - 49.007x^2 + 103.26x - 33.322$	88.6735 57.9617	30.71

[1] $\mathbf{y_1}$: gradation curve equation after crushing at 2700 kPa
$\mathbf{y_0}$: gradation curve equation before crushing
$\mathbf{y_2}$: gradation curve equation after crushing at 1500 kPa

The crushability under different magnitudes of stress was studied to a further extent for sample AB-5. The samples were loaded to 2 different stress levels; namely 1500, and 2700 kPa. Grain size distribution curves of the sample after crushing are presented in Figure 23.

As the stress increases, the percentage of fines generated increases. This is clearly manifested by looking at D_c at various stress levels, Table 19. On the other hand, the effect of crushing on grading evolution under 1500, and 2700 kPa is almost two times evidenced by D_c of 20.48, and 40.47, respectively. Figure 26 presents a bar chart of sand samples tested and their associated D_c value, while Figure 27 shows the degree of crushing of sample AB-5 under different stress level.

The degree of crushing can be expressed as a percentage using the following relationship:

$$D_{c\%} = \frac{A_1 - A_0}{A_0}$$

where A_1: is the area under gradation curve after crushing;

A_0: is the area under gradation curve before crushing

The values of $D_{c\%}$ for sand samples are presented in Table 20. It can be noticed that samples AB-2, AB-3, and AB-4 exhibited low crushing under the applied stress; having D_c value of 6.52, 1.20, and 4.54, respectively. These are the same samples which had shown gab gradation in the primary sieve analysis presented in Figure 18. These samples are relatively courser than other sand samples tested. Nonetheless, their corresponding $D_{c\%}$ values are as high as 67.50, 62.67, and 74.64 %, respectively which approximately rivals the other samples' values.

For comparison purpose, a sample of quartz white sand is tested for crushing following the

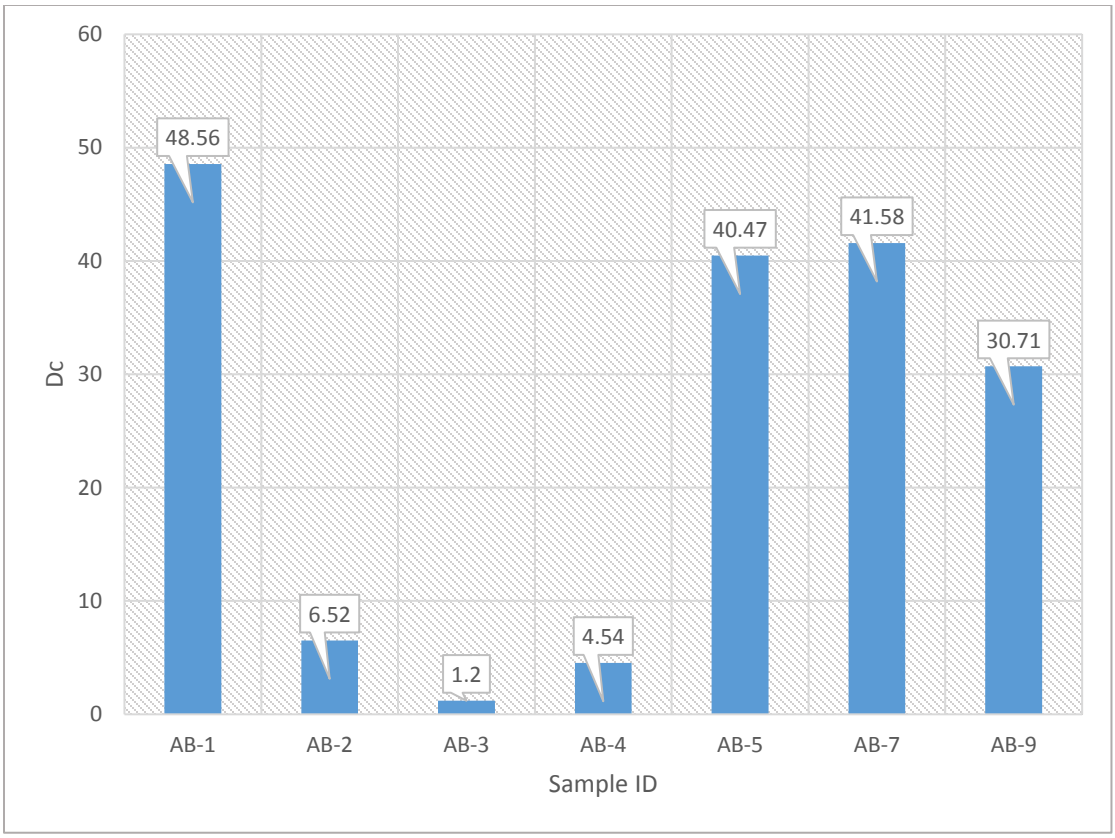

Figure 26: Degree of crushing of sand samples tested

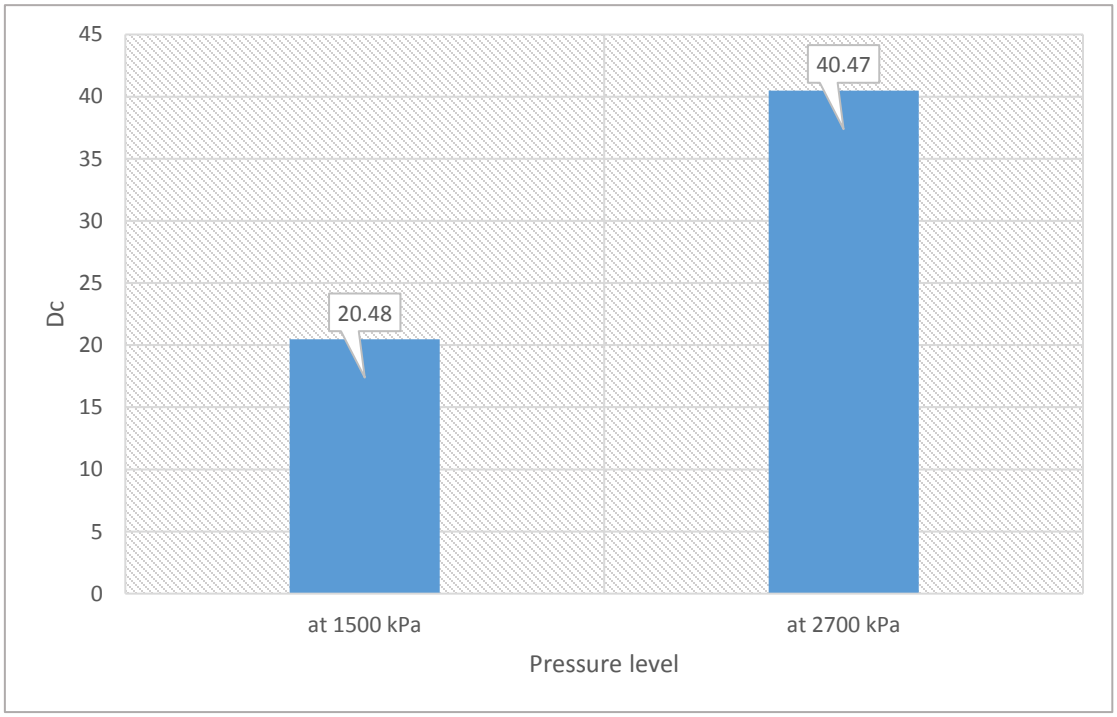

Figure 27: Degree of crushing of sample AB-5 at different stress levels

same procedure used for carbonate sand. The gradation curves before and after crushing and the stress-displacement relationship is displayed in Figure 28. The two curves are almost identical yielding D_c of only 1.69 even though the sample has been subjected to a higher level of stress up to 4000 kPa. Table 27 also shows a comparison between the degree of crushing of calcareous/carbonate sand and quartz sand samples tested. The average value of $D_{c\%}$ for calcareous sand is about 65.2%, compared to 2.23% for quartz sand. This means that the crushability of calcareous sand is about 30 times that of quartz sand.

Table 20: Comparison between degree of crushing of carbonate and quartzitic sands

Sample ID	Calcareous/Carbonate sand		Quartzitic sand	
	D_c	$D_{c\%}$	D_c	$D_{c\%}$
AB-1	48.56	73.25	1.69	2.23
AB-2	6.52	67.50		
AB-3	1.20	62.67		
AB-4	4.54	74.64		
AB-5	59.16	68.40		
AB-6	41.58	57.02		
AB-7	30.71	52.99		
Average	27.47	65.21		

4.3.2 SEM and XRD Analysis

The results of the XRD analysis on the calcareous and quartz sand samples showed a predominant presence for Calcite and Aragonite ($CaCO_3$) in calcareous sand. While quartz (SiO_2), and as the name indicates was the prime constituent mineral in the quartz sand. The XRD spectrum of each sample and its associated interpretation is presented in Figures 29 to 32.

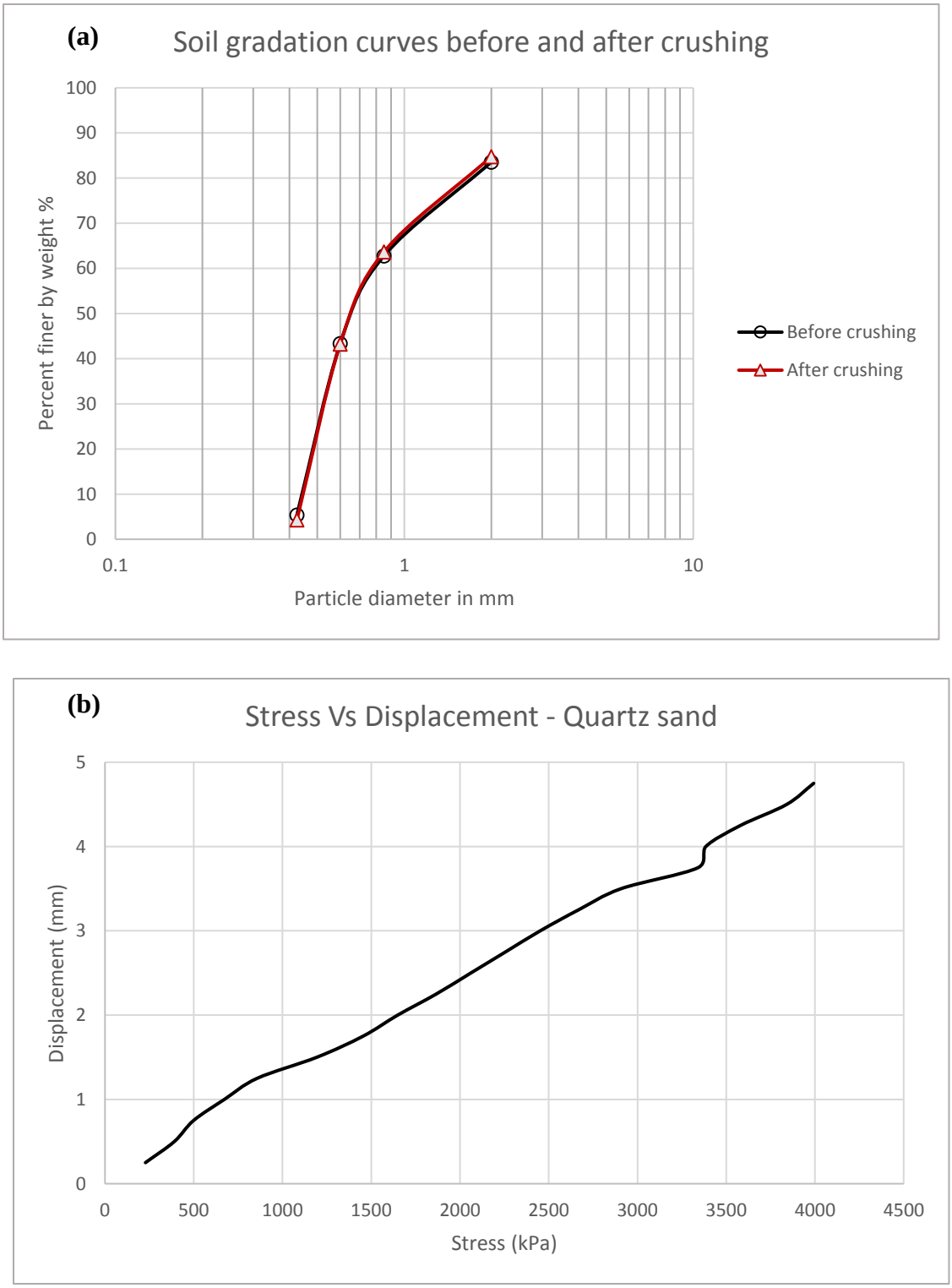

Figure 28: Crushability evaluation tests on quartz sand sample (a) Gradation curves before and after crushing, (b) stress-displacement curve

Scanning electron images of the calcareous and quartz sand samples tested are presented in Figures 33 to 36. Figures 35 and 36 illustrates the difference between calcareous and quartz sand. The particles of quartz sand look more rounded and have smoother surface unlike calcareous sand particles, which have rough surface and contain voids. That explains their vulnerability when subjected to high level of stress similar to pile driving.

Sample AB-1		
Mineral	**Formula**	**Content (%)**
Aragonite	$Ca(CO_3)$	68.9
Calcite	$CaCO_3$	31.1

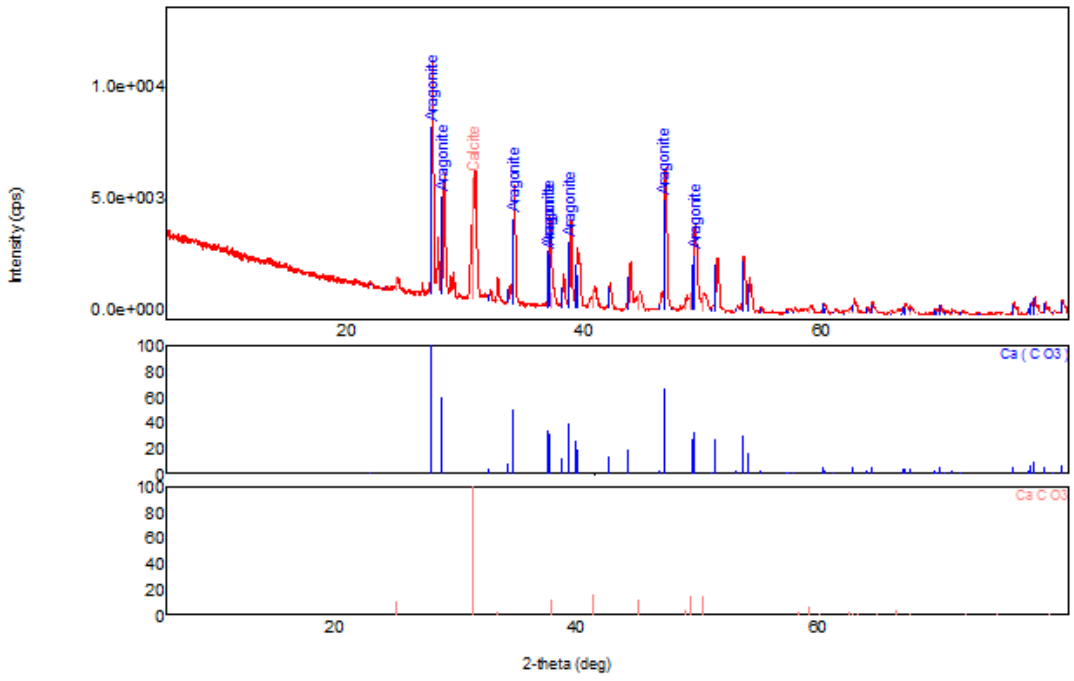

Figure 29: XRD spectrum and weight ratios of minerals for sample AB-1

Sample AB-5		
Mineral	**Formula**	**Content (%)**
Aragonite	$Ca(CO_3)$	29.3
Calcite	$CaCO_3$	54.3
Dolomite	$CaMg(CO_3)_2$	16

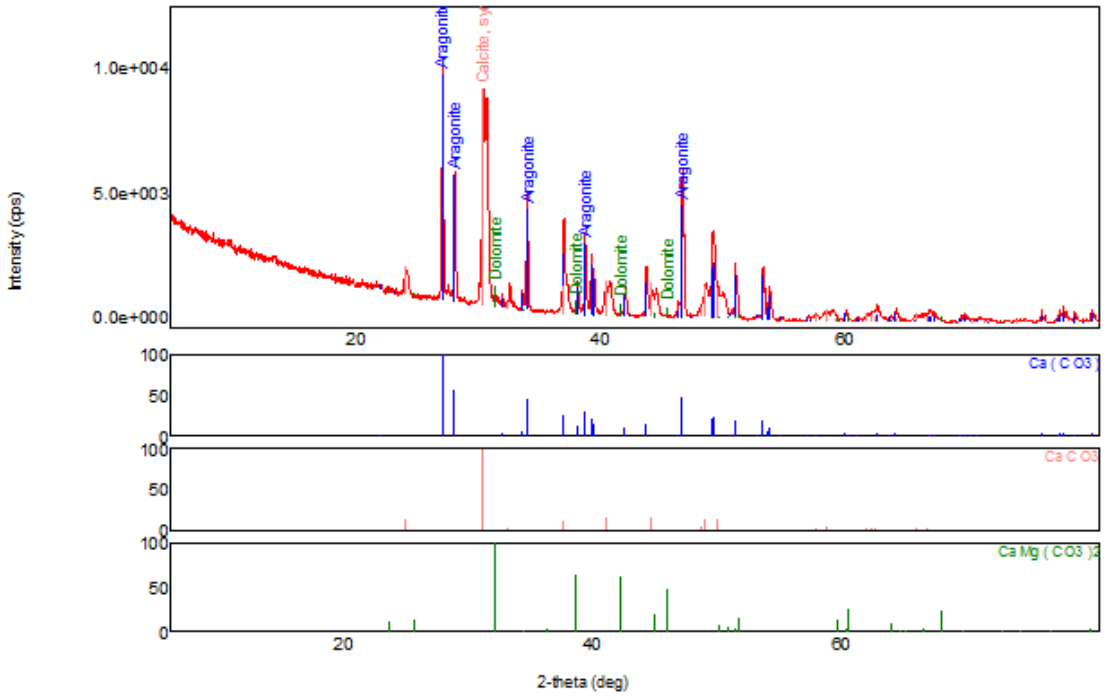

Figure 30: XRD spectrum and weight ratio of minerals for sample AB-5

Sample AB-7		
Mineral	**Formula**	**Content (%)**
Aragonite	$Ca(CO_3)$	60.7
Calcite	$CaCO_3$	35.7
Quartz	SiO_2	3.6

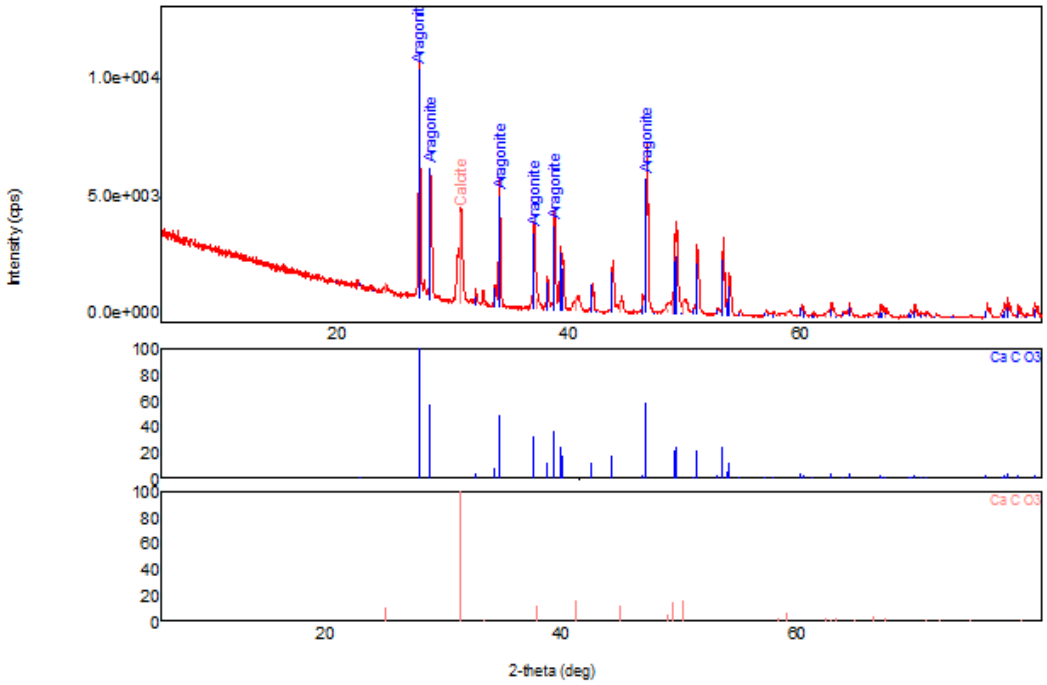

Figure 31: XRD spectrum and weight ratio of minerals for sample AB-7

Quartz sand sample		
Mineral	**Formula**	**Content (%)**
Quartz	SiO_2	100
Kaolinite	$Al_2Si_2O_5(OH)_4$	Very small

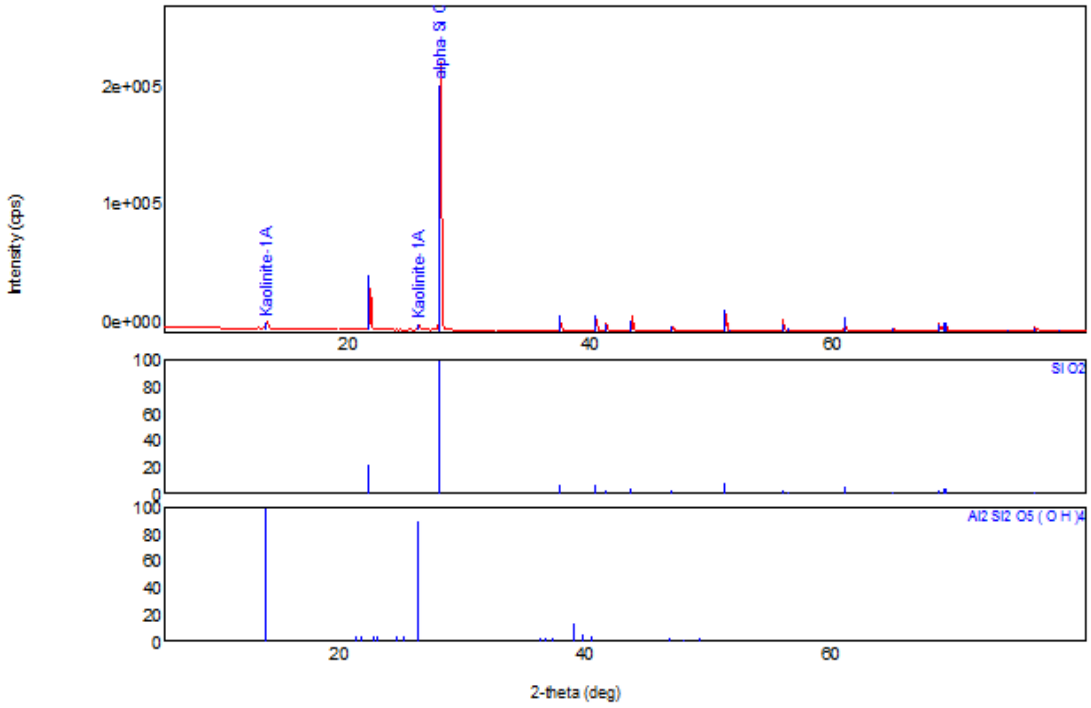

Figure 32: XRD spectrum and weight ratio of minerals for quartz sand sample tested

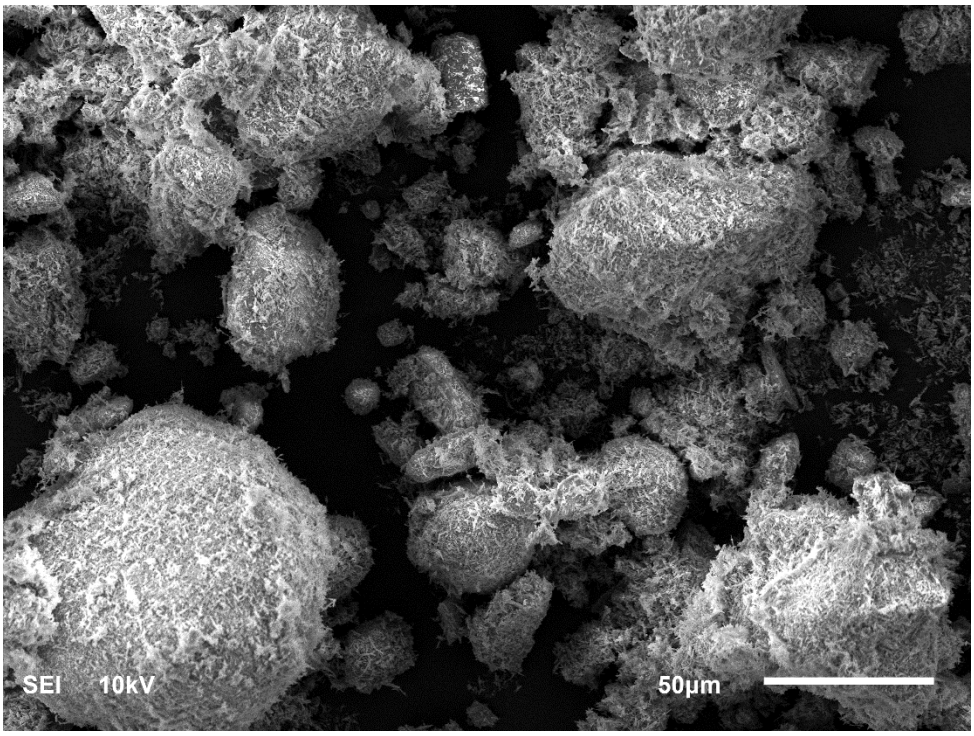

Figure 33: SEM image of sample AB-1

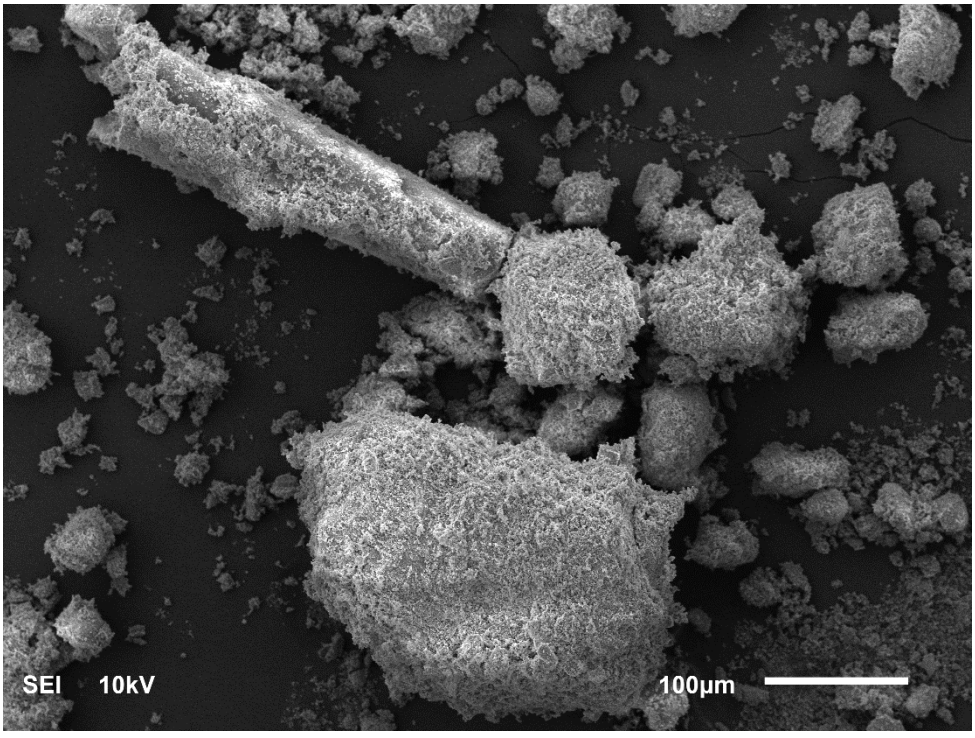

Figure 34: SEM image of sample AB-5

(a)

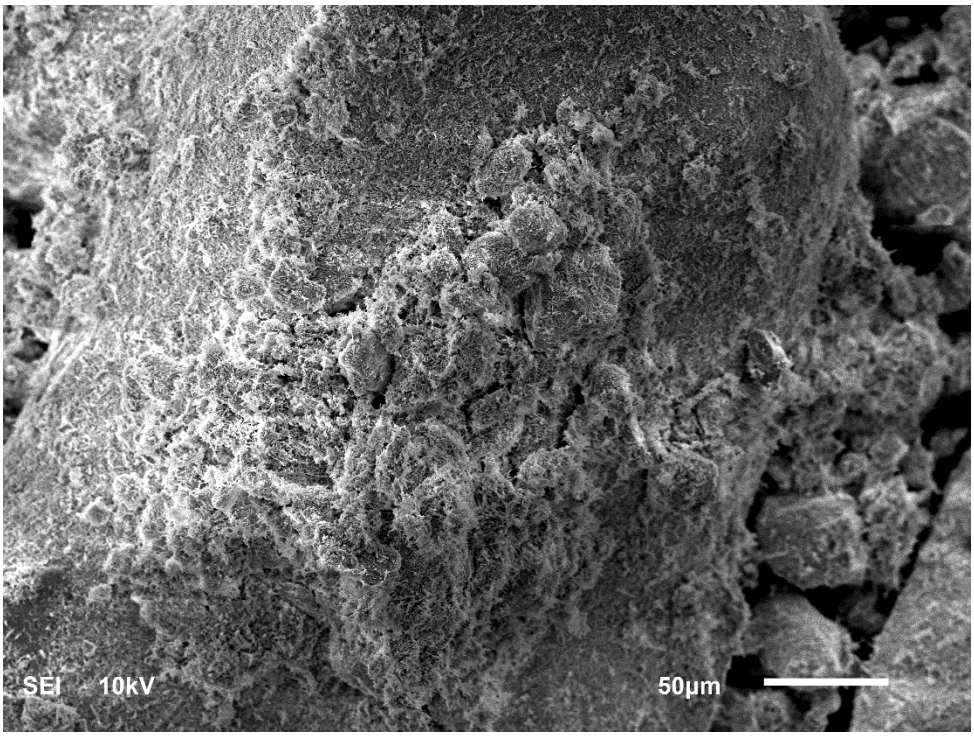

(b)

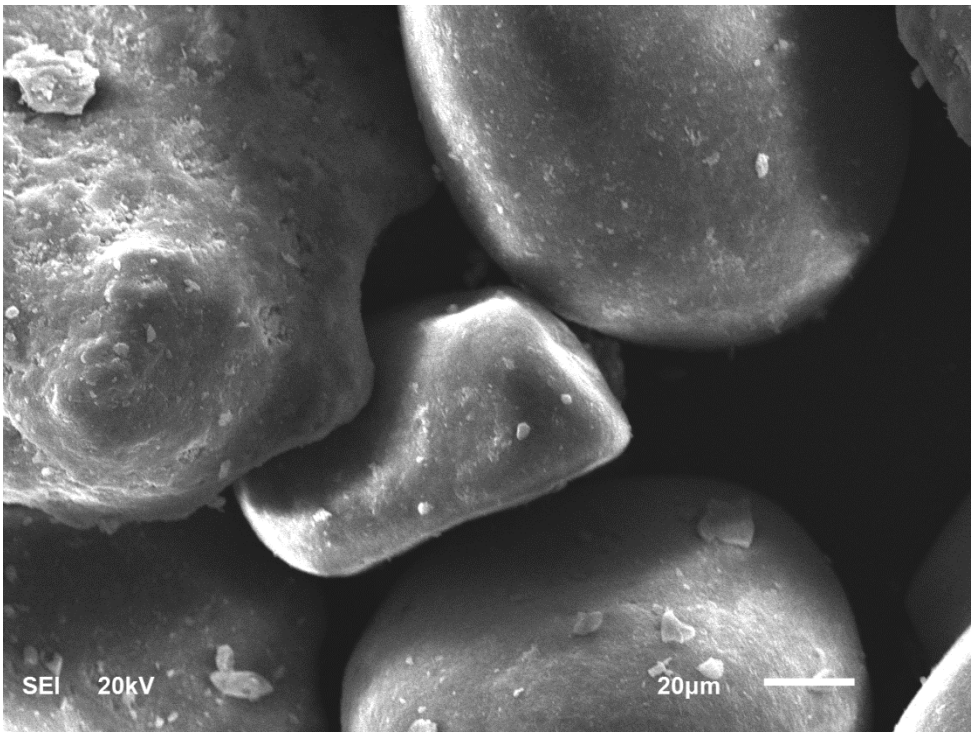

Figure 35: SEM images: (a) sample AB-7, (b) quartz sand

(a)

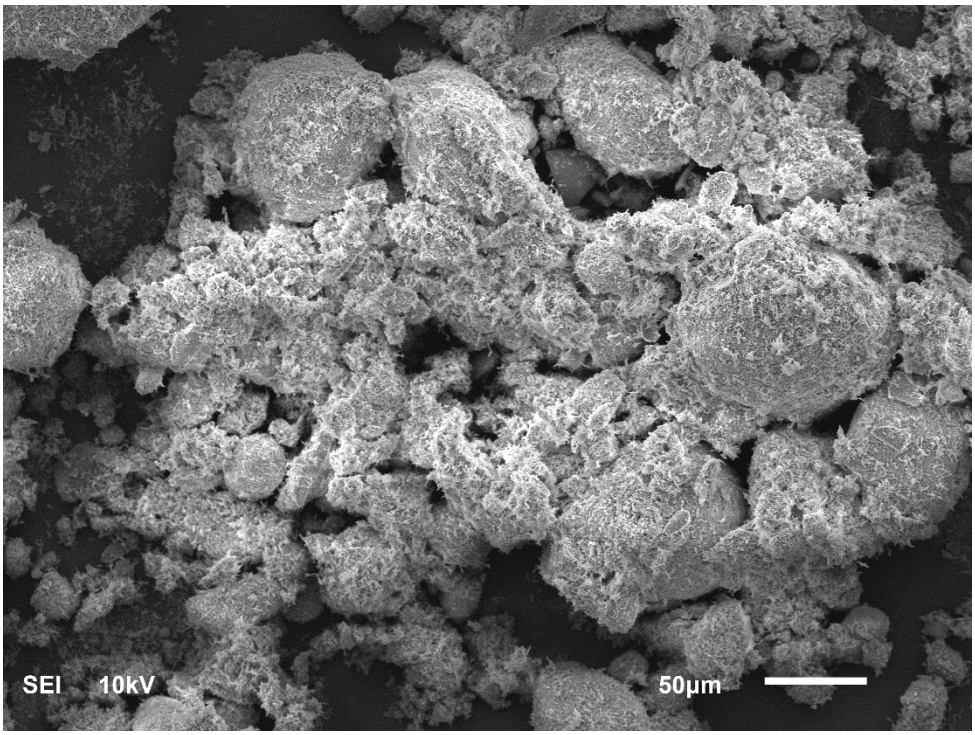

(b)

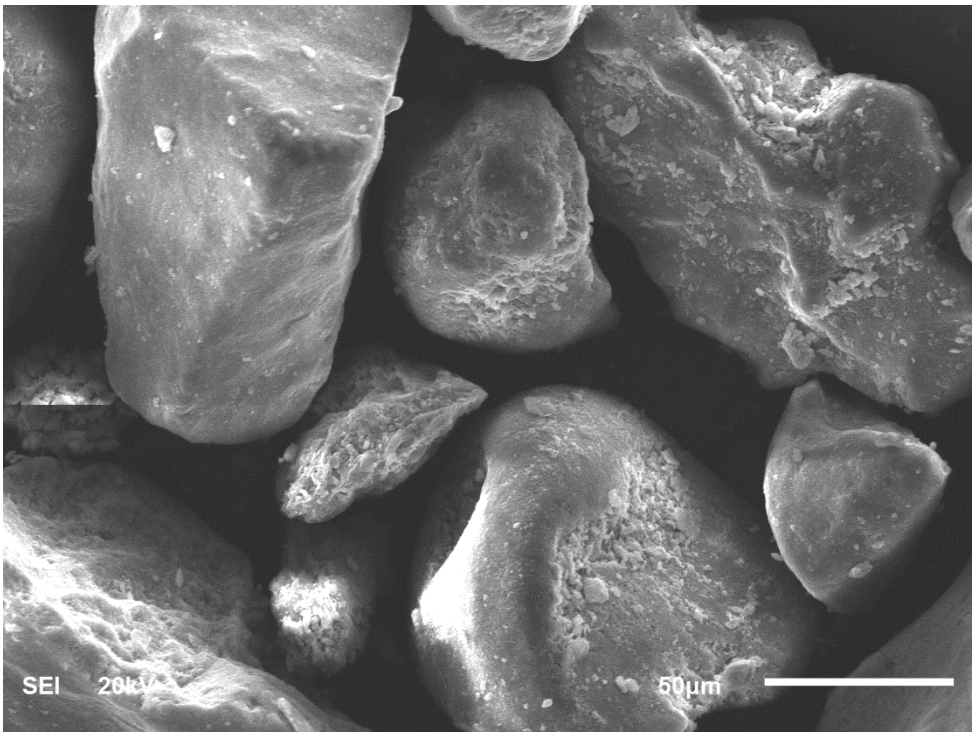

Figure 36: SEM images: (a) sample AB-6, (b) quartz sand

CHAPTER 5

SUMMARY, CONCLUSIONS, AND RECOMMENDATIONS

5.1 Summary

The especial conditions of marine sand and clay in the Arabian Gulf called for evaluation of the overconservatism in the present design parameters used for offshore pile capacity calculation. Assessing this degree of overconservatism was the primary objective of this research.

Sufficient number of offshore geotechnical reports have been collected and their corresponding dynamic pile monitoring reports, for more than 5 different locations within the Arabian Gulf. The evaluation of API capacity was conducted using the data of piles that have been subjected to restrike, and the corresponding data of sand and clay layers which the piles penetrate. The shaft friction was the basis for comparing the API with DMS capacity for piles in sand, while the α-factor was used for piles in clay. Statistical analyses were performed on the compiled data. Based on the results of these tests, it was found that generally, the pile design parameters obtained using API guidelines is smaller than that measured by DMS. The difference is presented in the form of overconservative factor of 2.36, 1.50, 2.03, 1.71, and 1.76 for very loose, loose, medium dense, dense, and very dense silica sand, respectively. While for the carbonate sand the overconservative factor was found to be as high as 3.67. Similarly, for clay overconservative factor was found to be 1.90, 1.44, and 1.35 for clay with OCR = 1, $1 < OCR \leq 4$, and $OCR > 4$, respectively.

The crushability of calcareous/carbonate sand samples is investigated. The samples were obtained from different locations in the Arabian Gulf. The results of the experimental tests manifested the high tendency to crushing of these soils. This fact was elucidated more by testing a quartz sand sample, which showed that the crushability of calcareous sand is almost 30 times that of quartz sand.

5.2 Conclusions

In light of the design parameters evaluation and the experimental programme conducted in this thesis, the following conclusions can be drawn:

- API design parameters are indeed overconservative. Consequently, there is a need to revise the presently used pile design parameters estimated as per this standard. The α-factor for piles in clay can be increased by multiplying it by an amount equal to the overconservative factor presented earlier, given that the soil layer satisfies the same conditions the factor was suggested for (i.e., OCR). Similarly, the API shaft friction may be multiplied by the proposed overconservative factor bearing in mind the relative density of the sand layer in question.
- The results of the experimental crushing test supported by what the SEM and XRD analyses have revealed, show good agreement with Kolk, 2000 findings.
- The major reason that some clay layers have very low α_{DMS} is that there was no enough energy in the hammer to displace the pile. Usually it takes about 2 mm displacement per blow (at least 1 mm/blow) to mobilise skin friction. So, with the available energy, shear strength could not be mobilised. The N-1 field is an extreme

example of this. Generally, the same can be said about other locations where α_{DMS} is found to be less than 0.3. That was the main reason why these values were excluded from the analysis.

5.3 Recommendations for Further Study

- The reliability of the overconservative factor estimated can be further enhanced by increasing the number of BOR piles, and hence soil layers involved in the analysis. The more data used, the better reliability the statistical analyses will bring about.
- Other approaches for classifying the sand and clay layers can be used instead of relative density and OCR, respectively. For instance, carbonate content or shear strength (angle of internal friction) can be the basis for classifying sand, while plasticity may be used for clay. Subsequently, statistical analyses can be performed on the compiled data to obtain new overconservative factors, so as to be compared with old values.
- An experimental programme can be performed to study the thixotropy of marine clay of the Arabian Gulf and its relation with the setup of piles driven in these soils.
- Developing a standardised test for assessing the crushability of carbonate sands is highly recommended.

References

[1] R. 2Geo API, *Geotechnical and Foundation Design Considerations*. 2011.

[2] M. F. Randolph and S. M. Gourvenec, *Offshore Geotechnical Engineering*. 2011.

[3] E. T. R. Dean, *Offshore Geotechnical Engineering. Principles and Practice*. 2010.

[4] M. Randolph, M. Cassidy, and S. Gourvenec, "Challenges of offshore geotechnical engineering Les défis de la géotechnique offshore," *Icsmge*, vol. 1, 2005.

[5] S. A. Chakrabarti, "Hydrodynamics of Offshore Structures." Wit Press, Southampton, UK, 2001.

[6] K. Sadeghi, "An Overview of Design , Analysis , Construction and Installation of Offshore Petroleum Platforms Suitable for Cyprus Oil/Gas Fields," *Int. J. Soc. Appl. Sci.*, vol. 2, no. 4, pp. 1–16, 2007.

[7] H. G. Poulos, *Marine Geotechnics*. The Academic Devision of Unwin Hyman Ltd, London, UK, 1988.

[8] J. F. Wilson, *Dynamics of Offshore Structures*. John Wiley & Sons, Inc., Hoboken, New Jersey, 2003.

[9] R. J. Barbour and C. T. Erbrich, "Analysis of in-situ Reformation of Flattened Large Diameter Foundation Piles using ABAQUS," in *UK ABAQUS Users Conference*, 1994.

[10] MSL, "A study of pile fatigue during driving and in-service and of pile tip integrity," Offshore Technology Report 200l/018. Prepared by MSL Engineering Limited for the Health and Safety Executive, HSE Books, 2001.

[11] T. R. Aldridge, T. M. Carrington, and N. R. Kee, "Propagation of pile tip damage during installation.," in *Int. Conf. Frontiers in Offshore Geotechnics*, 2005, pp. 823–827.

[12] R. J. Barbour and C. Erbrich, "Analysis of soil skirt interaction during installation of bucket foundations using 'ABAQUS,'" in *ABAQUS Users Conference*, 1995.

[13] T. Alm, R. O. Snell, K. M. Hampson, and A. Olaussen, "Design and installation of the Valhall piggyback structures," in *Annual Offshore Tech. Conf*, 2004.

[14] J. Angemeer, E. Carlson, and J. H. Klick, "Techniques and results of offshore pile load testing in calcareous soils," in *5th Offshore Technology Conference*, 1973, pp. 677–692.

[15] J. Angemeer, E. Carlson, S. Stroud, and M. Kurzeme, "Pile load tests in calcareous soils conducted in 400 feet of water from a semi submersible exploration rig," in *7th Offshore Technology Conference*, 1975, pp. 657–670.

[16] J. D. Murff, "Pile capacity in calcareous sands: state of the art report," *ASCE J. Geotech. Eng.*, vol. 113, no. GT5, pp. 490–507, 1987.

[17] A. F. Williams, T. W. Dunnavant, S. Anderson, D. W. Equid, and A. M. Hyden, "The performance and analysis of lateral load tests on 356 mm dia. piles in reconstituted calcareous sand," in *st Int. Conf. on Calcareous Sediments*, 1988, pp. 271–280.

[18] A. M. Hyden, J. M. Hulett, J. D. Murff, and A. F. Abbs, "Design practice for grouted piles in Bass Strait calcareous soils," in *1st Int. Conf. on Calcareous Sediments*, 1988.

[19] S. Al-Mandeel, "Behavior of laterally loaded pile group model in sand," Master of Science Thesis, King Fahd University of Petroleum and Minerals, Saudi Arabia, 2000.

[20] C. R. Golightly, "Engineering Properties of Carbonate Sands: The geological origins, classification, engineering, shear and triaxial stress path properties of four carbonate sands. The analysis of the transfer function for pile skin friction.," Doctor of Philisophy Dissertation, University of Bradford, UK, 1988.

[21] ASTM, "ASTM Standard 1143: Standard Test Method for Piles Under Static Axial Compression Load," West Conshohocken, PA., 1996.

[22] P. J. Hannigan, G. G. Goble, G. Thendean, G. E. Likins, and F. Raushe, "Design and Construction of Driven Pile Foundations," *FHWA-HI-97-013, Fed. Highw. Adm.*, vol. II, p. Washington, D.C., 2006.

[23] AASHTO, "Standard Specifications for Highway Bridges," Washington, D.C., 2002.

[24] M. T. Davisson, "High-Capacity Piles," in *Proceedings of Lecture Series on Innovations in Foundation Construction*, 1972, p. 81–112, Chicago, IL.

[25] T. Sandford and C. Stuart, "Development and Evaluation of Pile 'High Strain Dynamic Test Database' to Improve Driven Pile Capacity Estimates: Phase II Report," University of Maine, 2013.

[26] A. S. Bradshaw and C. D. Baxter, "Chapter 4. Dynamic And Static Pile Load Test Data," in *Design and Construction of Driven Pile Foundations: Lessons Learned on the Central Artery/Tunnel Project*, Federal Highway Administration, 2012.

[27] W. Yu, L. Liang, R. Givet, L. Qin, and X. Li, "Application of High Strain Dynamic Testing Technique to Underwater Skirt Pile Foundation," in *Twenty-third (2013) International Offshore and Polar Engineering*, 2013, vol. 9, pp. 428–435.

[28] N. V Nayak, "Static and High Strain Dynamic Test Correlation Studies on Cast-in-Situ Concrete Bored Piles," in *Deep Foundation Institute*, 2000, no. September.

[29] P. Lai and C. L. Kou, "Validity of Predicting Pile Capacity by Pile Drving Analyzer," in *International Conference on Design and Construction of Deep Foundations*, 1994, p. Vol II, Orlando, FL.

[30] J. Long, D. Bozkurt, J. KERRIGAN, and M. H. WYSOCKEY, "Value of Methods for Predicting Axial Pile Capacity," *Trnasportation Res. Rec.*, vol. 1663, no. 99, pp.

57–63, 1999.

[31] M.-005 SAES, “Design and Construction of Fixed Offshore Platforms,” 2011.

[32] Q.-004 SAES, *Installation of Piles and Conductors for Offshore Structures*. 2010.

[33] E. A. Wdtsie, R. . Stevens, and W. . Vines, “Pile Installation Acceptance in Strong Soil,” in *Proceedings, 2nd International Conference on the Application of Stress Wave Theory on Piles*, 1984, pp. 72–78.

[34] S. C. Helfrich, E. A. Wiltsie, W. R. Cox, and K. A. A.1-Shafei, “Pile Load Tests in Dense Sand - Planning, Instrumentation and Results,” in *Proceedings of the 7th Annual Offshore Technology Conference (OTC)*, 1985, pp. 55–64.

[35] K. A. Al-Shafei, W. R. Cox, and S. C. Helfrich, “Pile load tests in dense sand: analysis of static test results,” in *Proceedings, 26th Offshore Technology Conference*, 1994, pp. 83–103.

[36] R. F. Stevens and K. Al-Shafei, “The Applicability of the Ras Tanajib Pile Capacity Method to Long Offshore Piles,” in *Offshore Technology Conference*, 1996, pp. 171–180.

[37] R. J. Jardine, A. S. Merritt, and F. C. Schroeder, “The ICP Design Method and Application to a North Sea Offshore Wind Farm,” in *IFCEE*, 2015, pp. 1–10.

[38] R. J. Jardine, R. . Overy, and J. R. Standing, *ICP Design Methods for Driven Piles in Sands and Clays*. Thomas Telford Ltd, London, 2005.

[39] B. M. Lehane, J. A. Schneider, and X. Xu, “A Review of Design Methods for Offshore Driven Piles in Siliceous Sand,” UWA Report GEO 05358, 2005.

[40] H. G. G. Poulos, “A Review of the Behaviour and Enginerring Properties of Carbonate Soils,” *Australian Geomechanics News*, no. 6. 1983.

[41] B. Gerwick, *Construction of Marine and Offshore Structures*. CRC Press, New York, 2007.

[42] H. J. Kolk, “Deep Foundations in Calcareous Sediments,” in *Al-Shafei, K.A. (Ed.), Engineering for Calcareous Sediments, Proc 2nd Intl. Conf. on Eng. for Calcareous Sediments, Vol 2*, 2000, pp. 313–344.

[43] Fugro, “Engineering Assessments, Zulf Field Developement (Phase II), Arabian Gulf, Saudi Arabia,” Geotechnical report No. 1758/06/215, 2007.

[44] P. G. Fookes and I. E. Higginbotham, “The Classification and Description of Near-shore Carbonate Sediments for Engineering Purposes,” *Geotechnique*, vol. 25, no. 2, pp. 406–4011, 1975.

[45] A. R. Clark and B. F. Walker, “A Proposed Scheme for the Classification and Nomenclature for Use in Engineering Description of Middle Eastern Sedimentary Rocks,” *Geotechnique*, vol. 17, no. 1, pp. 93–99, 19777.

[46] R. W. King, W. R. Van Hooydonk, H. J. Kolk, and D. Windle, “Geotechnical

Investigations of Calcareous Soils of the Northern West Shelf, Australia," in *Proc. 12th Annual OTC, Houston*, 1980, pp. 303–313.

[47] M. Datta, G. V. Rao, and S. . Gulhati, "The Nature and Engineering Behaviour of Carbonate Soils at Bombay High," *Mar. Geotechnol.*, vol. 4, no. 4, pp. 307–341, 1981.

[48] K. L. Lee and I. Farhoomand, "Compressibility and Crushing of Granular Soil in Anisotropic Triaxial Compression," *Can. Geotech. J.*, vol. 4, no. 1, pp. 68–100, 1967.

[49] T. Ramamurthy and R. S. Lal, "Influence of Crushing on the Properties of Badarpur Sand," *J. Indian Natl. Soc. Soil Mech. Found. Eng.*, vol. 9, no. 3, pp. 305–321, 1970.

[50] M. Datta, S. K. Gulhati, and G. V. Rao, "Crushing of Calcareous Sands During Shear," in *11th Annual OTC*, 1979.

[51] G. Miao and D. Airey, "Breakage and Ultimate States for a Carbonate sand," *Géotechnique*, vol. 63, no. 14, pp. 1221–1229, 2013.

[52] B. C. Gerwick, "Pile Installation in Difficult Soils," *J. Geotech. Geoenvironmental Eng.*, vol. 130, no. 5, pp. 454–460, 2004.

[53] T. B. Edil and C. H. Benson, "Comparison of Basic Laboratory Test Results with more Sophisticated Laboratory and In-Situ Tests Methods on Soils in Southeastern Wisconsin," Geo Engineering Program No 0092-06-05, Department of Civil and Environmental Engineering, University of Wisconsin-Madison, 2009.

[54] R. D. Holtz and W. D. Kovacs, *An Introduction to Geotechnical Engineering*. Prentice Hall, Englewood Cliffs, New Jersey, 1981.

[55] J. K. Mitchell and K. Soga, *Fundamentals of Soil Behaviour*, Third edit. New York: John Wiley & Sons, Inc., Hoboken, New Jersey, USA, 2005.

[56] BS 5930, "Code of Practice for Site Investigations," 1999.

[57] M. Jamiolkowski, V. N. Ghionna, R. Lancellotta, and E. Pasqualini, "New Correlations of Penetration Tests for Design Practice," in *De Ruiter, J. (Ed.), Penetration Testing 1988: Proceedings of the, First International Symposium on Penetration Testing, ISOPT-1*, 1988, pp. 263–296.

[58] R. B. Peck, W. E. Hanson, and T. H. Thornburn, *Foundation Engineering*, Second edi. John Wiley & Sons, Inc., 1974.

[59] J. G. Eisenhauer, "Regression through the Origin," *Teach. Stat.*, vol. 25, no. 3, pp. 76–80, 2003.

[60] A. Ghasemi and S. Zahediasl, "Normality tests for statistical analysis: A guide for non-statisticians," *Int. J. Endocrinol. Metab.*, vol. 10, no. 2, pp. 486–489, 2012.

[61] D. Altman and J. Bland, *Statistics Notes: the normal distribution*. BMJ. 310(6975):298, 1995.

[62] J. Pallant, *SPSS survival manual*, *a step by step guide to data analysis using SPSS for windows*, 3rd ed. McGraw Hill, Sydney, 2007.

[63] A. Elliott and W. Woodward, *Statistical analysis quick reference guidebook with SPSS examples*, 1st ed. London: Stage Publications, 2007.

[64] PDI, "http://www.pile.com/pdi/," 2017.

VITAE

Name	Ahmed H. Bukhary
Nationality	Sudanese
Date of Birth	September 30, 1989
Email	ahmed.bukhary@hotmail.com
Address	P.O. Box 13350, Omdurman, Khartoum 11111, Sudan
Academic Background	B.Sc. (Honours) in Civil Engineering

List of Publications:

"Hamzah. M. Al-Hashemi, and **Ahmed. H. Bukhary**, "Correlation Between California Bearing Ration (CBR) and Angle of Repose of Granular Soil", *Electronic Journal of Geotechnical Engineering*, vol. 21, 2016, pp. 5655 – 5660.

"Yassir Mustafa, Hamzah Al-Hashemi, and **Ahmed Bukhary***, "Characterisation and Index Properties Correlations for Marlstone and Marly Limestone of Saudi Arabia", *Proceedings of the 2nd World Congress on Civil, Structural, and Environmental Engineering*, 2017, Barcelona, Spain.

Mohammed T. Mahmoud, **Ahmed H. Bukhary**, Ahmed G. Ramadan and Muhammad A. Al-Zahrani, "Prediction of Breach Peak Outflow and Failure Time of Earthen Dams Using Artificial Neural Network Approach", *Proceedings of the 2nd World Congress on Civil, Structural, and Environmental Engineering*, 2017, Barcelona, Spain.

APPENDIX

SECTION 1
GENERAL INFORMATION

Table A-1: General information of piles after restrike in different offshore fields in the Arabian Gulf

	Location											
	N-1	**F-1**	**F-2**	**F-3**	**F-4**	**F-5**	**F-6**	**F-7**	**F-8**	**F-9**	**F-10**	**F-11**
DMS report No.	D1	D2	D3	D4	D5	D6	D7	D8	D9	D10	D11	D12
Geotechnical report No.	G1	G2	G3	G4	G5	G6	G7	G8	G9	G10	G11	G12
Pile section	B3 (P3)	B1 (P1)	B1 (P1)	A1 (P1)	B2 (P2)	B1 (P1)	B1 (P1)	A2 (P2)	B1 (P2)	A1 (P2)	B1 (P1)	B1 (P1)
Pile outside diameter (m)	1.22	0.76	0.76	0.76	0.76	0.76	0.76	0.76	1.07	1.07	1.07	1.07
Pile Penetration (m)	86.00	22.00	22.50	19.00	23.00	30.25	27.75	30.50	29.80	43.75	25.00	27.75
Blow count/0.25 m	2917	120	50	25	49	75	400	270	70	110	90	50
Total capacity Qc (kN)	36900	10100	9000	9400	5400	13800	13450	16350	17540	20370	19280	13830
Required FOS	2.00	2.00	1.50	2.00	1.50	1.50	2.00	2.00	1.50	2.00	1.50	1.50
Actual FOS	3.00	11.20	5.40	5.90	4.10	7.14	15.80	8.20	2.80	2.00	3.00	2.30
Waiting time of restrike (hours)	82	12	17	15	15.5	12	19	12	12	12.75	NR	NR
Setup	0.97	1.20	1.20	1.32	1.15	1.41	1.14	1.27	1.37	1.36	1.39	1.25

Table A-1 continued.

	Location											
	F-12	**F-13**	**J-1**	**J-2**	**J-3**	**J-4**	**Y-1**	**Y-2**	**Y-3**	**Y-4**	**Y-5**	**Y-6**
DMS report No.	D13	D14	D15	D16	D17	D18	D19	D20	D21	D22	D23	D24
Geotechnical report No.	G13	G14	G15	G16	G17	G18	G19	G20	G21	G22	G23	G24
Pile section	B1 (P1)	A1 (P3)	A1 (P3)	A2 (P3)	A2 (P3)	A2 (P3)	B2 (P1)	B2 (P1)	B2 (P1)	A1 (P2)	A1 (P1)	B1 (P1)
Pile outside diameter (m)	1.07	1.07	1.07	1.07	1.07	1.07	0.76	1.07	0.76	1.07	1.07	1.07
Pile Penetration (m)	26.75	58.00	54.00	58.00	58.00	68.10	29.75	31.75	23.75	39.50	33.05	22.95
Blow count/0.25 m	60	180	500	430	520	230	120	200	30	135	90	100
Total capacity Qc (kN)	16800	22700	28717	27906	30262	27000	14098	25350.20	8819.80	22262.60	16900	22499.90
Required FOS	2.00	2.00	2.00	1.50	1.70	1.50	2.00	2.00	1.50	2.00	2.00	1.50
Actual FOS	3.30	2.20	2.40	1.54	1.50	1.50	14.10	4.53	4.99	2.00	1.70	2.30
Waiting time of restrike (hours)	28.50	17.75	16	20	67	16	14	13	15	12	758	14.50
Setup	1.34	1.39	1.61	1.99	1.68	1.73	1.27	1.42	1.29	1.36	1.72	1.45

Table A-1 continued.

	Location											
	Y-7	**Y-8**	**Y-9**	**Y-10**	**Y-11**	**U-1**	**U-2**	**U-3**	**U-4**	**U-5**	**U-6**	**U-7**
DMS report No.	D25	D26	D27	D28	D29	D30	D31	D32	D33	D34	D35	D36
Geotechnical report No.	G25	G26	G27	G28	G29	G30	G31	G32	G33	G34	G35	G36
Pile section	B1 (P1)	A1 (P3)	A1 (P3)	A2 (P3)	A2 (P3)	A2 (P3)	B2 (P1)	B2 (P1)	B2 (P1)	A1 (P2)	A1 (P1)	B1 (P1)
Pile outside diameter (m)	1.07	1.07	1.07	1.07	1.07	1.07	0.76	1.07	0.76	1.07	1.07	1.07
Pile Penetration (m)	26.75	58.00	54.00	58.00	58.00	68.10	29.75	31.75	23.75	39.50	33.05	22.95
Blow count/0.25 m	60	180	500	430	520	230	120	200	30	135	90	100
Total capacity Qc (kN)	16800	22700	28717	27906	30262	27000	14098	25350.20	8819.80	22262.60	16900	22499.90
Required FOS	2.00	2.00	2.00	1.50	1.70	1.50	2.00	2.00	1.50	2.00	2.00	1.50
Actual FOS	3.30	2.20	2.40	1.54	1.50	1.50	14.10	4.53	4.99	2.00	1.70	2.30
Waiting time of restrike (hours)	28.50	17.75	16	20	67	16	14	13	15	12	758	14.50
Setup	1.34	1.39	1.61	1.99	1.68	1.73	1.27	1.42	1.29	1.36	1.72	1.45

Table A-2: Pile (BOR) general information for N-1 location

Location: N-1									
Soil layer depth range (m)		Thickness (m)	Pile segment No.	Depth below the grade (m)	Segment length (m)	SF_{DMS} (kN)	SF_{DMS} (kPa)	SF_{API} (kPa)	Segment surface area (m^2)
0.90	2.50	1.60	1	1.70	1.70	224.90	34.48	0.96	6.51
2.50	4.60	2.10	2	3.70	2.00	147.10	19.14	7.27	7.66
4.60	7.70	3.10	3	5.70	2.00	81.00	10.54	33.75	7.66
7.70	8.80	1.10	4	7.70	2.00	110.80	14.41	32.04	7.66
8.80	17.50	8.70	5	9.70	2.00	201.60	26.23	64.84	7.66
8.80	17.50	8.70	6	11.70	2.00	244.50	31.81	69.09	7.66
8.80	17.50	8.70	7	13.70	2.00	237.60	30.91	71.49	7.66
8.80	17.50	8.70	8	15.80	2.10	280.40	36.48	75.51	8.04
17.50	18.50	1.00	9	17.80	2.00	371.50	48.33	73.46	7.66
19.80	22.40	2.60	10	19.80	2.00	429.40	55.86	65.92	7.66
19.80	22.40	2.60	11	21.80	2.00	440.90	57.36	72.69	7.66
22.40	26.80	4.40	12	23.80	2.00	456.00	59.32	84.55	7.66
22.40	26.80	4.40	13	25.80	2.00	588.10	76.51	87.54	7.66
26.80	28.00	1.20	14	27.80	2.00	856.90	111.47	83.50	7.66
28.00	30.30	2.30	15	29.80	2.00	839.80	109.25	108.01	7.66
30.30	33.30	3.00	16	31.80	2.00	839.80	109.25	120.43	7.66
33.30	36.50	3.20	17	33.80	2.00	925.00	120.33	50.38	7.66
33.30	36.50	3.20	18	35.80	2.00	786.30	102.29	44.85	7.66
37.60	45.50	7.90	19	37.80	2.00	740.10	96.28	66.79	7.66
37.60	45.50	7.90	20	39.80	2.00	717.40	93.33	119.85	7.66
37.60	45.50	7.90	21	41.80	2.00	752.50	97.89	123.83	7.66
37.60	45.50	7.90	22	43.90	2.10	882.80	114.84	130.91	8.04
45.50	48.60	3.10	23	45.90	2.00	1014.90	132.03	135.32	7.66
45.50	48.60	3.10	24	47.90	2.00	1121.20	145.86	136.73	7.66
49.50	50.60	1.10	25	49.90	2.00	1292.00	168.07	151.52	7.66
50.60	52.50	1.90	26	51.90	2.00	1408.80	183.27	117.64	7.66
52.50	55.60	3.10	27	53.90	2.00	1251.60	162.82	81.21	7.66
55.60	63.40	7.80	28	55.90	2.00	890.40	115.83	158.84	7.66
55.60	63.40	7.80	29	57.90	2.00	591.90	77.00	164.31	7.66
55.60	63.40	7.80	30	59.90	2.00	478.20	62.21	169.05	7.66
55.60	63.40	7.80	31	61.90	2.00	436.80	56.82	171.71	7.66
63.40	68.00	4.60	32	63.90	2.00	386.40	50.27	179.91	7.66
63.40	68.00	4.60	33	65.90	2.00	386.40	50.27	199.36	7.66
63.40	68.00	4.60	34	67.90	2.00	386.40	50.27	221.05	7.66
69.50	71.00	1.50	35	69.90	2.00	386.40	50.27	323.10	7.66
71.80	73.50	1.70	36	72.00	2.10	386.40	50.27	86.70	8.04
73.50	76.15	2.65	37	74.00	2.00	386.40	50.27	81.13	7.66
73.50	76.15	2.65	38	76.00	2.00	386.40	50.27	208.90	7.66
77.50	81.50	4.00	39	78.00	2.00	386.40	50.27	81.21	7.66
77.50	81.50	4.00	40	80.00	2.00	386.40	50.27	80.94	7.66
81.50	82.50	1.00	41	82.00	2.00	2010.70	261.57	14.62	7.66
82.50	85.55	3.05	42	84.00	2.00	2599.50	338.17	16.57	7.66
85.55	86.50	0.95	43	86.00	2.00	2572.00	334.59	175.33	7.66

Table A-3: Pile (BOR) general information for F-1 location

Location: F-1									
Soil layer depth range (m)		Thickness (m)	Pile segment No.	Depth below the grade (m)	Segment length (m)	SF_{DMS} (kN)	SF_{DMS} (kPa)	SF_{API} (kPa)	Segment surface area (m^2)
0	4.50	4.50	1	1.90	1.90	20.00	4.33	4.00	4.55
0	4.50	4.50	2	3.90	2.00	20.00	4.16	5.00	4.79
4.50	7.00	2.50	3	6.00	2.10	20.00	4.16	10.00	5.03
7.00	8.50	1.50	4	8.00	2.00	70.00	14.55	30.00	4.79
9.45	12.65	3.20	5	10.00	2.00	300.00	62.35	40.00	4.79
9.45	12.65	3.20	6	12.00	2.00	500.00	103.92	45.00	4.79
12.65	18.10	5.45	7	14.00	2.00	800.00	166.27	70.00	4.79
12.65	18.10	5.45	8	16.00	2.00	1020.00	212.00	85.00	4.79
12.65	18.10	5.45	9	18.00	2.00	1050.00	218.23	95.00	4.79
18.10	20.50	2.40	10	20.00	2.00	1050.00	218.23	95.00	4.79
20.50	22.25	1.75	11	22.00	2.00	1050.00	218.23	100.00	4.79

Table A-4: Pile (BOR) general information for F-2 location

Location: F-2									
Soil layer depth range (m)		Thickness (m)	Pile segment No.	Depth below the grade (m)	Segment length (m)	SF_{DMS} (kN)	SF_{DMS} (kPa)	SF_{API} (kPa)	Segment surface area (m^2)
1.50	3.75	2.25	1	2.40	2.40	50.00	8.88	5.00	5.75
3.75	5.40	1.65	2	4.40	2.00	200.00	41.45	20.00	4.79
5.40	8.30	2.90	3	6.40	2.00	300.00	62.18	32.00	4.79
8.30	10.45	2.15	4	8.40	2.00	600.00	124.36	45.00	4.79
8.30	10.45	2.15	5	10.40	2.00	600.00	124.36	65.00	4.79
10.45	12.80	2.35	6	12.40	2.00	600.00	124.36	55.00	4.79
13.90	17.50	3.60	7	14.40	2.00	600.00	124.36	65.00	4.79
13.90	17.50	3.60	8	16.50	2.10	600.00	124.36	75.00	5.03
17.50	21.00	3.50	9	18.50	2.00	600.00	124.36	85.00	4.79
17.50	21.00	3.50	10	20.50	2.00	650.00	134.72	93.00	4.79
21.00	25.20	4.20	11	22.50	2.00	700.00	145.08	103.00	4.79

Table A-5: Pile (BOR) general information for F-3 location

Location: F-3									
Soil layer depth range (m)		Thickness (m)	Pile segment No.	Depth below the grade (m)	Segment length (m)	SF_{DMS} (kN)	SF_{DMS} (kPa)	SF_{API} (kPa)	Segment surface area (m^2)
2.25	6.00	3.75	1.00	2.80	2.80	120.00	17.97	10.00	6.70
2.25	6.00	3.75	2.00	4.80	2.00	215.00	44.32	15.00	4.79
6.00	9.75	3.75	3.00	6.80	2.00	380.00	78.33	21.00	4.79
6.00	9.75	3.75	4.00	8.90	2.10	570.00	117.50	31.00	5.03
9.75	13.80	4.05	5.00	10.90	2.00	785.00	161.82	52.00	4.79
9.75	13.80	4.05	6.00	12.90	2.00	840.00	173.16	62.00	4.79
13.80	18.00	4.20	7.00	14.90	2.00	990.00	204.08	87.00	4.79
13.80	18.00	4.20	8.00	17.00	2.10	1000.00	206.14	93.00	5.03
18.00	21.00	3.00	9.00	19.00	2.00	1000.00	206.14	98.00	4.79

Table A-6: Pile (BOR) general information for F-4 location

Location: F-4									
Soil layer depth range (m)		Thickness (m)	Pile segment No.	Depth below the grade (m)	Segment length (m)	SF_{DMS} (kN)	SF_{DMS} (kPa)	SF_{API} (kPa)	Segment surface area (m^2)
0	12.80	12.80	1.00	2.50	2.50	30.00	5.02	4.00	5.98
0	12.80	12.80	2.00	4.50	2.00	30.00	6.11	5.00	4.79
0	12.80	12.80	3.00	6.60	2.10	30.00	6.11	6.00	5.03
0	12.80	12.80	4.00	8.70	2.10	30.00	6.11	7.00	5.03
0	12.80	12.80	5.00	10.70	2.00	30.00	6.11	8.00	4.79
0	12.80	12.80	6.00	12.80	2.10	50.00	10.18	16.00	5.03
12.80	15.25	2.45	7.00	14.80	2.00	200.00	40.72	27.00	4.79
16.75	18.50	1.75	8.00	16.90	2.10	500.00	101.81	45.00	5.03
18.50	20.85	2.35	9.00	18.90	2.00	800.00	162.90	83.00	4.79
20.85	22.40	1.55	10.00	21.00	2.10	800.00	162.90	76.00	5.03
22.40	29.15	6.75	11.00	23.00	2.00	500.00	101.81	80.00	4.79

Table A-7: Pile (BOR) general information for F-5 location

Location: F-5									
Soil layer depth range (m)		Thickness (m)	Pile segment No.	Depth below the grade (m)	Segment length (m)	SF_{DMS} (kN)	SF_{DMS} (kPa)	SF_{API} (kPa)	Segment surface area (m^2)
0	1.50	1.50	20.00	0.90	0.90	8.80	4.11	0.00	2.15
1.50	4.30	2.80	21.00	1.90	1.00	13.00	5.36	4.40	2.39
1.50	4.30	2.80	22.00	2.90	1.00	17.00	7.02	6.60	2.39
1.50	4.30	2.80	23.00	3.90	1.00	21.60	8.91	8.80	2.39
4.30	7.50	3.20	24.00	4.90	1.00	44.90	18.53	17.80	2.39
4.30	7.50	3.20	25.00	6.00	1.10	68.20	28.14	22.20	2.63
4.30	7.50	3.20	26.00	7.00	1.00	91.50	37.76	24.40	2.39
7.50	11.70	4.20	27.00	8.00	1.00	149.80	61.82	22.20	2.39
7.50	11.70	4.20	28.00	9.00	1.00	149.80	61.82	24.40	2.39
7.50	11.70	4.20	29.00	10.00	1.00	188.00	77.58	26.70	2.39
7.50	11.70	4.20	30.00	11.00	1.00	188.00	77.58	31.10	2.39
11.70	15.00	3.30	31.00	12.00	1.00	200.00	82.90	66.70	2.39
11.70	15.00	3.30	32.00	13.00	1.00	210.90	87.03	71.10	2.39
11.70	15.00	3.30	33.00	14.10	1.10	220.90	91.16	75.60	2.63
15.00	16.00	1.00	34.00	15.10	1.00	231.10	95.37	55.60	2.39
16.00	17.00	1.00	35.00	16.10	1.00	265.10	109.40	60.00	2.39
17.00	17.50	0.50	36.00	17.10	1.00	265.10	109.40	62.20	2.39
17.50	20.00	2.50	37.00	18.10	1.00	265.10	109.40	102.20	2.39
17.50	20.00	2.50	38.00	19.10	1.00	265.10	109.40	106.70	2.39
20.00	21.00	1.00	39.00	20.10	1.00	324.90	134.07	111.10	2.39
21.00	22.70	1.70	40.00	21.10	1.00	324.90	134.07	80.00	2.39
21.00	22.70	1.70	41.00	22.20	1.10	433.00	178.68	13.30	2.63
22.70	24.00	1.30	42.00	23.20	1.00	433.00	178.68	13.30	2.39
24.00	28.50	4.50	43.00	24.20	1.00	488.50	201.58	13.30	2.39
24.00	28.50	4.50	44.00	25.20	1.00	488.50	201.58	137.80	2.39
24.00	28.50	4.50	45.00	26.20	1.00	488.50	201.58	142.22	2.39
24.00	28.50	4.50	46.00	27.20	1.00	488.50	201.58	146.70	2.39
24.00	28.50	4.50	47.00	28.20	1.00	488.50	201.58	155.60	2.39
28.50	30.00	1.50	48.00	29.20	1.00	488.50	201.58	46.70	2.39
30.00	31.00	1.00	49.00	30.30	1.10	488.50	201.58	46.70	2.63

SECTION 2

CLAY LAYERS INFORMATION

Table A-8: Clay information at J-1 location

Location: J-1														
S_u (kPa)	LL (%)	PI (%)	φ	α_{API}	$\alpha_{API\ 2}$	α_{DMS}	$\alpha_{DMS}/\alpha_{API}$	$\alpha_{DMS}/\alpha_{API\ 2}$	OCR	G_s	γ (kN/m^3)	w.c. (%)	$p'_0(z)$ (kPa)	$p'_{0,\ tip}$ (kPa)
80.00	42.0	22.0	2.60	0.3936	0.0689	0.0233	0.0591	0.3376	8.57	2.67	19.20	27.00	30.720	30.720
137.50	55.0	30.0	1.23	0.4747	0.3799	0.0327	0.0689	0.0861	4.28	2.62	20.00	23.00	111.72	114.00
137.50	55.0	30.0	0.91	0.5252	0.4380	0.1740	0.3312	0.3972	3.27	2.62	20.00	23.00	151.72	154.00
170.00	78.0	52.0	0.74	0.5807	0.4399	0.3195	0.5502	0.7264	2.87	2.65	18.80	30.00	229.32	219.96
300.00	78.0	52.0	1.12	0.4862	0.4059	0.1742	0.3583	0.4291	4.02	2.65	19.50	25.00	268.32	267.15
487.50	53.0	29.0	1.59	0.4455	0.3603	0.1277	0.2865	0.3542	5.50	2.65	19.50	25.00	307.32	306.15
487.50	53.0	29.0	1.41	0.4590	0.3862	0.1927	0.4198	0.4990	4.94	2.65	19.50	25.00	346.32	345.15
525.00	68.0	44.0	1.35	0.4637	0.3868	0.2003	0.4320	0.5178	4.66	2.65	20.00	20.00	388.32	396.00
525.00	68.0	44.0	1.23	0.4752	0.3959	0.2003	0.4215	0.5059	4.28	2.65	20.00	20.00	428.32	436.00
600.00	68.0	44.0	1.28	0.4700	0.3915	0.2003	0.4262	0.5116	4.46	2.65	20.00	20.00	468.32	476.00
600.00	68.0	44.0	1.18	0.4797	0.4008	0.2128	0.4437	0.5311	4.14	2.65	20.00	20.00	508.32	516.00
600.00	68.0	44.0	1.09	0.4889	0.4055	0.2253	0.4609	0.5558	3.87	2.65	20.00	20.00	548.32	556.00
300.00	80.0	52.0	0.51	0.6996	0.4459	0.5508	0.7874	1.2355	1.99	2.60	19.50	25.00	587.32	581.10
300.00	80.0	52.0	0.48	0.7224	0.5038	1.0015	1.3863	1.9880	1.88	2.60	19.50	25.00	626.32	620.10
525.00	52.0	32.0	0.74	0.5812	0.4506	0.7869	1.3539	1.7463	2.73	2.60	20.00	22.00	709.37	718.00
525.00	52.0	32.0	0.70	0.5974	0.4563	0.8012	1.3412	1.7558	2.60	2.60	20.00	22.00	749.37	758.00
275.00	58.0	38.0	0.33	0.8680	0.4777	1.3657	1.5734	2.8591	1.33	2.65	20.00	22.00	828.77	838.00
600.00	62.0	37.0	0.63	0.6289	0.4692	0.1885	0.2997	0.4017	2.35	2.62	20.20	20.00	949.19	969.60
450.00	80.0	50.0	0.42	0.7686	0.4092	0.1316	0.1713	0.3217	1.68	2.60	19.50	26.00	1063.39	1053.00

Table A-9: Clay information at J-2 location

Location: J-2														
S_u (kPa)	LL (%)	PI (%)	φ	α_{API}	$\alpha_{API\ 2}$	α_{DMS}	$\alpha_{DMS}/\alpha_{API}$	$\alpha_{DMS}/\alpha_{API\ 2}$	OCR	G_s	γ (kN/m^3)	w.c. (%)	$p'_0(z)$ (kPa)	$p'_{0,\ tip}$ (kPa)
5.00	52.0	29.0	0.1389	1.3416	0.4372	0.9660	0.7200	2.2094	0.61	2.61	18.00	37.00	36.00	36.00
125.00	52.0	29.0	1.6667	0.4401	0.3419	0.0532	0.1209	0.1556	5.62	2.63	19.50	25.00	75.00	78.00
100.00	47.0	25.0	0.8929	0.5292	0.4108	0.0492	0.0930	0.1198	3.33	2.59	18.50	30.00	112.00	111.00
175.00	47.0	25.0	1.1667	0.4811	0.4033	0.1319	0.2741	0.3270	4.16	2.59	19.00	30.00	150.00	152.00
375.00	70.0	43.0	1.6447	0.4415	0.3672	0.0985	0.2230	0.2682	5.49	2.56	20.00	20.00	228.00	240.00
375.00	70.0	43.0	1.3993	0.4597	0.3801	0.0990	0.2154	0.2605	4.77	2.56	20.00	20.00	268.00	280.00
375.00	70.0	43.0	1.2175	0.4760	0.3943	0.0999	0.2099	0.2533	4.23	2.56	20.00	20.00	308.00	320.00
375.00	70.0	43.0	1.0776	0.4907	0.4083	0.1011	0.2061	0.2477	3.80	2.56	20.00	20.00	348.00	360.00
375.00	70.0	43.0	0.9665	0.5086	0.4215	0.0929	0.1826	0.2203	3.45	2.56	20.00	20.00	388.00	400.00
375.00	70.0	43.0	0.8762	0.5342	0.4289	0.0908	0.1700	0.2117	3.16	2.56	20.00	20.00	428.00	440.00
375.00	70.0	43.0	0.8013	0.5586	0.4386	0.1362	0.2438	0.3105	2.92	2.56	20.00	20.00	468.00	480.00
375.00	66.0	43.0	0.7382	0.5820	0.4470	0.2380	0.4090	0.5325	2.72	2.60	20.00	20.00	508.00	520.00
450.00	72.0	46.0	0.6747	0.6087	0.4601	0.3027	0.4972	0.6578	2.46	2.58	20.50	20.00	667.00	697.00
90.00	72.0	46.0	0.1211	1.4366	1.0587	2.6656	1.8554	2.5178	0.56	2.58	18.50	27.00	743.00	703.00
400.00	44.0	23.0	0.4283	0.7640	0.4987	0.9286	1.2154	1.8622	1.69	2.55	19.50	22.00	934.00	936.00
400.00	44.0	23.0	0.4111	0.7798	0.5427	0.9480	1.2156	1.7469	1.63	2.55	19.50	22.00	973.00	975.00
400.00	73.0	44.0	0.3953	0.7953	0.5525	0.9093	1.1433	1.6459	1.57	2.55	19.50	22.00	1012.00	1014.00
220.00	52.0	27.0	0.2026	1.1109	0.7647	0.5980	0.5383	0.7820	0.87	2.55	19.00	25.00	1086.00	1064.00
220.00	52.0	27.0	0.1957	1.1302	0.7827	0.2110	0.1867	0.2696	0.85	2.55	19.00	25.00	1124.00	1102.00

Table A-10: Clay information at J-3 location

Location: J-3														
S_u (kPa)	LL (%)	PI (%)	φ	α_{API}	$\alpha_{API\ 2}$	α_{DMS}	$\alpha_{DMS}/\alpha_{API}$	$\alpha_{DMS}/\alpha_{API\ 2}$	OCR	G_s	γ (kN/m^3)	w.c. (%)	$p'_0(z)$ (kPa)	$p'_{0,\ tip}$ (kPa)
90.00	61.0	35.3	5.5556	0.3257	0.3967	0.1180	0.3623	0.2975	17.40	2.71	9.00	34.14	16.20	16.20
140.00	37.0	18.5	3.8674	0.3565	0.3314	0.0923	0.2588	0.2784	11.98	NR	10.00	24.20	36.20	38.00
130.00	48.0	25.0	2.2727	0.4072	0.4123	0.1232	0.3024	0.2987	7.29	2.79	10.50	23.20	57.20	60.90
275.00	55.0	32.0	1.9615	0.4225	0.4156	0.0799	0.1892	0.1923	6.85	2.73	10.00	25.40	140.20	138.00
275.00	55.0	32.0	1.7166	0.4368	0.4287	0.0827	0.1894	0.1930	6.06	2.73	10.00	25.40	160.20	158.00
275.00	55.0	32.0	1.5261	0.4499	0.4415	0.0856	0.1903	0.1939	5.43	2.73	10.00	25.40	180.20	178.00
325.00	60.4	50.0	1.6153	0.4435	0.3846	0.0869	0.1960	0.2260	5.72	NR	10.00	25.27	201.20	199.00
325.00	60.4	50.0	1.4693	0.4541	0.4175	0.2679	0.5900	0.6417	5.24	NR	10.00	25.27	221.20	219.00
325.00	60.4	50.0	1.3474	0.4641	0.4397	0.2771	0.5971	0.6302	4.84	NR	10.00	25.27	241.20	239.00
325.00	60.4	50.0	1.2443	0.4734	0.4615	0.2948	0.6227	0.6387	4.50	NR	10.00	25.27	261.20	259.00
325.00	60.4	50.0	1.1558	0.4822	0.4945	0.3047	0.6319	0.6162	4.20	NR	10.00	25.27	281.20	279.00
325.00	60.4	50.0	1.0790	0.4906	0.5166	0.3342	0.6812	0.6469	3.95	NR	10.00	25.27	301.20	299.00
447.50	49.0	27.2	1.3889	0.4606	0.4311	0.2784	0.6044	0.6458	4.76	2.72	10.50	20.93	322.20	334.95
447.50	49.0	27.2	1.3039	0.4679	0.4628	0.3553	0.7594	0.7677	4.51	2.72	10.50	20.93	343.20	355.95
447.50	49.0	27.2	1.2287	0.4749	0.4947	0.4975	1.0475	1.0055	4.28	2.72	10.50	20.93	364.20	376.95
460.00	73.0	48.0	1.0171	0.4979	0.4659	0.9145	1.8367	1.9629	3.65	2.71	10.50	24.00	452.25	462.00
380.00	78.3	48.7	0.7704	0.5697	0.5826	0.8261	1.4502	1.4179	2.96	2.75	10.00	25.00	493.25	480.00
450.00	49.4	27.6	0.8407	0.5453	0.5080	0.3530	0.6474	0.6949	2.94	2.70	11.00	21.93	535.25	572.00
450.00	49.4	27.6	0.8075	0.5564	0.5398	0.3069	0.5516	0.5686	2.84	2.70	11.00	21.93	557.25	594.00
450.00	49.4	27.6	0.7769	0.5673	0.5713	0.2794	0.4924	0.4890	2.75	2.70	11.00	21.93	579.25	616.00
450.00	49.4	27.6	0.7484	0.5780	0.5953	0.2597	0.4494	0.4362	2.66	2.70	11.00	21.93	601.25	638.00

Table A-11: Clay information at J-4 location

Location: J-4														
S_u (kPa)	LL (%)	PI (%)	φ	α_{API}	$\alpha_{API\ 2}$	α_{DMS}	$\alpha_{DMS}/\alpha_{API}$	$\alpha_{DMS}/\alpha_{API\ 2}$	OCR	G_s	γ (kN/m^3)	w.c. (%)	$p'_0(z)$ (kPa)	$p'_{0,\ tip}$ (kPa)
150.00	59.0	35.0	1.9355	0.4239	0.3122	0.0000	0.0000	0.0000	6.70	2.62	18.80	27.00	77.50	77.08
175.00	28.0	9.0	1.4894	0.4526	0.3067	0.0170	0.0376	0.0555	5.08	2.62	20.00	22.00	117.50	122.00
250.00	56.0	33.0	1.0544	0.4934	0.1763	0.0597	0.1210	0.3385	3.80	2.65	19.80	23.00	237.10	239.58
200.00	77.0	52.0	0.6327	0.6286	0.4629	0.0746	0.1187	0.1612	2.43	2.65	19.50	28.00	316.10	313.95
200.00	77.0	52.0	0.5623	0.6668	0.4740	0.0746	0.1119	0.1574	2.15	2.65	19.80	23.00	355.70	358.38
200.00	77.0	52.0	0.5072	0.7021	0.4866	0.0746	0.1063	0.1533	2.00	2.65	19.30	27.00	394.30	387.93
200.00	77.0	52.0	0.4620	0.7356	0.5084	0.2984	0.4056	0.5868	1.84	2.65	19.30	27.00	432.90	426.53
350.00	105.0	72.0	0.7401	0.5812	0.4486	0.4262	0.7333	0.9500	2.74	2.65	20.00	22.00	472.90	482.00
350.00	105.0	72.0	0.6824	0.6053	0.4565	0.5114	0.8450	1.1204	2.54	2.65	20.00	22.00	512.90	522.00
400.00	55.0	33.0	0.6312	0.6293	0.4584	0.5967	0.9481	1.3016	2.34	2.65	20.40	21.00	633.70	654.84
400.00	55.0	33.0	0.5930	0.6493	0.4751	0.5967	0.9189	1.2559	2.21	2.65	20.40	21.00	674.50	695.64
550.00	55.0	33.0	0.7290	0.5856	0.4474	0.4339	0.7410	0.9700	2.72	2.60	20.00	23.00	754.50	762.00
550.00	55.0	33.0	0.6923	0.6009	0.4573	0.4068	0.6769	0.8896	2.60	2.60	20.00	23.00	794.50	802.00
550.00	55.0	33.0	0.6591	0.6159	0.4639	0.3797	0.6165	0.8184	2.48	2.60	20.00	23.00	834.50	842.00
500.00	68.0	45.0	0.5465	0.6764	0.4966	0.4177	0.6175	0.8410	2.13	2.65	19.70	25.00	914.90	908.17
600.00	68.0	45.0	0.6287	0.6306	0.4692	0.3481	0.5520	0.7418	2.42	2.65	19.70	25.00	954.30	947.57
450.00	70.0	46.0	0.3691	0.8230	0.4055	0.1989	0.2417	0.4905	1.56	2.60	18.50	30.00	1219.30	1148.85
450.00	70.0	46.0	0.3573	0.8364	0.5850	0.1326	0.1585	0.2267	1.41	2.60	20.00	23.00	1259.30	1282.00
600.00	70.0	46.0	0.4618	0.7358	0.4924	0.0995	0.1352	0.2020	1.78	2.60	20.00	23.00	1299.30	1322.00

SECTION 3
SAND LAYERS INFORMATION

Table A-12: Sand information at U-7 location

Location: U-7									
$CaCO_3$ (%)	G_s	γ (kN/m^3)	w.c. (%)	D_r (%)	N_q	δ (deg.)	Sand type	$p'_0(z)$ (kPa)	$p'_{0,\ tip}$ (kPa)
17.00	2.73	10.00	25.67	Very dense	50	35	Silica	44.30	47.00
31.00	NR	10.50	23.29	Very dense	50	28	Calcareous	65.30	70.35
31.00	NR	10.50	23.29	Very dense	50	28	Calcareous	86.30	91.35
30.00	2.70	9.50	23.00	Dense	40	25	Calcareous	124.30	120.65
24.00	2.80	10.50	26.57	Medium dense	50	32	Calcareous	164.30	175.35
30.00	2.71	10.00	24.00	Dense	50	29	Calcareous	205.30	207.00
32.00	2.80	11.00	22.60	Dense	40	24	Calcareous	227.30	249.70
32.00	2.80	11.00	22.60	Dense	40	24	Calcareous	249.30	271.70
32.00	2.80	11.00	22.60	Dense	40	24	Calcareous	271.30	293.70
27.00	2.78	10.50	20.50	Dense	50	30	Calcareous	308.30	322.35
27.00	2.78	10.50	20.50	Dense	50	30	Calcareous	329.30	343.35
24.00	NR	10.00	26.00	Medium dense	40	28	Calcareous	370.30	387.00
33.00	2.75	11.00	15.00	Medium dense	20	20	Calcareous	432.30	491.70

Table A-13: Sand information at F-1 location

Location: F-1									
$CaCO_3$ (%)	G_s	γ (kN/m^3)	w.c. (%)	D_r (%)	N_q	δ (deg.)	Sand type	$p'_0(z)$ (kPa)	$p'_{0,\ tip}$ (kPa)
71	2.71	9.00	35.01	Loose	12	10.6	Calcareous	17.10	17.10
71	2.71	9.00	35.01	Loose	12	10.6	Calcareous	35.10	35.10
57	2.72	9.00	39.51	Very loose	8	10.6	Calcareous	54.00	54.00
20	NR	9.00	29.46	Medium dense	20	25.0	Calcareous	72.00	72.00
6	NR	10.00	21.75	Medium dense	20	25.0	Silica	92.00	100.00
6	NR	10.00	21.75	Medium dense	20	25.0	Silica	112.00	120.00
4	NR	10.00	21.41	Very dense	70	35.0	Silica	132.00	140.00
4	NR	10.00	21.41	Very dense	70	35.0	Silica	152.00	160.00
4	NR	10.00	21.41	Very dense	70	35.0	Silica	172.00	180.00
3	NR	10.00	21.52	Dense	55	32.5	Silica	192.00	200.00
3	NR	10.50	20.70	Dense	40	30.0	Silica	213.00	231.00

Table A-14: Sand information at J-3 location

Location: J-3									
$CaCO_3$ (%)	G_s	γ (kN/m³)	w.c. (%)	D_r (%)	N_q	δ (deg.)	Sand type	$p'_0(z)$ (kPa)	$p'_{0,\ tip}$ (kPa)
41.00	2.70	10.50	23.55	Very dense	50	23	calcareous	78.20	81.90
41.00	2.70	10.50	23.55	Very dense	50	23	calcareous	99.20	102.90
41.00	2.70	10.50	23.55	Very dense	50	23	calcareous	120.20	123.90
48.00	2.70	11.00	21.50	Medium dense	40	18	calcareous	386.20	416.90
48.00	2.70	11.00	21.50	Medium dense	40	18	calcareous	408.20	438.90
48.00	2.70	11.00	21.50	Medium dense	40	18	calcareous	430.20	460.90
46.00	2.70	10.50	22.00	Medium dense	20	16	calcareous	473.25	483.00
37.00	NR	10.00	24.00	Loose	40	22	calcareous	513.25	500.00

Table A-15: Sand information at F-6 location

Location: F-6									
$CaCO_3$ (%)	G_s	γ (kN/m³)	w.c. (%)	D_r (%)	N_q	δ (deg.)	Sand type	$p'_0(z)$ (kPa)	$p'_{0,\ tip}$ (kPa)
74.00	2.77	8.00	31.49	Very loose	8.00	9.93	Calcareous	9.60	9.60
21.00	2.68	11.00	17.93	Loose	16.00	21.80	Calcareous	32.70	36.30
21.00	2.68	11.00	17.93	Loose	16.00	21.80	Calcareous	54.70	58.30
21.00	2.68	11.00	17.93	Loose	16.00	21.80	Calcareous	77.80	81.40
4.00	NR	10.50	21.84	Very dense	70.00	35.00	Silica	98.80	98.70
6.00	NR	10.00	22.37	Medium dense	20.00	25.00	Silica	118.80	114.00
10.00	NR	11.00	19.03	Dense	55.00	32.50	Silica	141.90	148.50
10.00	NR	11.00	19.03	Dense	55.00	32.50	Silica	163.90	170.50
10.00	NR	11.00	19.03	Dense	55.00	32.50	Silica	187.00	193.60
10.00	NR	11.00	19.03	Dense	55.00	32.50	Silica	209.00	215.60
10.00	NR	11.00	19.03	Dense	55.00	32.50	Silica	231.00	237.60
8.00	NR	11.00	NR	Very dense	70.00	35.00	Silica	254.10	260.70
8.00	NR	11.00	NR	Very dense	70.00	35.00	Silica	276.10	282.70
4.00	2.66	10.00	24.58	Medium dense	30.00	27.50	Silica	297.10	278.00